APPLICATION OF SANDWICH BEAM IN AUTOMOBILE FRONT BUMPER FOR FRONTAL CRASH ANALYSIS

A Thesis by

Amarnath Donga

Bachelor of Engineering, JNTU, India 2005

Submitted to the Department of Mechanical Engineering
and the faculty of the Graduate School of
Wichita State University
in partial fulfillment of
the requirement for the degree of
Masters of Science

December 2011

APPLICATION OF SANDWICH BEAM IN AUTOMOBILE FRONT BUMPER FOR FRONTAL CRASH ANALYSIS

The following faculty members have examined the final copy of this thesis for form and content and recommend that it be accepted in partial fulfillment of the requirements for the degree of Master of Science with a major in Mechanical Engineering.

_____
Hamid M.Lankarani, Committee Chair

_____
Neeraj Jaggi, Committee Member

_____
Prasannakumar Bhonge, Committee Member

DEDICATION

To My Parents Rama Rao and Dhanalakshmi

ACKNOWLEDGEMENTS

I take this opportunity to extend my sincere gratitude and appreciation to many great people who made these masters possible. First I would like to thank my academic advisor Dr. Hamid M. Lankarani for his excellent guidance, advice, precious time, and constant support throughout my graduate career at Wichita state university, without which my efforts would not have been complete and fruitful.

I would also like to express my thanks and appreciation to Dr. Neeraj Jaggi and Dr. Prasannakumar Bhonge for their time and efforts in reviewing this manuscript.

I am greatful to my friends Sachin, Shravan, Jaya Prakash, Arun, for their assistance to complete my task successfully. Finally my greatful thanks to my parents, my brothers Nagendra Prasand and Venkata Ramana who are source for my emotional peace and encouragement throughout my life.

ABSTRACT

The study of energy-absorbing behavior in sandwich beams under static loading has become the basis for the design of crashworthy structure in automobile applications. Unlike metals, composite sandwich materials display little or no plastic deformation. Research has shown that foam-cored sandwich beam has significantly higher energy absorption than low carbon/high carbon steel used in automobiles.This thesis is aimed at developing a structural component that provides better kinetic energy absorption, than the existing car front bumper. Occupants of motor vehicles are injured or killed in several different types of crash situations. These are frontal, side, rear, and rollover. The most severe accident situations are frontal impact. The car front bumper is a major structural component, and it carries most of the impact load in crash events. Therefore, in order to improve the front bumper performance, an attempt is made in this study to use sandwich material in the front bumper. And for that, a study is carried out to arrive at a combination of core and face sheet that offers maximum energy absorption.

A Finite Element (FE) model of a Ford Taurus is first utilized and validated, using the LS-Dyna FE software. Frontal crash analysis is then performed on the car with sandwich bumper model according to the Federal Motor Vehicle Safety Standard 208 (FMVSS 208) and the New Car Assessment Program (NCAP). The vehicle displacements, energy absorption, and deceleration levels are compared for both the steel and sandwich models. Occupant injuries are then evaluated for frontal impact sled test at 35 mph, using the LS-Dyna, for both steeel and the new composite models. The injury levels including, head, neck and chest injuries are evaluated and compared for the both models. It is demonstrated that foam-cored sandwich beam with carbon/epoxy face sheet is more effective than the present steel car bumper.

TABLE OF CONTENTS

TABLE OF CONTENTS (Continued)

LIST OF FIGURES

Figure Page

LIST OF FIGURES (continued)

Figure Page

LIST OF FIGURES (continued)

Figure Page

LIST OF FIGURES (continued)

Figure Page

LIST OF TABLES

CHAPTER 1

INTRODUCTION

1.1 Background

Occupants of motor vehicles are injured or killed in different types of crash events, such as frontal, side, rear, rollovers, and others. With each type of crash, there are different crash severities, causes, and risk of injuries to the occupant for a given type of vehicle. The most severe accident situations are frontal impact crashes. After frontal impact crashes, the second most severe type of automobile impacts in the United States are side impacts, which result in serious head and pelvic injuries to the occupants. The statistics in Figure 1.1 are derived from Volvo's accident database, containing 27,500 crashes involving Volvo cars only [1].

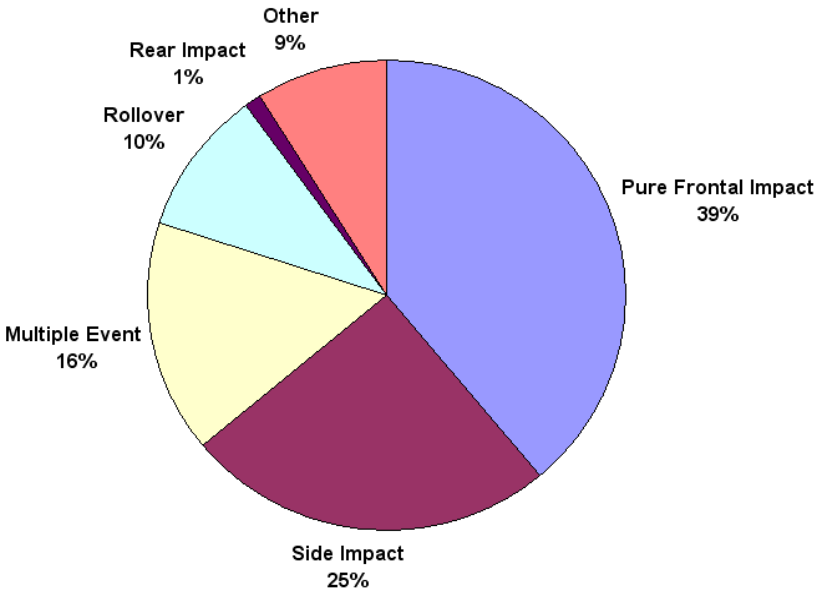

Figure 1.1 Volvo's distribution of serious-to-fatal crashes [1]

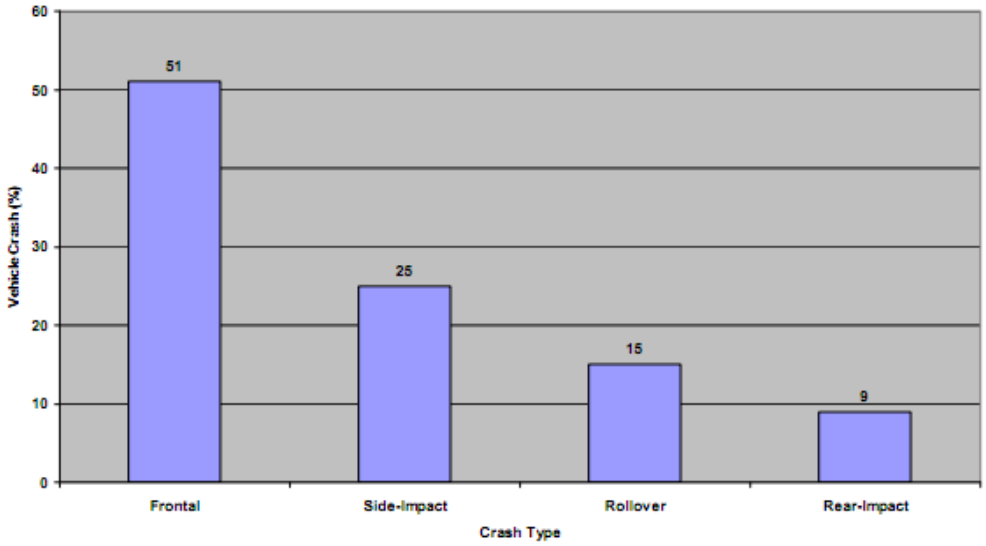

Figure 1.2 Vehicle crashes by crash type [1]

Over the years, researchers have carried out a wide range of studies and analyses on front impact crashes. They have largely been successful in reducing the injury parameters sustained by the vehicle occupant [1]. Figure 1.2 shows vehicle crashes by crash type, and Figure 1.3 provides a comparison of the injuries involved in frontal and side impact scenarios. This clearly indicates that researchers have been successful in the reduction of injury levels in frontal impacts; however the injuries involved in side impact crashes have increased. Many design and material changes have been made in an effort to reduce injury severity, mainly by improving frontal impact protection techniques [1].

Nearly 30,000 vehicle occupants die every year in front impact crashes, of which more than 50% of deaths are due to head injuries. Impacts with poles represent a significant portion of the vehicular collisions [1]. Fixed object collisions account for less than 8% of all crashes in the USA, but they represent nearly 30% of overall fatal crashes [2].

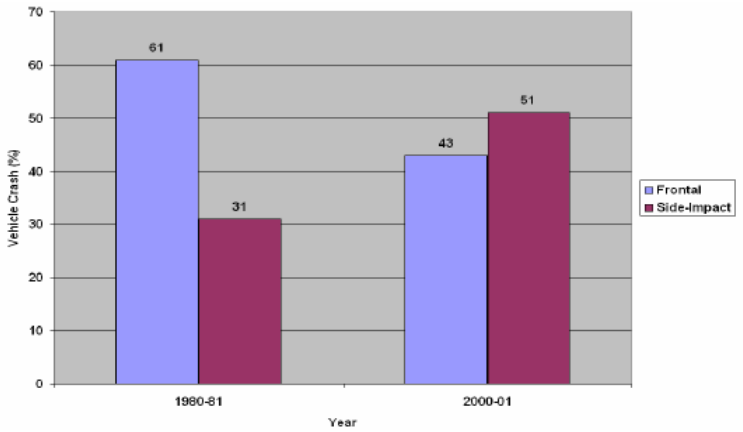

Figure 1.3 Comparison of frontal and side impact crash injuries [1]

1.2 Motivation

Much automotive research has been aimed at developing automotive structures to sustain impact loading in diverse crash conditions such as, frontal perpendicular, angular, offset and side collisions. This research has enabled manufacturers to replace existing structural parts with newer materials and designs that improve the structural performance of the automobile. An increased focus on occupant safety has been the basis for developing the most comfortable, as well as fuel and environmentally efficient cars [2]. The increasing application of composite materials in the automobile industry, and the specific strength that they offer, is the core reason for replacing the existing front bumper of the Ford Taurus with sandwich beam material. Sandwich beam material is the combination of solid laminate as the face sheet, and rigid foam as the core. This offers better strength and absorbs more impact energy, when compared with existing front bumpers [2].

1.3 Crashworthiness

The ability of the vehicle to absorb energy and to prevent occupant injuries in the event of an accident is referred to as “crashworthiness”. The vehicle must be designed so

that, at higher speeds, its occupant does not experience a net deceleration greater than 20g. Crashworthiness can be categorized into three basic areas: material engineering and design, combustion and fire, and medical engineering (biomechanics). Crashworthiness features include air bags, seat belts, crumple zones, side impact protection, interior padding, and head rests. These features are updated with new, safer, and better designs.

Structural crashworthiness involves absorption of kinetic energy by considering designs and materials suitable for controlled and predictive energy absorption. In this process, the kinetic energy of the colliding bodies is partly converted into internal work of the bodies involved in the crash. Crash events are non-linear, and may involve material failure, global and local structural instabilities, and failure of joints. In addition, strain-rate and inertia effects may play an important role in the response of the structure involved.

Crashworthiness of a material is expressed in terms of its specific energy absorption, $E_S = F/D_S$, where D_S is the density of the composite material and F is the crush stress. In order to protect passengers during an impact, a structure based on strength and stiffness is far from being optimal. Rather, the structure should collapse in a well-defined deformation zone, and keep the forces well below dangerous acceleration levels. However, since the amount of absorbed energy equals the area under the load deflection curve, the two above mentioned criteria are somewhat contradictory. Thus showing that it is not only important to know how much energy is absorbed, but also the *way* that it is absorbed. That is to say, how inertia loads are transferred from the impact point to the supporting structural components.

1.4 Composite Sandwich Materials in Crashworthiness

The fuel efficiency and gas emission regulation of the car are very important in the contemporary world. Every day the price of fuel and the requirements of the fuel are increasing. Consequently, vehicle exhaust is polluting the environment and increasing the global temperature. A composite material helps in reducing the weight of the structure, thus reducing fuel consumption. The use of composite sandwich structures in aerospace and automotive applications is increasing, especially due to their extremely low weight, high flexural and transverse shear stiffness, and corrosion resistance [2]. In addition, these materials are capable of absorbing large amounts of energy under impact loads, which results in high structural crashworthiness [2]. In its simplest form a structural sandwich, which is a special form of laminated composites, is composed of two thin stiff face sheets and a thick lightweight core bonded between them. A sandwich structure will offer different mechanical properties with the use of different types of materials. The overall performance of sandwich structures depends on the properties of the constituents [2]. Hence, optimum material choice is often obtained according to the design needs. Various combinations of core and face sheet materials are utilized by researchers worldwide, in order to achieve improved crashworthiness [2].

Generally, in a sandwich structure the bending loads are carried by the force couple formed by the face sheets, and the shear loads are carried by the lightweight core material [3]. The face sheets are strong and stiff, both in tension and compression, as compared to the low-density core material, whose primary purpose is to maintain a high moment of inertia. The low-density of the core material results in low panel density; therefore, under flexural loading, sandwich panels have high specific mechanical

properties relative to the monologue structures. Consequently, sandwich panels are highly efficient in carrying bending loads.

Under flexural loading, face sheets act together to form a force couple, where one laminate is under compression and the other is under tension. On the other hand, the core resists transverse forces and stabilizes the laminates against global buckling and local buckling [4]. The critical properties of sandwich structures vary according to the application area of the structure. In automotive industry, the out-of-plane compressive properties are more critical, whereas in wind turbines, the in-plane compressive properties are more important. Therefore, depending on the application area, different properties or characteristics of sandwich panels need to be evaluated [5].

The most widely-used method of selecting the correct configuration for sandwich structures according to the design specifications is by numerically modeling them [6]. For this purpose, finite element modeling is used worldwide, and the behavior of the structures can be seen before manufacturing the real parts. The objectives of this study are to understand the mechanical behavior and failure mechanisms of sandwich structures with Divinyle Chloride Foam core and carbon/epoxy face sheets [7]. For this purpose, three-point bending tests were conducted on composite sandwich specimens with various core thicknesses. Figure 1.4shows the front bumper construction used in automobiles.

1.5 NHTSA Standards

The National Highway Traffic Safety Administration (NHTSA), under the U.S. Department of Transportation, was established by the Highway Safety Act of 1970. As the successor to the National Highway Safety Bureau, its purpose is to carry out safety programs under the National Traffic and Motor Vehicle Safety Act of 1966, and the

Highway Safety Act of 1966 [5]. The Vehicle Safety Act has subsequently been recorded under Title 49 of the U. S. Code in Chapter 301, Motor Vehicle Safety. NHTSA also performs consumer programs established by the Motor Vehicle Information and Cost Savings Act of 1972, which has been recorded in various Chapters under Title 49. NHTSA is responsible for reducing deaths, injuries and economic losses resulting from motor vehicle crashes [8]. This is accomplished by setting and enforcing safety performance standards for motor vehicles and motor vehicle equipment, and through grants to state and local government to conduct effective local highway safety programs.

Figure 1.4 Metallic front bumper used in cars [11]

NHTSA investigates safety defects in motor vehicles, sets and enforces fuel economy standards, and helps state and local communities reduce the threat of drunk drivers. It also promotes the use of safety belts, child safety seats and air bags, investigates odometer fraud, establishes and enforces vehicle anti-theft.

1.6 FMVSS 208 Regulation

The objective of a crash test for Federal Motor Vehicle Safety Standard (FMVSS) 208 is to measure the crashworthiness of a passenger vehicle [8]. The standard specifies

requirements for the protection of vehicle occupants in crashes [8]. Historically, this has encouraged improvements to the vehicle structure and restraint systems, to enhance occupant crash protection. Structural design for crashworthiness seeks to mitigate two adverse effects of a crash – (1) degradation of the occupant compartment survival space and (2) the occupant compartment deceleration severity [8]. Both effects have the potential to cause injuries – first, because of the increase in probability of occupant contact with intruding vehicle components, and second, because of the potential for internal injuries to occupants.

The degradation of the occupant compartment survival space is measured by intrusion, while occupant compartment deceleration severity is measured by the amplitude and time duration of the crash pulse [5]. The ideal frontal crash test procedure will evaluate the potential for occupant injury, from both deceleration severity and from intrusion. Furthermore, in addition to occupant protection, the ideal test procedure will not lead to designs which jeopardize the vehicle's crash compatibility with its collision partners. Finally, the test conditions (i.e., impact speed, impact angle, and impact partner) must encompass and be representative of the frontal crash environment to which passenger vehicles are exposed on the highway [8].

1.7 New Car Assessment Program (NCAP)

The rigid barrier test is used in the New Car Assessment Programs (NCAP) of the U.S., Japan, and Australia [8]. Unlike the FMVSS No. 208 rigid barrier test, the NCAP test is applied to belted occupants only, at a speed of 35mph [5]. Figure 1.5 shows the frontal impact test set-up as per FMVSS 208 standard. According to FMVSS 208, NCAP testing has led to designs with reduced intrusion and softer crash pulses for both cars, and

light trucks and vans [8]. In the U.S., until the recent adoption of the alternative sled test, this test (including the oblique test) was the only basis for occupant protection standard FMVSS No. 208 (S.5.1) for unbelted and belted occupants [8]. NCAP is a full-systems test, which evaluates the protection provided by both the energy-absorbing vehicle structure and the occupant restraint system. In the rigid barrier test, the vehicle changes velocity very quickly upon hitting the barrier [8]. The crash produces a high deceleration crash pulse of short time duration – frequently referred to as a 'stiff pulse' [8].

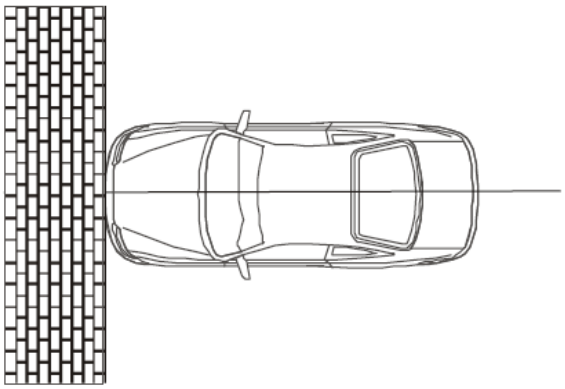

Figure 1.5 US-NCAP test setup [15]

In rigid barrier tests, only minimal intrusion has been measured in the testing vehicles of the U.S. fleet. Prior to the mandatory requirements of FMVSS 208 and of NCAP, in the late 1970s and early 1980s, extensive intrusion, particularly of the steering columns in light trucks, was a common occurrence. The kinetic energy of the crash (½ MV^2) is dissipated by the crush of the vehicle and the rebound velocity [5]. To minimize the delta-V, structural designs attempt to minimize the residual rebound velocity away from the wall. Figure 1.5 shows the test setup for frontal impact test according to FMVSS 208 standards [8].

1.8 Oblique Frontal Fixed Barrier Test

The frontal barrier crash test of FMVSS 208 requires a rigid barrier test of up to 30 mph, at angles from perpendicular to the line of travel, to 30 degrees. A schematic of the test configuration is shown in Figure 1.6. Oblique Frontal Fixed Barrier tests result in a lower acceleration crash pulse of longer duration, than the full frontal fixed barrier tests – frequently referred to as a 'soft crash pulse.' The oblique frontal fixed barrier test is intended to represent most real-world crashes, with less frontal engagement, more oblique, with changes in velocity up to approximately 35 mph. The angled barrier test exposes the belted or unbelted occupants to the same change in velocity (approximately 0 to 35 mph), for any vehicle. Like the perpendicular barrier test, it is a full systems test which evaluates the protection provided by both the energy-absorbing vehicle structure, and the occupant restraint system [9]. It ensures that the restraint system provides the same level of protection in single vehicle crashes, regardless of vehicle mass/size.

1.9 Car Front Bumper

The automotive front bumper is the main load-carrying and energy-absorbing component during frontal and angled impacts [8]. The front bumper can absorb up to 25% of the impact energy through progressive plastic deformation, when the vehicle crashes.

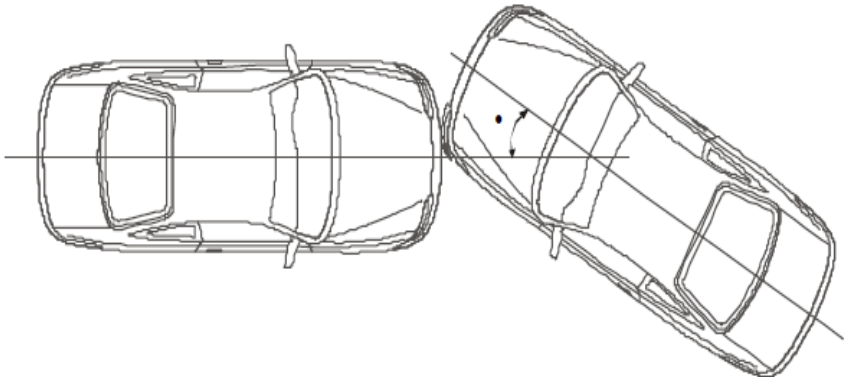

Figure 1.6 Car-to-car oblique impact test [15]

For the structural analysis of the car front bumper FEM is used, since it is the most extensively used computational method in the automotive industry. The FE model of a car front bumper structural component does not perform exactly the same in a crash as it does in the full vehicle test. This is due to complex boundary conditions that exist in an actual car. Crashworthiness of a structure is a complex system, and the individual performance of components do not necessarily compare across platforms. However, the general trends and energy absorption capabilities of component analysis are indicative of actual performance for each platform, and are extensively used for design and analysis [8].

Steel is still used as the material for car front bumpers. However lighter materials, such as fiber reinforced plastics (FRPs), are being used in the automotive industry. FRPs can be used as a substitute for steel for this component, as they offer higher energy absorption than steel. As discussed earlier, composite sandwich structures have high strength and stiffness-to-weight ratio in the fiber direction, as well as the in the direction perpendicular to the fiber, even though their Young's modulus is less than steel. This means that the composite sandwich structure has an increased thickness and larger

moment of inertia, to reduce the effect of combined bending. There are some disadvantages of composites, though, which include higher production and tooling costs, although the actual processing of the complex parts in one piece is much easier [8]. Also, by using composites as the materials for these beams, the resultant reduction in weight can lead to less fuel consumption.

CHAPTER 2

LITERATURE REVIEW

Over the past several decades, the importance of crashworthiness has been growing in virtually every transportation sector. Newer designs are proposed every day to improve the crashworthiness of a structure. There are constant efforts, in the field of crashworthiness, to reduce the injuries sustained by vehicle occupants. It is preferable to design a vehicle to collapse in a controlled manner, thereby ensuring the safe dissipation of kinetic energy, and limiting the seriousness of injuries incurred by the occupants [2].

The use of composites, as discussed earlier, has increased dramatically over the last few decades. Fiber-reinforced composite sandwich structures are characterized by specific stiffness and strength, exceeding that of similar metal structures. With emphasis on light-weight vehicles, the use of composite materials in aerospace and automotive structures has created a need to further understand the energy-absorption characteristics of composite materials.

2.1 Composites in Automobile Parts

Due to increasing legal and market demands for safety, the weight of the car body will most likely increase in the future. At the same time, environmental demands will become stronger and lower weight will play an important part in meeting them [2]. In the European Union, car manufacturers have agreed to an overall 25% increase in fuel efficiency by the year 2010, over 1990 figures [2]. Fuel efficiency of the vehicle directly depends on the weight of the vehicle [2]. The carbon fiber composite body structure is 57% lighter than steel structure of the same size, and provides superior crash protection,

improved stiffness, and favorable thermal and acoustic properties [2]. Composite materials may be used in the automotive industry as a means of increasing fuel efficiency [2]. With 75% of fuel consumption relating directly to vehicle weight, the automotive industry can expect an impressive 6 to 8% improvement in fuel usage with a mere 10% reduction in vehicle weight. This translates into a reduction of approximately 20 kilograms of carbon dioxide per kilogram of weight reduction, over the vehicle's lifetime.

Fiber Reinforced Polymers (FRP's) were introduced to Formula-1 racecars for the first time by the McLaren team. Since then, the crashworthiness of racing cars has improved beyond all recognition [2]. Carbon fiber composite has been used to manufacture the car body, giving it low weight, high rigidity and providing high crash safety standards. Reports from the United States and Canada predicted that plastics and composites would be widely used in body panels, bumper systems, flexible components, trims, and drive shaft and transport parts of cars [2]. In addition, rotors manufactured using RTM (Resin Transfer Moldings) for air compressors or superchargers of cars have been used to substitute for metal rotors, which are difficult to machine [2].

2.2. Definition of Sandwich Structures

A sandwich structure is a special form of laminated composites. A typical sandwich structure consists of two thin, high-strength face sheets bonded to a thick, light-weight core, as shown in Figure 2.1. Face sheets are rigid and the core is relatively weak and flexible, but when combined in a sandwich panel they produce a structure that is stiff, strong, and lightweight [2]. In structural sandwiches, face sheets are mostly identical in material and thickness, and they primarily resist in-plane and bending loads. These structures are called symmetric sandwich structures.

However, in some special cases, face sheets may vary in thickness or material because of different loading conditions or working environment. This configuration is known as ‘asymmetric sandwich structures’ [10].

d= width of sandwich panel,

t= thickness of face sheet,

b= width of sandwich panel

c= core thickness

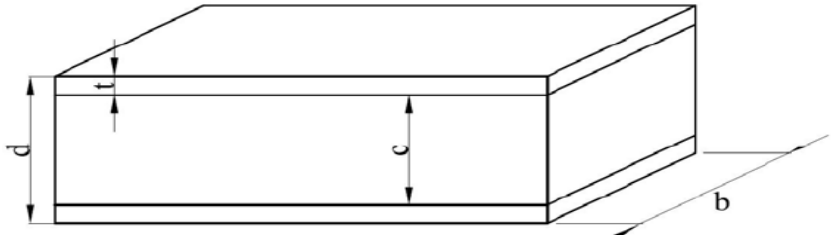

Figure 2.1 Sandwich structure construction [10].

In general, sandwich structures are symmetric; the variety of sandwich constructions basically depends on the configuration of the core [10, 11]. The core of a sandwich structure can be almost any material or architecture, but usually they are classified into four types: foam or solid core, honeycomb core, web core, and corrugated or truss core. The adhesion of face sheets and core is another important criterion for load transfer, and for the functioning of the sandwich structure as a whole [11].

The basic concept of a sandwich structure is that the face sheets carry the bending loads, while the core carries the shear loads. The face sheets are strong and stiff in tension and compression, compared to the low-density core material. The core material’s primary purpose is to keep the face sheets separated in order to maintain a high section modulus

(a high “moment of inertia” or “second moment of the area”) [11].The core material has relatively low density (e.g., honeycomb or foam), which results in high specific mechanical properties - in particular, high flexural strength and stiffness properties relative to the overall panel density [11]. Therefore, sandwich panels are efficient in carrying bending loads. Additionally, they provide increased buckling resistance to shear panels and compression members.

Sandwich structures should be designed to meet basic structural criteria. For instance, the face sheets should be thick enough to withstand tensile, compressive and shear stresses. The core should have sufficient strength to withstand shear stresses induced by design loads [7]. Adhesive must have adequate strength to carry shear stress into the core. The core should be thick enough, and have enough shear modulus, to prevent overall buckling of the sandwich under load, preventing crimping [7]. Compressive modulus of the core and face sheets should be sufficient to prevent wrinkling of the face sheets under design load [10]. The core should have sufficient compressive strength to resist crushing design loads acting normal to the panel face sheets, or by compressive stresses induced through flexure. The sandwich structure should have sufficient flexural and shear rigidity to avoid unnecessary deflections under design load [10]. In order to sustain these criteria, sandwich structures may also be produced as complex structures. These complex structures would include localized reinforcements in the form of FRP tubes, cones, or corrugation connecting the external face plates [10].

2.3 Application Areas of Sandwich Structures

The use of composite sandwich structures in aeronautical, automotive, aerospace, marine, and civil engineering applications is growing. This is because these structures have excellent stiffness to weight ratios, leading to weight reduction and decreased fuel consumption. Also, they have high structural crashworthiness, because they are capable of absorbing large amounts of energy in a sudden collision [10]. Figure 2.2 shows various application parts in automobiles. Different combinations of core and face sheet materials are being studied by researchers worldwide, in order to achieve improved crashworthiness [10]. In aerospace applications, various honeycomb-cored sandwich structures were used for space shuttle constructions. They are also used for both military and commercial aircraft. For more than 20 years, both the U.S. Navy and the Royal Swedish Navy have used honeycomb sandwich bulkheads to reduce ship weight and to withstand underwater explosions [10].

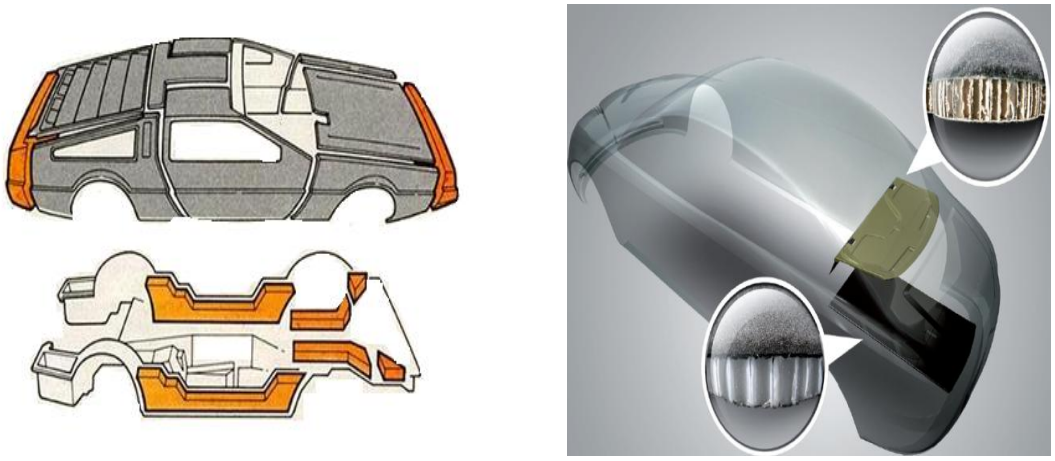

Figure 2.2 Sandwich material application in different car parts [11]

Sandwich material is being used in locomotives, to help resist pressure waves that occur when high-speed trains pass one another in tunnels [12]. More recently, sandwich

constructions are being used in civil engineering projects such as bridge decks, and wall and roof claddings for buildings, because of their low cost and thermal performance. Also, railcars for rapid transit trains, buses, sailboats, racing boats, race cars, snow skis, water skis, and canoes are all employing sandwich constructions [12].

2.4 Constituents of aSandwich Structure

There are various types of face sheet and core materials, with every different combination of these components resulting in sandwich constructions having different mechanical behaviors. It is important to produce a sandwich structure having required properties according to the working environment. In order to employ the proper components, the following conditions must be satisfied [10]:

- Determination of the absolute minimum weight for a given structural geometry, loading, and material system.
- Comparison of one type of sandwich construction with others.
- Comparison of the best sandwich construction, with alternative structural configurations (monocoque, rib-reinforced, etc.).
- Selection of the best face sheet and core materials in order to minimize structural weight.
- Selection of the best stacking sequence for faces composed of laminated composite materials.
- Comparison of the optimum construction weight with weights required by some restrictions; i.e., the weight penalty due to restrictions of cost, minimum gage, manufacturing, material availability, etc.

2.4.1 Face sheet material

In a sandwich structure, the face sheet can be made of many different materials. It can be isotropic monologue material, anisotropic monologue material, or a composite material [12]. Aluminum, fiberglass, graphite, and aramid are the widely used face sheet materials. However, in order to minimize the weight of the structure, composite face sheets are generally preferred [12].

2.4.2 Composite face sheets

Available composite face sheet thicknesses range from 0.152mm to 2.2 mm, according to the design specifications. Design flexibility is an advantage for the manufacturer, because unnecessary material can be removed from areas with little stress, and unnecessary weight can be decreased [10]. Composite materials have superior resistance to most environments, and they can be used by most individuals without a major investment in equipment [12]. The purpose or use of the composite material must be clear, in order to select proper constituent matrix material and reinforcement. In composites, the fiber is used to carry the load exerted on the composite structure. It also provides stiffness, strength, thermal stability, and other structural properties to the face sheet. Matrix material carries out several functions in a composite structure. These include binding the fibers together and transferring the load to the fibers. Matrix material protects reinforcing fibers from chemical attack, mechanical damage, and other environmental effects like moisture, humidity, etc [10].

2.4.3 Face sheet matrix material

The mechanical performance and durability of polymer-matrix based composite laminates is strongly linked to the mechanical performance of the matrix. Polymers

behave as viscoelastic or viscoplastic solids, depending on strain and stress rate at room temperature. Creep and stress relaxation are other consequences which have to be taken into account during the design phase.

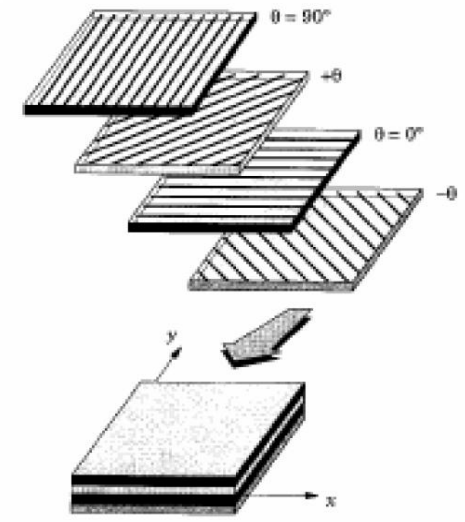

Figure 2.3 FRP composite plies in different orientations [10]

The combined effects of creep, fatigue, moisture, and temperature on mechanical properties, and the time to failure are very complex and still under research [8]. The viscoelastic properties of materials can be expected to depend on temperature, as well as time. Moisture acts on the polymeric matrix as a plasticizer, lowering the glass transition temperature. Also, moisture changes the time-dependent mechanical response. Therefore, composite material options must be considered carefully [10].

There are two main types of resins; they are thermosetting and thermoplastic resins. Epoxy, unsaturated polyester, and vinyl ester are the most widely used thermosetting resins. A wide range of physical and mechanical properties can be obtained by employing these resins. The formation of rigid solid from liquid resin is done while the composite is being manufactured. Figure 2.3 shows ply orientation during the

construction of solid laminate, face sheet for a sandwich panel. In Figure 2.3, the horizontal, vertical, and inclined lines on the four layers show how fiber orientation changes depending on the angle of cut, during sandwich panel construction.

The mechanical properties of the resin depend on both the resin chemical and curing chemical. The resin chemical controls the mechanical properties, while the curing chemical controls the density and the length of the formed network. Curing is generally completed through a schedule involving heating, and keeping the resin to one or more levels of temperature at prescribed times. This way, the optimum cross-linking and optimum resin properties can be achieved. When compared to thermoplastics, it can be easily seen that thermoplastics can undergo plastic deformation, while thermosets are brittle. However, thermosets have different properties when compared to each other [10]. For example, epoxies are generally tougher than unsaturated polyesters or vinyl esters. Also, epoxies have good resistance to heat distortion and they shrink less during curing, compared to polyester. In fact, epoxy resins are better in most properties than other thermosetting resins. Epoxy is used in weight critical, high strength, and dimensionally accurate [12] applications. Polyester resins are less expensive, offer more corrosion resistance, and are more forgiving than epoxies [12]. For this reason, they are the most widely used [10].

2.4.4 Face sheet reinforcement material

The physical properties of composites are fiber dominant [12]. When resin and fiber are combined, their performance remains most like the individual fiber properties [13]. For this reason, fabric selection is critical when designing composite structures [13]. There are many reinforcement materials available to use in matrix systems, but all

reinforcement materials have high stiffness and relatively low density, with numerous types and styles. Glass, carbon, and aramid fibers are widely used in polymer matrix composites. Glass fibers are based on silica (SiO2) with additions of calcium, boron, sodium, iron, or aluminum oxides. E-glass (E meaning electrical) is the most commonly used glass fiber since it has good strength, stiffness, electrical, and weathering properties [10]. C-glass (C meaning corrosion) is employed where more resistance to corrosion with respect to E-glass is needed, but C-glass has lower strength. For applications where higher strength than E-glass is needed, S-glass (S meaning strength) is used as reinforcement material. S-glass has higher Young's modulus and temperature resistance compared to E-glass. Glass fibers are produced by the mechanical drawing of the flow of melted raw materials, using the gravity. The control of the diameter of the glass is possible by controlling different parameters like the head level of the melted glass in the tank, the viscosity of the glass, and the diameter of the holes that the raw material is drawn through. The diameter of the E-glass is generally from 8-15 μm.

Carbon fiber is a modern reinforcement characterized by extremely low weight [13], high tensile strength, and high stiffness. The material handling is easy, and it can be molded like fiberglass. However, some advanced techniques are necessary to attain the maximum properties of this material [13]. Carbon fiber is also the most expensive of the reinforcing fibers [13]. This fact often limits its use. Carbon fibers consist of small crystallites of graphite, and are generally about 8 μm in diameter. Aramid fibers are developed from aromatic polyamides, and they form the most important high modulus polymer fiber group [10]. Aramid fibers were first developed by Du Pont under the trade name Kevlar™. Kevlar exhibits the lowest density of any fiber reinforcement, high

tensile strength for its weight, and superior toughness. It is priced between fiberglass and carbon fiber [13]. Kevlar is puncture and abrasion resistant, making it the reinforcement of choice for canoes, kayaks [13], and leading edges of airfoils. On the other hand, Kevlar is difficult to cut and machine during part fabrication. It also has a low service temperature and poor compressive properties [13]. It is possible to unite Kevlar with other materials, creating a hybrid [13] laminate which can compensate for its shortcomings.

2.5 Core Materials

The other main component of composite sandwich structures is the core material. For all sandwich structures, both in-plane and bending loads are carried by the face sheets, and the core carries transverse shear loads. Usually the face sheets are identical in material and thickness. The variety in the types of sandwich constructions basically depends upon the configuration of the core. To maintain the effectiveness of the sandwich structure, the core must be strong enough to withstand the compressive, or crushing, load placed on the panel. The core must also resist the shear forces involved. If the core collapses, the mechanical stiffness advantage is lost. Core densities range from 16kg/m3 to 900kg/m3 [10]. The core materials are generally divided into four types. These are foam or solid core, honeycomb core, web core, and corrugated or truss core. Foam or solid cores are relatively inexpensive, and can consist of balsa wood and an almost infinite selection of foam/plastic materials, with a wide variety of densities and shear moduli [12].

There are various types of foam cores, and one of them, vinyl sheet foam, is probably the most versatile core material on the market. It is a rigid, closed-cell material

that resists hydrocarbons, sea water, gasoline, and diesel oil. It has been used extensively in aircraft and performance automotive structures, but it can be applied anywhere that high properties and easy handling are needed. Vinyl foam can be thermoformed in an oven or with a heat gun while applying gentle pressure. Another foam type is polyurethane foam which is a rigid, closed-cell material with excellent thermal insulation and flotation properties. This core has been widely used in the marine industry for decades, and is fairly inexpensive when a lower property cored laminate is needed. It is compatible with both polyester and epoxy resin systems [12].

It is assumed that in sandwich structures having foam or honeycomb core, all of the primary loading is carried by the face sheets. However, in web or truss-cored structures, a portion of the primary load is carried by the core. There may be many other core architectures in addition to those mentioned above. For example, recent studies propose sandwich structures having composite vertical laminate-reinforced foam [12].

CHAPTER 3

OBJECTIVE AND METHODOLOGY

3.1 Objective

The main aim of this study is to model and analyze the current and a new composite bumper for a Ford Taurus front vechicle. This analysis shell be done using a foam-cored sandwich beam which performs better than the existing bumper, thus reducing the injuries sustained by the occupant. Efforts are made to reduce the weight of the new design, without sacrificing the safety of the occupant. This is done in accordance with crashworthiness standards, which require minimal progressive crushing and higher kinetic energy absorption.

There are several areas of crash-impact dynamics that need to be considered, in order to improve the crashworthy design of the front bumper. So far, there have been many contributions toward understanding and analyzing the energy absorption characteristics of composites. In this study, FEM is used as an alternative method in studying the energy absorption of a front bumper. In addition, one can try to actually understand the behavior by conducting full-size crash simulations. This is the best possible method, but this is, again, a quite expensive method and can provide information for only a few limited impact conditions and designs.

3.2 Methodology

In this study, an attempt is made to design an efficient, energy-absorbing car front bumper structure, and compare the testing and analysis results with the existing front bumper. The new material modification is then evaluated, noting its efficiency in impact

energy absorption and reduction of the injuries sustained by occupant. To evaluate occupant injuries sustained due to the replacement of the existing front bumper with sandwich beam material, a frontal impact sled test is performed. The sled test considers the acceleration pulse obtained, due to frontal impact of the sandwich beamed car front bumper at 35 mph. Finally, a comparison is made between the original and the new front bumper. The Figure 3.1 flow chart below, describes the sequence of steps followed during this research in the form of a flow chart.

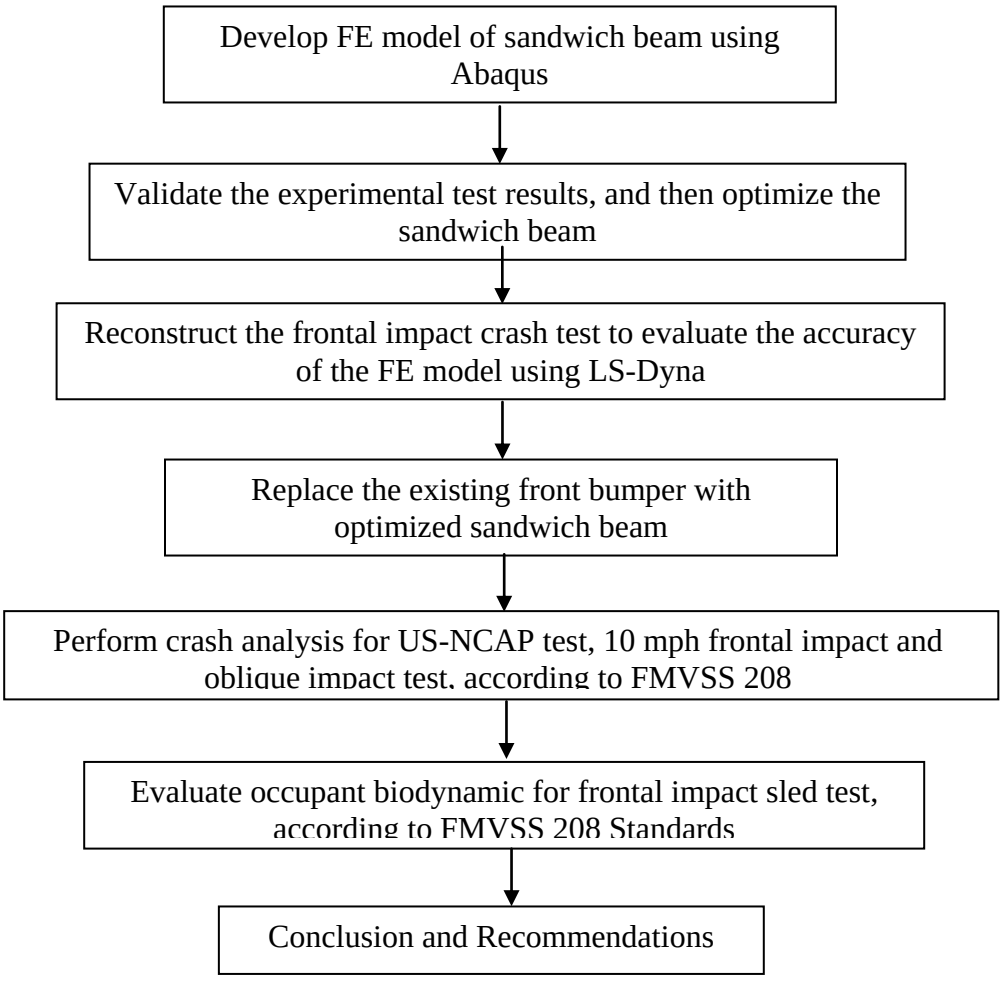

Figure 3.1 Methodology

From Figure 3.1, the methodology carried out in this research is depicted in the following steps.

- This research work starts with FE modeling of the composite sandwich beam, using CAE software, Abaqus.

- FE analysis is performed to validate the experimental test results. Once a good correlation is obtained between tested data and FE analysis, optimization of sandwich beam is done.

- Optimization of sandwich beam is accomplished by increasing the number of plies and including more angled plies.

- Optimization of sandwich beam is carried out to meet the design and specific strength requirements of the existing car front bumper.

- Reconstruction of the Ford Taurus frontal impact crash event is performed to evaluate the accuracy of the FE model using LS-Dyna.

- Optimized sandwich beam replaces the existing front bumper, and again the frontal impact crash analysis is carried out to know the performance of the new design in a crash event.

- To find the performance of the new design in a car-to-car oblique impact and its deformation at low speeds, a crash analysis is performed at 35 mph, at 45 degrees angle impact, and 10 mph full-width frontal crash against a rigid barrier.

- Occupant dynamic response is performed using seat belt restrained frontal impact sled test, with acceleration pulse recorded from frontal impact with new design.

- Occupant response and injury levels are compared, using test results from the actual front bumper and the newly developed sandwich material.

- Conclusions and the further work recommendations are made.

CHAPTER 4

FINITE ELEMENT MODELING AND ANALYSIS TOOLS

The advantages of FEA are numerous and important. A new design concept may be modeled to determine its real-world behavior under various load environments. Based on results of the modeling, it may be refined prior to the creation of drawings, when few dollars have been committed, and changes are inexpensive [2]. Once a detailed CAD model has been developed, FEA can then analyze the design in detail, saving time and money by reducing the number of prototypes required. An existing product which is experiencing a field problem, or is simply being improved, can be analyzed to speed up an engineering change and reduce its cost. Finite element analysis is used to break a large stress analysis problem into many smaller ones, which are then collectively solved by computer [2].

The explicit finite element software codes of LS-Dyna, MSC Dytran, and Pam-crash are commercial tools employed within various engineering industries. Both the aerospace and automotive industries have accepted simulations as part of the design process, to minimize design codes and create structures that are more efficient. Prototyping and testing are always performed to verify the design [2].

When considering structural analysis applications, implicit FE methods can be used in static and dynamic analyses, where linear and nonlinear effects are to be investigated. The tools used in this study are briefly explained below.

4.1 Hypermesh

Hypermesh is a versatile software that deals with design and finite element analysis. It is a finite element modeler used to perform a variety of CAD and CAE tasks including modeling, meshing, and post processing for FEM solvers LS-Dyna, Nastran, Abaqus, etc. Hypermesh provides direct access to geometry from the world's leading CAD systems and standards. Using sophisticated geometry access tools, Hypermesh addresses many of the traditional barriers to shared geometry, including topological incompatibilities, solid body healing, mixed tolerances, and others [2].

Hypermesh provides an open, integrated, CAE environment for multidisciplinary design analysis. This feature can be used to simulate product performance and manufacturing process early in the design-to-manufacture process. This has the ability to import geometry from any CAD system, and various data exchange standards. Powerful and flexible meshing is available, with capabilities that range from fully automatic solid meshing to detailed node and element editing. Loads and boundary conditions can vary, and may be associated with the design geometry or with the analysis model [2].

The resulting visualization tools enable identification of critical information, including minimums, maximums, trends, and correlations. Iso-surfaces and other advanced visualization tools help to speed and improve the results evaluation. In this study, hypermesh has been used to model the sandwich beam. The mesh needed for FEA is generated by this software. The major part of this study involves modeling the composite sandwich beam, and it is meshed using hypermesh. This serves as a very helpful tool in modeling [2].

4.2 Abaqus

The Abaqus FEA product offers powerful and complete solutions for both routine and sophisticated engineering problems, covering a vast spectrum of industrial applications. In the automotive industry, engineering work groups are able to consider full vehicle loads, dynamic vibration, multi-body systems, impact/crash, nonlinear static, thermal coupling, and acoustic-structural coupling using a common model data structure and integrated solver technology [9].

Abaqus FEA provides the most complete and flexible solution to get the job done. The software suite delivers accurate, robust, high-performance solutions for challenging nonlinear problems, large-scale linear dynamics applications, and routine design simulations. Its unmatched integration of implicit and explicit FEA capabilities enables researchers to use the results of one simulation directly in a subsequent analysis. This could include capturing the effects of prior history, such as manufacturing processes on product performance. User programmable features, scripting, and GUI customization features allow proven methods to be captured and deployed, enabling more design alternatives to be analyzed in less time [9].

Abaqus FEA takes advantage of the latest high-performance parallel computing environments, allowing you to include details in your models previously excluded due to computing limitations. This allows you to minimize assumptions, while reducing turnaround time for high-fidelity results.

CHAPTER 5

MODEL VALIDATION AND OPTIMIZATION

As stated earlier, the objective of this research work is to develop a structural component that can absorb high kinetic energy during a frontal crash, while also focusing on reducing vehicle occupant injury severity. For this we have selected composite sandwich material, where the core material is polyvinylchloride foam core, and the face sheets are carbon/epoxy laminates [5]. According to the sandwich concept, the face sheets form the stress couple countering the external bending moments. We have selected this combination because of its higher strength and very high energy absorption, qualities that have been proven by the research done on composite material in the past few decades [14].

In the present material validation procedure, an FE model of the sandwich beam is developed using Abaqus/Standard Finite Element software code. It is validated through experimental test results, and observations of nonlinear mechanical behavior of foam core polymer composite sandwich beams, when subjected to sudden impact loading.

5.1 FE Modeling of the Sandwich Beam

The skin used for modeling the sandwich beam is made from four plies of carbon /epoxy uni-directional pre-preg (300 gsm per layer). Each ply thickness is 0.152mm, and the orientation used is cross-ply from (0,90,0,90), giving a total skin area density of 1200 gsm and total thickness of 0.608. The core was constructed from foams made by Divinycell H200. It has a density of 200 kg m^{-3}, as denser foams are used for highly loaded areas, which has been observed from past research. The dimensions of the

sandwich beam modeled, is shown in Figure 5.1. The FE model is developed using the shell element S4R for face sheet, and the solid elements C3D8 for core. Element size used is 4mm for both face sheet and core [7]. The Figure5.2 shows the experimental setup of three-point bending of sandwich beam, under static loading.

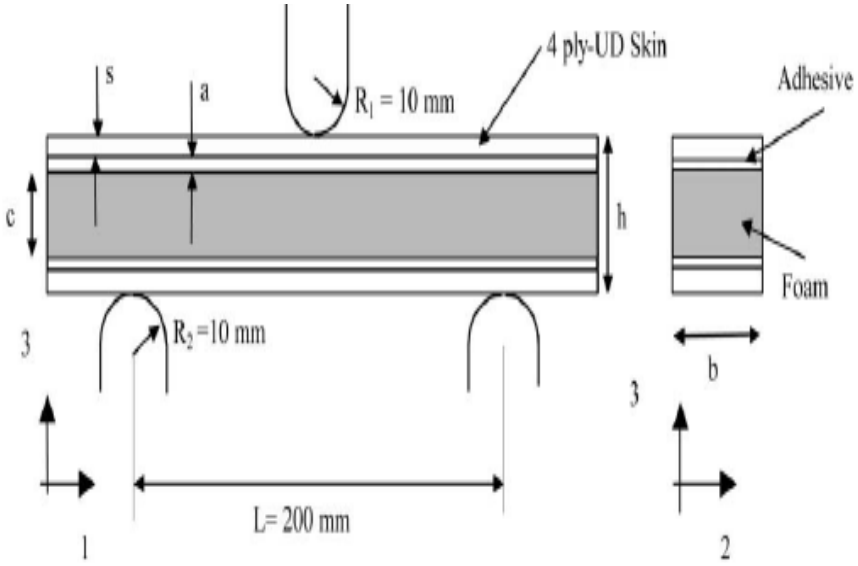

Figure 5.1 Experimental setup for three-point bending test [5]

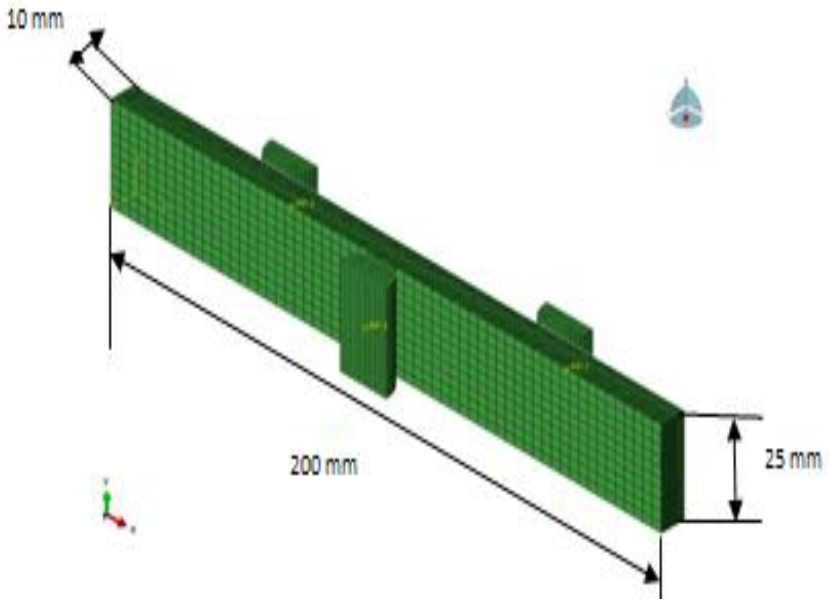

Figure 5.2 FE model reconstructed in Abaqus

Abaqus, a widely used non-linear finite element code and standard implicit version, is used for modeling the sandwich beam. Figure 5.2 shows the finite mesh generated using Abaqus. The skin is modeled as a solid laminate of four plies using S4R shell element, and the core is modeled as a solid element, using C3D8 which is used in the contact analysis problems. The thickness of the beam is 10 mm and the width is 25 mm. A mesh sensitivity study was conducted with respect to the number of elements and the bias ratio, to ensure that the mesh was fine enough to give reliable results. The study suggests that 10 elements through its depth, with 1200 elements along the face sheet and the core surface gives better results. Simple supports for the sandwich beam are modeled, using rigid solid elements as shown in Figure 5.3. The contact between the face sheet and the indenter were defined using element-based surface-to-surface contact. Contact between the foam and the face sheet were defined using the node-to-node based tie contact option in Abaqus.

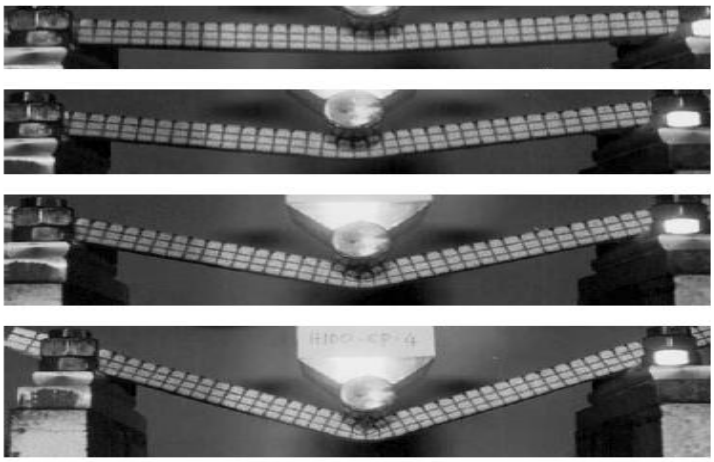

Figure 5.3 Three-point bending test of sandwich beam [5]

The rigid supports used at the bottom of the sandwich beam are constrained with respect to the rigid node created at the center of each support, modeled using solid elements. This node is constrained in all degrees of freedom, and the contact between the

support and the bottom face sheet outer layer is defined using surface-to-surface contact. The indenter is constrained in five degrees of freedom; expect y-translation in y-direction. Contact between the outer surface of the top sheet and the indenter is defined using surface-to-surface contact. Displacement for the indenter is given using time displacement curve over a time of 0.6 sec, and the history output and field output were defined to post-process the analysis results.

5.2 Skin Failure Model

During FE modeling of the skin, the main focus was on damage initiation due to failure. As observed from the experimental test results, failure is initiated through the top face sheet failure. When investigating failure modes in FRP composite material, there exists a great number of material failures theories for laminated composite. The relevance of a given failure theory is dependent on the type of composite, the structural configuration, and mode of loading. Also of importance is the extent of material property data required to input into the model. The skin construction was cross-ply, and the mode of loading was simple beam bending, with loading introduced as a point line load. Inspection of the experimental beam failure mode, suggested that upper skin failure was controlled by strain along the beam. So it is decided to use the maximum strain criterion for skin failure. In order to raise the issue concerning the modes of laminate failure in three dimensional effects, we have used the Hashin Failure Theory, since it depends on the type of composite, structural configuration, and mode of loading. Hashin has identified four lamina failure modes namely fiber tension, fiber compression, matrix tension, and matrix compression [7]. Failure is expressed in terms of stress for three-

dimensional cases [7]. Equations used to model the failure criteria are shown in Figure 5.4.

Fibre tension failure:

$$\left(\frac{\sigma_{11}}{\sigma_A^+}\right)^2 + \frac{1}{\tau_A^2}\left(\sigma_{12}^2 + \sigma_{13}^2\right) = 1$$

Fibre compression failure:

$$\sigma_{11} = \left(-\sigma_A^-\right)$$

Matrix tension failure:

$$\frac{1}{\sigma_T^{+2}}(\sigma_{22} + \sigma_{33})^2 + \frac{1}{\tau_T^2}\left(\sigma_{23}^2 - \sigma_{22}\sigma_{33}\right) + \frac{1}{\tau_A^2}\left(\sigma_{12}^2 + \sigma_{13}^2\right) = 1$$

Matrix compression failure:

$$\frac{1}{\sigma_T^-}\left(\left(\frac{\sigma_T^-}{2\tau_T}\right)^2 - 1\right)(\sigma_{22} + \sigma_{33}) + \frac{1}{4\tau_T^2}(\sigma_{22} + \sigma_{33})^2 + \frac{1}{\tau_T^2}\left(\sigma_{23}^2 - \sigma_{22}\sigma_{33}\right) + \frac{1}{\tau_A^2}\left(\sigma_{12}^2 + \sigma 1_{13}^2\right) = 1$$

Figure 5.4 Equations used to model the Hashin Laminate Failure criteria [5]

5.3 Foam Crushing Model

The H100 foam core (Divinycell) was modeled as an elastic-plastic material with hardening. In this relation, the crushable foam and crushable foam hardening options in the Abaqus program system were used. The hardening behavior was defined on the basis of the stress-strain curve obtained from uni-axial compression testing, and was used to calibrate the crushable foam hardening material model. For this purpose, characteristic points were selected along the curve [14]. Their coordinates in terms of engineering (nominal) stress σ_{nom} and ε_{nom} were transformed in to true stress σ_{true} and volumetric logarithermic plastic strain ε_v by the equations:

$$\sigma t_{rue} = \sigma_{nom}(1+ \sigma_{nom}) \quad (5.1)$$

$$\varepsilon_{true} = \ln(1+ \varepsilon_{nom}) \quad (5.2)$$

$$\varepsilon_{pl} = \varepsilon_{true} - \sigma_y/E \quad (5.3)$$

$$\varepsilon_v = \ln(1+\varepsilon_{pl}) \quad (5.1)$$

where σ =1.5306, Mpa is uni-axial yield stress, E =35, MPa is Young's modulus. The nominal stress and strain in uni-axial compression are defined as: σ_{nom} =F/A, where F is the compressive force, and A is the cross-section of the cylindrical foam specimen used for uni-axial compression. Large deformations in the three-point test were taken into account via NLGEOM option in Abaqus [14].

Table 5.1 Elastic properties of carbon/epoxy material [5]

E_{11}(Gpa)	E_{22} (Gpa)= E_{33} (Gpa)	G_{12} (Gpa)	G_{13} (Gpa)	G_{23} (Gpa)	$v_{12} = v_{12}$
100	8.11	4.65	4.65	5	0.3

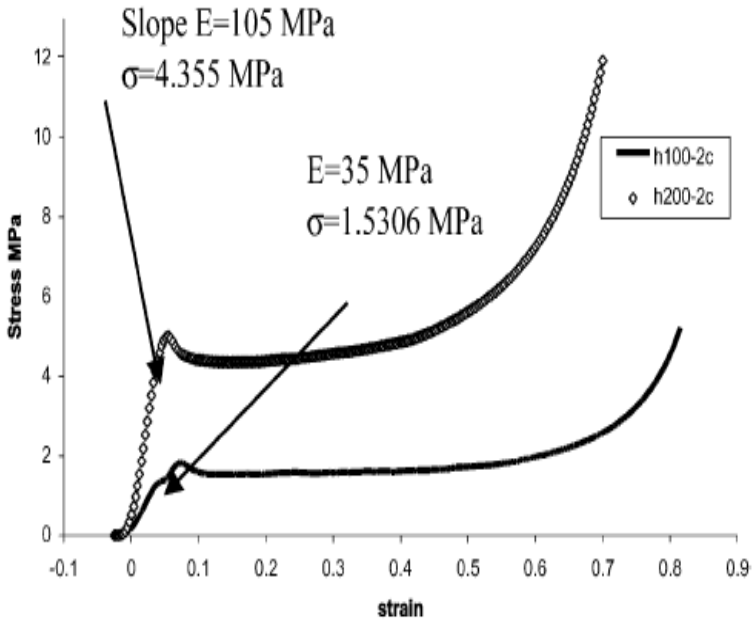

Figure 5.5 Uni-axial compression test true stress and volumetric strain [5]

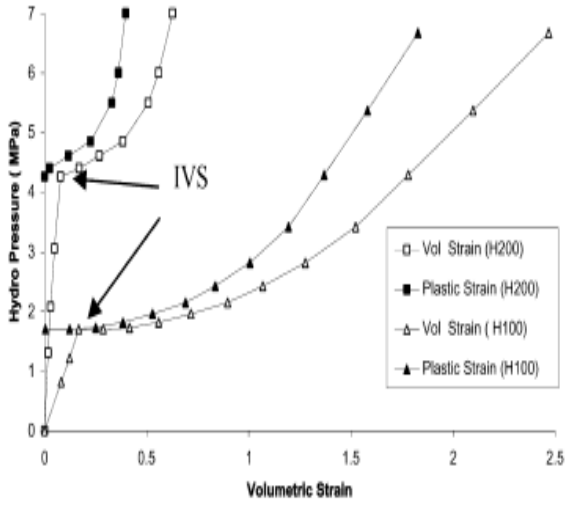

Figure 5.6 Volumetric strain vs. hydro-pressure curve used to define foam in Abaqus [5]

Table 5.2 Hashin failure criteria[7]

X_t (Mpa)	X_c (Mpa)	Y_t (Mpa)	Y_c (Mpa)	S_{12} (Mpa)
2000	1000	100	160	140

Table 5.3 Laminate damage evolution[7]

G_f^t (KJ/m^2)	G_f^c (KJ/m^2)	G_m^t (KJ/m^2)	G_m^c (KJ/m^2)	G_s (KJ/m^2)
100	25	2	2	2

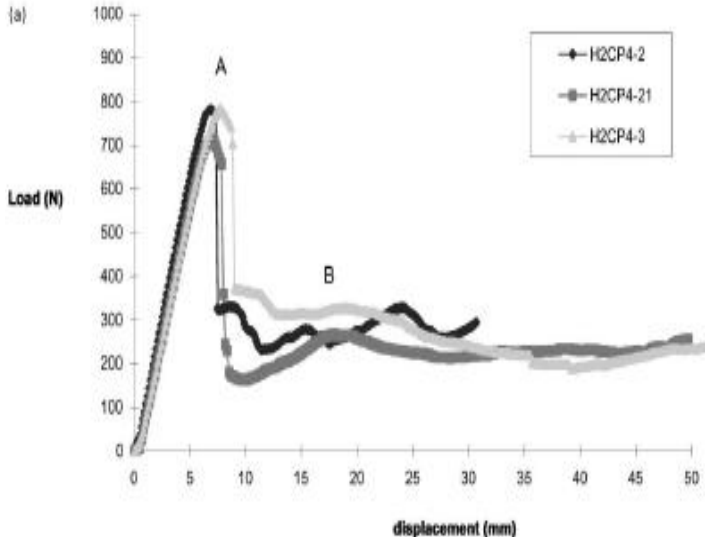

Figure 5.7 Experimental test results [5]

Table 5.4 Mechanical properties of Divinycell foam [5]

Property	H100 Foam
Compression Modulus (Mpa)	35
Poission's ratio	0
Compression Failure (Mpa)	1.53
Initial Volumetric Strain	0.19
Hydrostatic Failure Stress (Mpa)	0.6
Tension Yeild Stress (Mpa)	2.5
Tension Failure Stress (Mpa)	3.2
Shear Yeild Stress (Mpa)	1.35
Shear Failure Stress (Mpa)	1.47
Tension Modulus (Gpa)	120

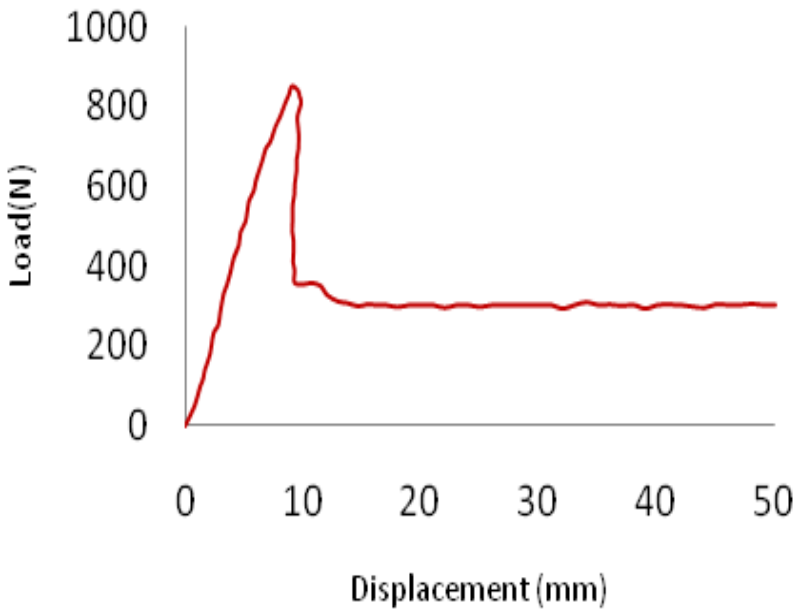

Figure 5.8 Results from FE model reconstructed

Figures 5-5 and 5-6 give the data required for defining the strain hardening of the foam, and Table 5.1 is used to define the elastic properties of the carbon/epoxy material in Abaqus. Tables 5.2 and 5.3 are used to define Hashin failure criteria and damage

initiation. Table 5.4 defines the mechanical properties of Divinycell foam. With all of the elastic properties defined, the material is validated and good correlation between experimental test results and the FE model is achieved. Peak load recorded, and initial failure loads observed, were within the displacement range shown in Figures 5.7 and 5.8. Experimental test result of sandwich beam under static loading is 790 N, and the peak load recorded from the FE analysis is 820 N. This is a 3% error; an error of up to 10% is acceptable while performing FE analysis.

5.4 Optimization

Increasing the thickness of the face sheet by introducing angled plies in the laminate is a method for optimizing sandwich panels. The plies configuration used for optimization is [(0/30/-30/-60/60/90/0/S]. The main reason for optimizing the validated sandwich beam, is to match the energy absorbed by the selected sandwich panel combination with the specific design and strength requirements of the current front beam used in the Ford Taurus. It is important to note here, that only the face sheet thickness is increased; nothing else is changed. The mesh quality has not changed, contact definition between the foam and face sheet is the same, and the indentor and face sheet contact remain unchanged. Here we intend to observe improvement in the performance of the sandwich panel by observbing higher kinetic energy than what was validated initially. Subsequently, it is observed that there is an increase of approximately 900% in the peak lode carried by the optimized sandwich beam. Figure 5.9 shows the load displacement curve profile. By observing the profile, it is evident that the area covered by the load displacement curve is much greater than the area under the curve in Figure 5.8. This proves that the optimized sandwich beam is displaying higher energy absorbtion when

compared to the validated sandwich beam, which is a required strength for the application of high-impact absorbing structures like car front bumpers.

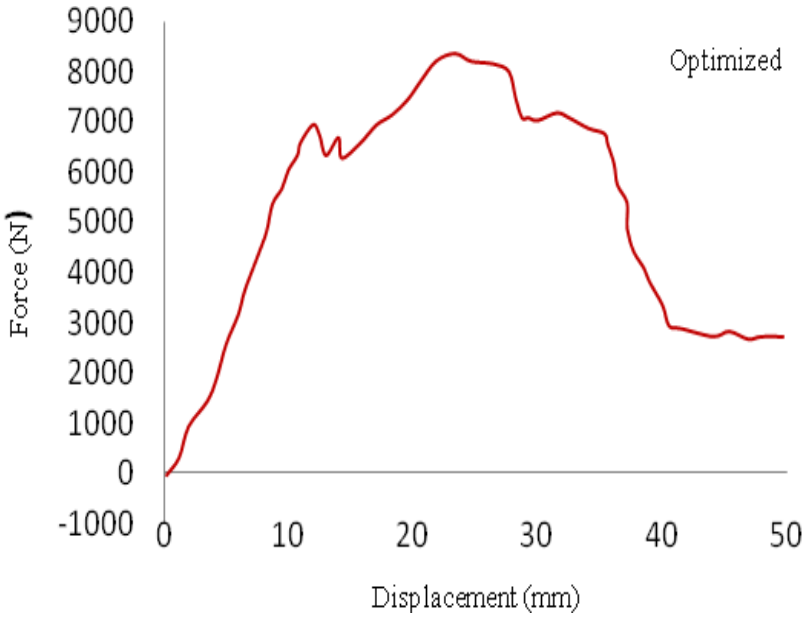

Figure 5.9 Force vs. displacement curve for optimized sandwich beam

The figures below show face sheet failure according to the Hashin failure theory. Figure 5.12 is Hashin failure due to matrix compression, where the top face sheet fails under compressive loads. Hashins failure theory depends on strain energy. Once the elements of the face sheet reach the critical strain energy value defined in the damage evolution criteria mentioned in the Abaqus, the elements start deleting. Figure 5.13 is Matrix failure under tension, where the bottom face sheet stretches with the core material, According to beam theory, the section above the neutral axis fails due to compression, and section below the neutral axis fails due to tension. So, in this test, the bottom face sheet fails in tension. Figure 5.14 is Hashin failure due to fiber under compression, and Figure 5.15 is fiber failure under tension.

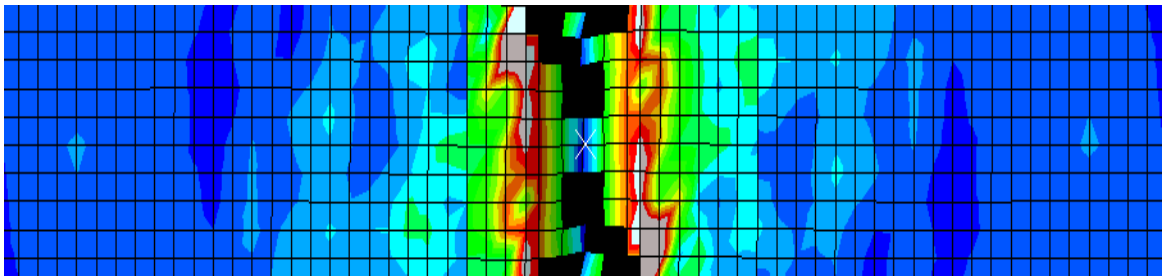

Figure 5.10 Hashin matrix failure in compression

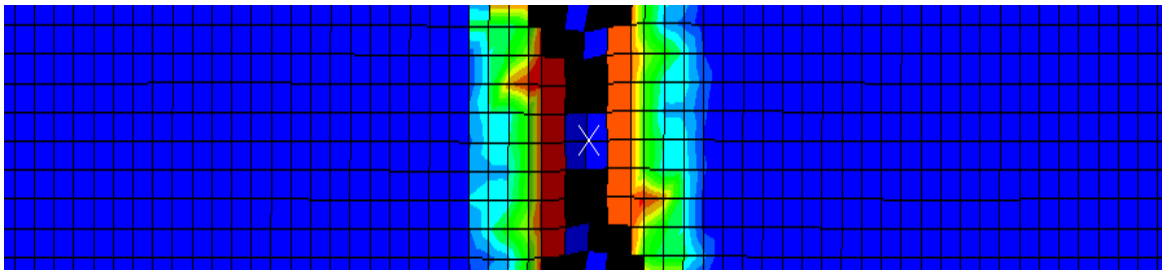

Figure 5.11 Hashin matrix failure in tension

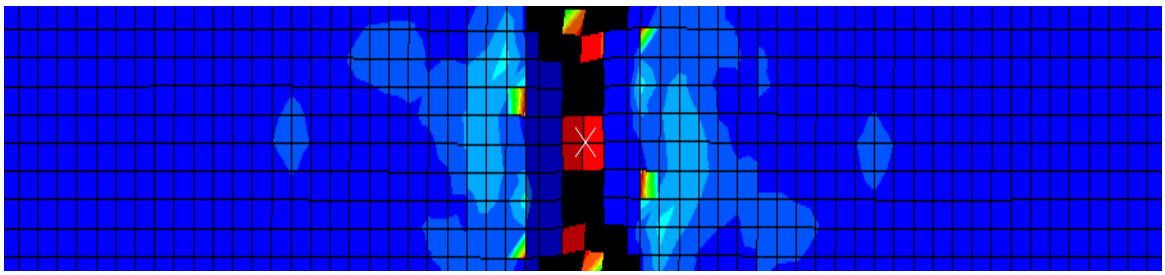

Figure 5.12 Hashin fiber failure in compression

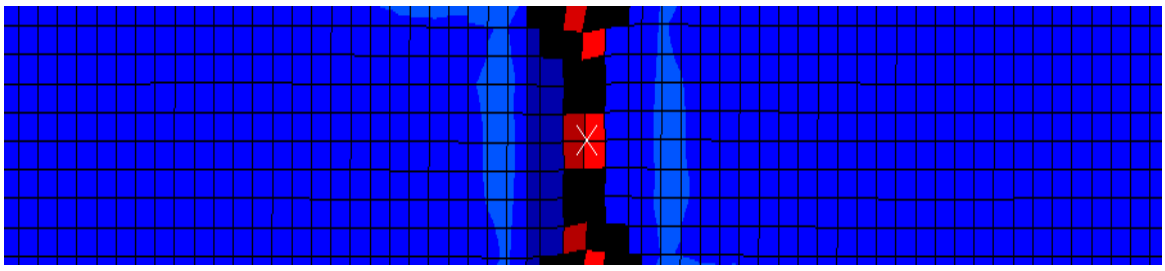

Figure 5.13 Hashin fiber failure in compression

Figures 5.14 through 5.21 show different stages of the simulation representing parameters that were requested while defining the history output in Abaqus.

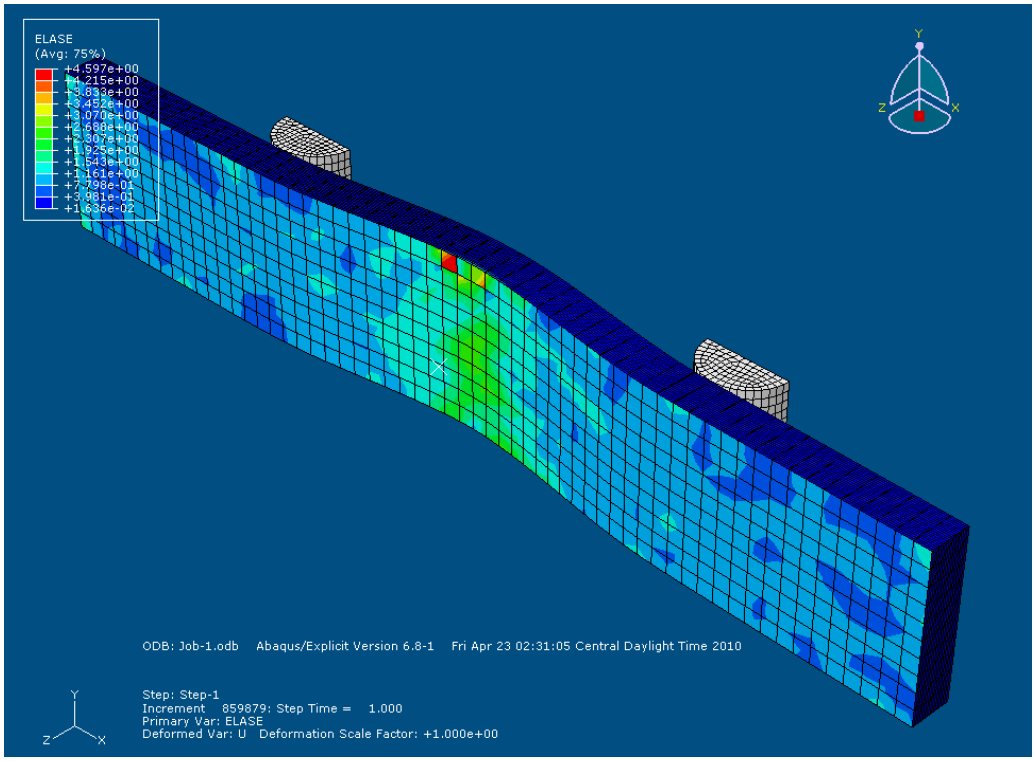

Figure 5.14 Artificial strain energy (hourglass energy)

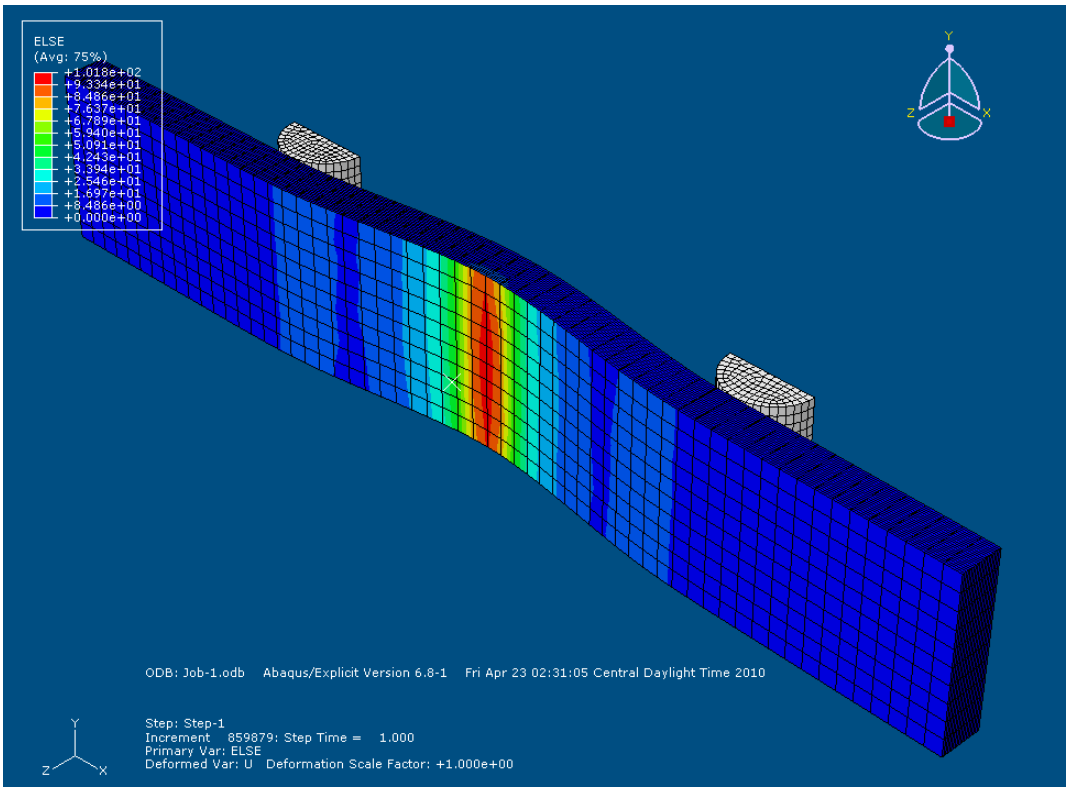

Figure 5.15 Total elastic strain energy

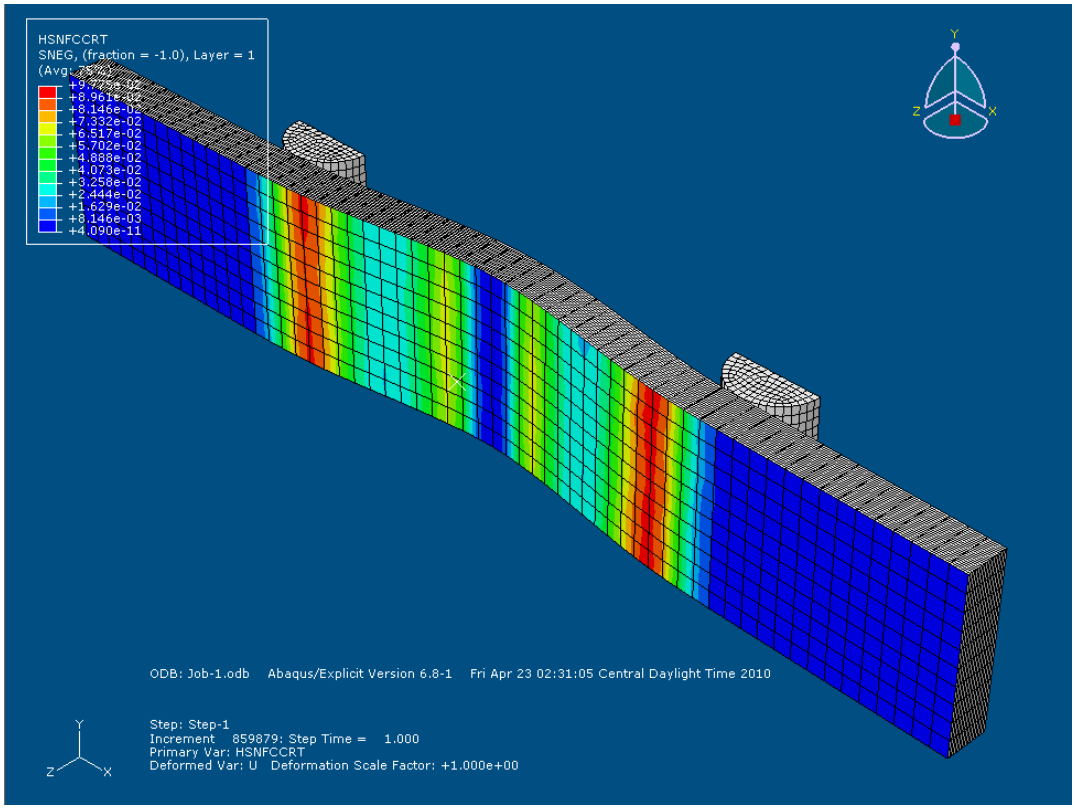

Figure 5.16 Hashin fiber failure in compression

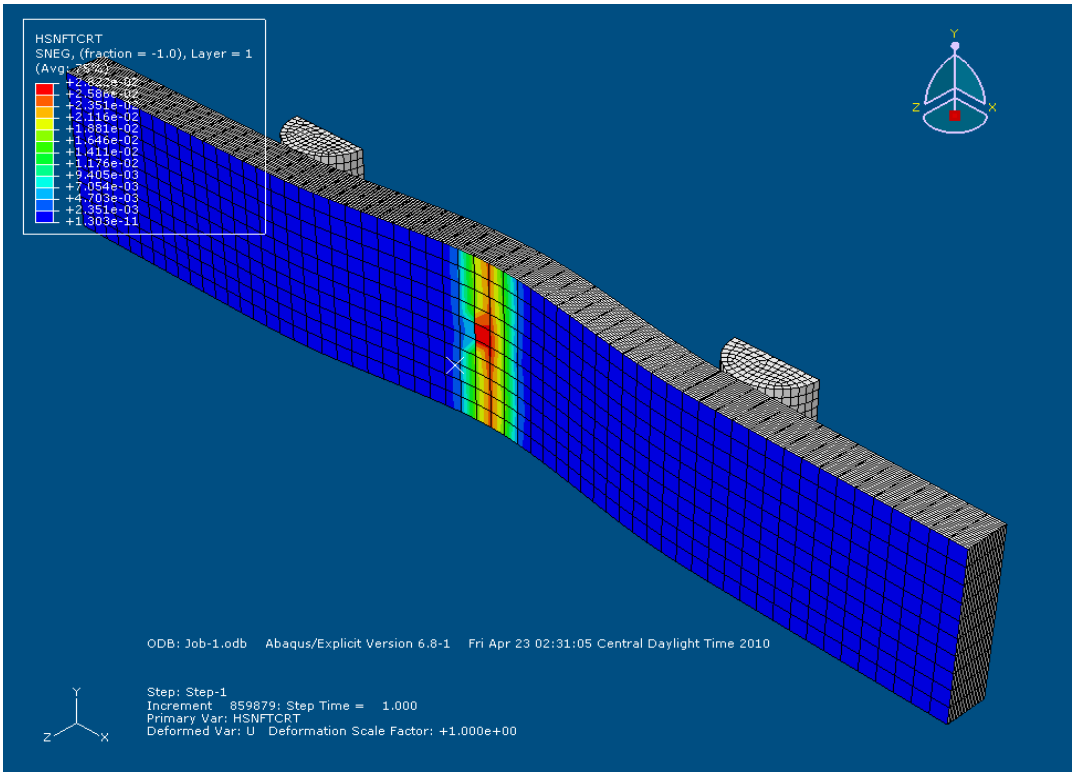

5.17 Hashin fiber failure in tension

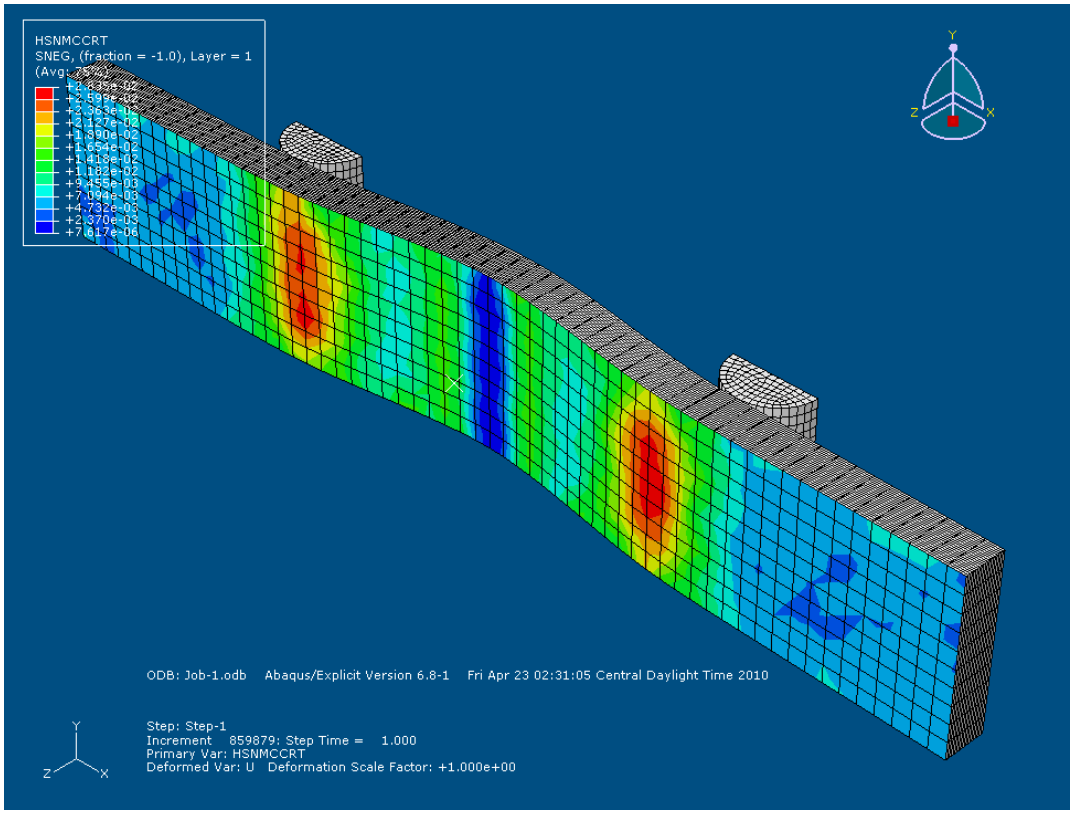

Figure 5.18 Hashin matrix failure in compression

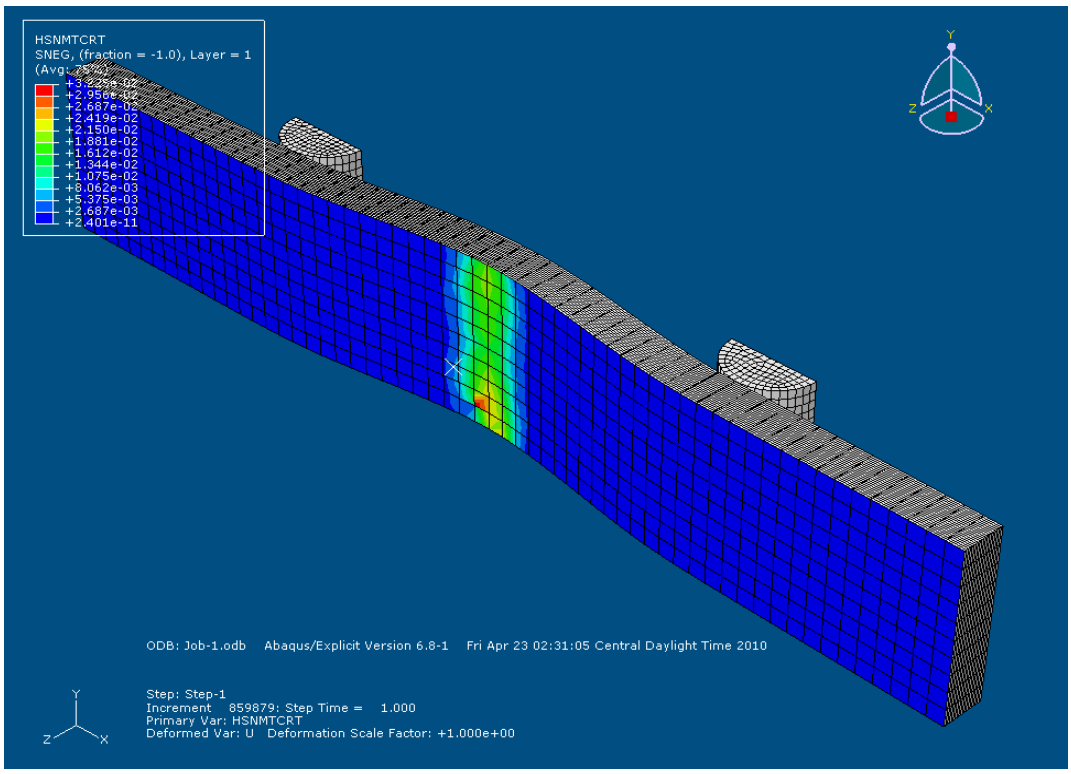

Figure 5.19 Hashin matrix failure in tension

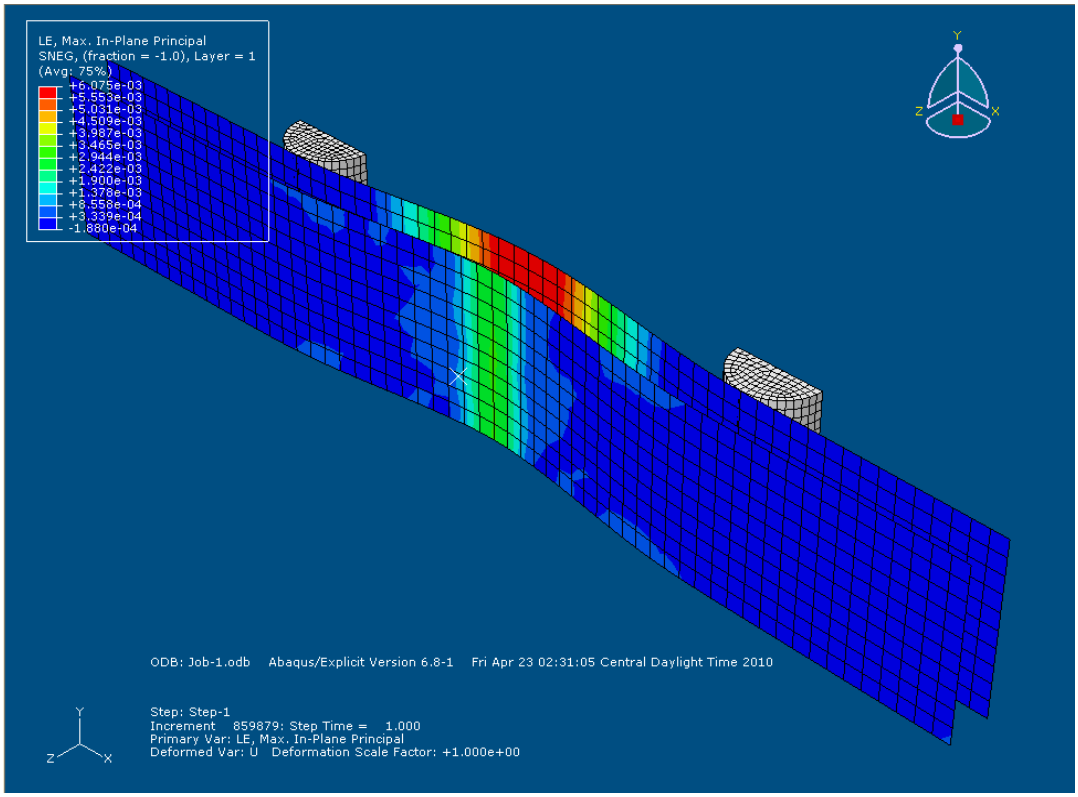

Figure 5.20 Logarithmic strain

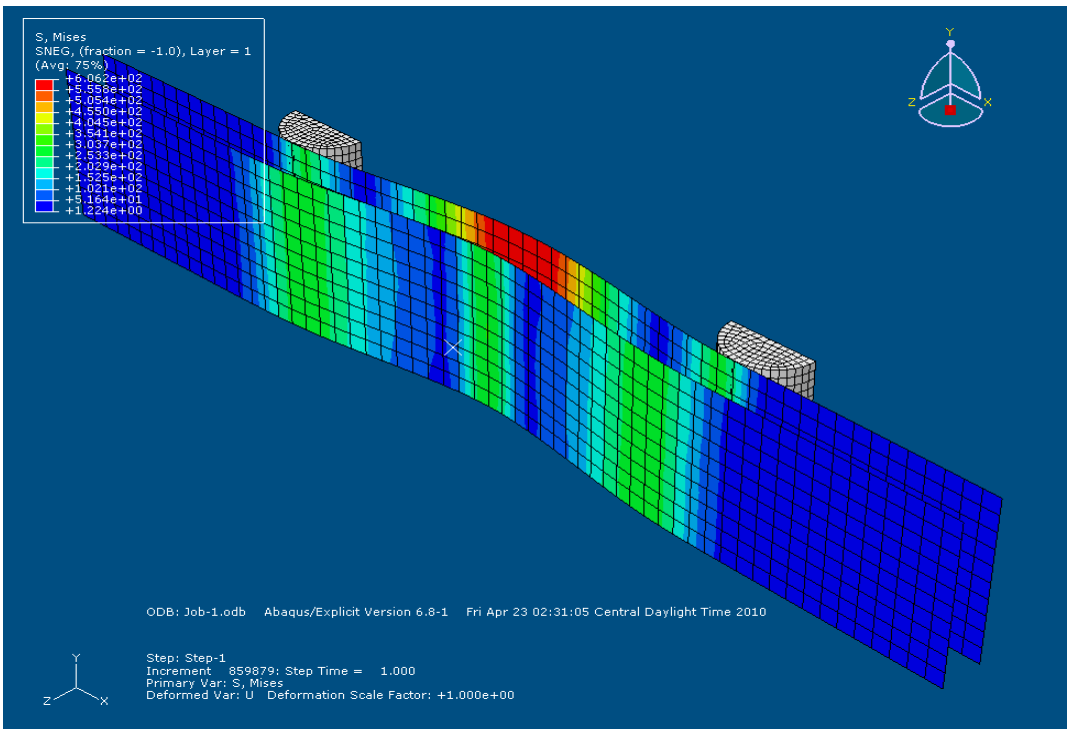

Figure 5.21 Stress distribution

It can be noted from Figures 5.14 through 5.21, that we do not see any face sheet failure criteria, even though we defined the damage evolution criteria while defining the model in Abaqus. The stress distribution and energy levels observed in the face sheet when loaded individually, are much higher than when it is loaded in the combination of H100 foam with the same strain rate, in both cases. We don't see any skin failure in the sandwich beam, because the foam core in the sandwich beam is supporting the top and bottom face sheets when loaded with constant strain rate, and taking the excessive load thereby avoiding complete skin failure. Contours plotted for ELASE, ELAS, S, LE, HSNFTCRT, HSNFCCRT, HSNFMTCRT and HSNFMCCRT give an idea of how stress and strain is distributed in the sandwich beam for three-point bending under constant static loading.

CHAPTER 6

DYNAMIC CRASH ANALYSIS OF FORD TAURUS

The use of finite element vehicle model for crash analysis is increasing in the automobile industry. The main reason for this is the repeatability of tests, and reduction in production costs. With the increase in the use of FE models, the models are improving in terms of accuracy, robustness, fidelity and size [2].

The Ford Taurus model which we have used for our analysis is a four-door sedan, 5 meters in length with a 2.76 m wheelbase. It is developed by the National Crash Analysis Center [2]. Figure 6.1 shows the frontal impact test setup. Usually in frontal impacts, the vehicle undergoes heavy deformations on the front end, whereas the central and the rear portions hardly undergo any deformation [2]. Since these models are developed for frontal impacts, the front portion of the vehicle is meshed finely and the middle and the rear portions of the vehicle are coarsely meshed. Some parts are modeled as beam elements and joined with spot welds [2]. Such modeling does not affect the accuracy of the model, as long as the mass and inertia distribution is consistent within the actual model [2].

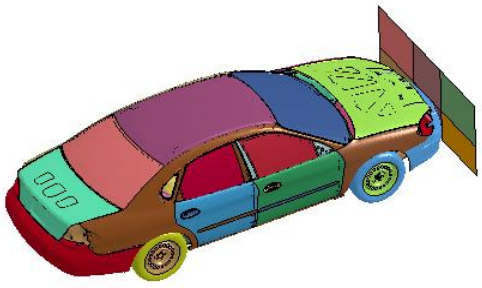

Figure 6.1 FE model of Ford Taurus [8]

6.1 Development of the FE Models

The Ford Taurus FE model has been developed by a method called *digitizing*. In this method, the real-time vehicle model is disassembled into different groups like front inner, front outer, frame, cabin, doors, rear trunk, etc [2]. Three dimensional geometric data of each component is obtained using a passive digitizing arm connected to the computer [2]. The digitized data is stored in IGES format, using some CAD software. Next, this IGES data is imported into pre-processors such as Patran or Hypermesh and meshed accordingly [2]. The output file obtained from the pre-processors is then submitted to the processor, LS-Dyna, to check the accuracy of the model. Many features are included in the FE models, such as suspension characteristics, radiator, engine, frame rails, etc., and are digitized in detail, minimizing any loss in the part's geometry [2].

6.2 Detailed Description of Finite Element Model

The detailed finite element model of the vehicle is made of 778 parts [8]. The parts represent the different structural components of the vehicle; 104 parts are made of shell elements, and 18 parts are made of beam elements [8]. One part is made of brick elements that represent the radiator. Two different types of shell elements are used, triangular and quadrilateral [8]. The shell elements are assigned with isotropic elastic plastic material, the stress strain relationship being defined by eight stress strain points [8]. Beam elements are assigned with isotropic elastic material, and solid elements are assigned with honeycomb material, with constant stress element formulation. The parts are joined by rigid body constrained options and spot welds [8]. The contacts between different parts are modeled as single surface-sliding interface also known as automatic

contact for beam, shell and solid elements with arbitrary segment orientation. Table 6.1 gives a summary of the vehicle model [8].

Table 6.1 FE model of details of Ford Taurus [8]

Number of Parts	778
Number of Nodes	936258
Number of Shell	805505
Number of Beams	4
Number of Solids	99486
Number of Elements	1057113
Weight	1665

6.3 Model validation

The accuracy of the simulation is evaluated by comparing the simulation test results with the actual test results [2]. In order for the simulation be fairly accurate, the profiles of force vs. displacement, force vs. time, displacement vs. time, and acceleration vs. time data presented by NHTSA should closely match the data obtained by performing FE analysis using LS-Dyna. Figure 6.2 shows the simulation obtained for FE analysis of frontal impact of Ford Taurus.

Figure 6.3 shows the engine x-acceleration comparison of the simulation and the test result. From the above figure we can clearly see that the acceleration profile obtained from simulation closely matches the acceleration profile obtained from the actual sled test results. The accelerometers are located on the engine and are defined as rigid bodies assigned with time history to that particular set of nodes of rigid body.

6.4 Modification of Front Bumper of the Ford Taurus

Once the model is corrected and running fine with the given velocity of 35 mph, we will replace the existing steel front bumper with the sandwich material that is validated and optimized. We will check its performance during frontal crash impact, and observe the improvement in impact energy absorption. Here we are not making any geometric changes to the existing front bumper. We are just replacing the steel material, which is already defined in the LS-Dyna model, with the material model of enhanced composite damage. We used the MAT_COMPOSITE_DAMAGE material card which is based on lamination shell theory; this material is MAT_54 in LS-Dyna. It deals with failure of composite structures under compression. For the foam material, MAT_CRUSHABLE_FOAM is used. FE analysis is performed again, using LS-Dyna for sandwich beam in the front bumper.

Reconstruction of US-NCAP frontal impact test of Ford Taurus

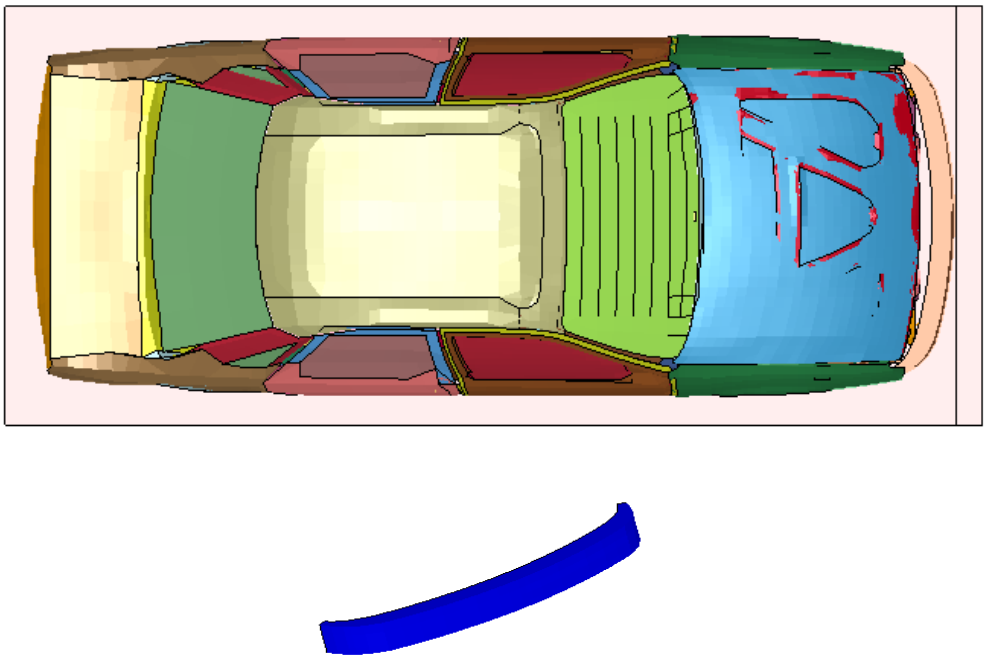

Figure 6.2 Frontal impact of Ford Taurus at T=0.0 sec.

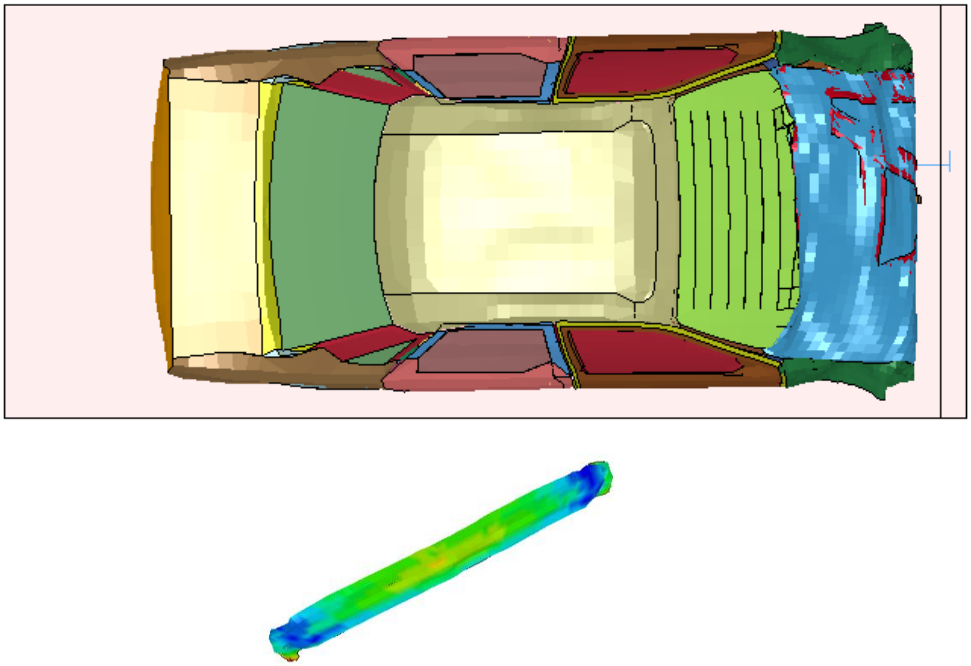

Figure 6.3 Frontal impact of Ford Taurus at T=0.14 sec.

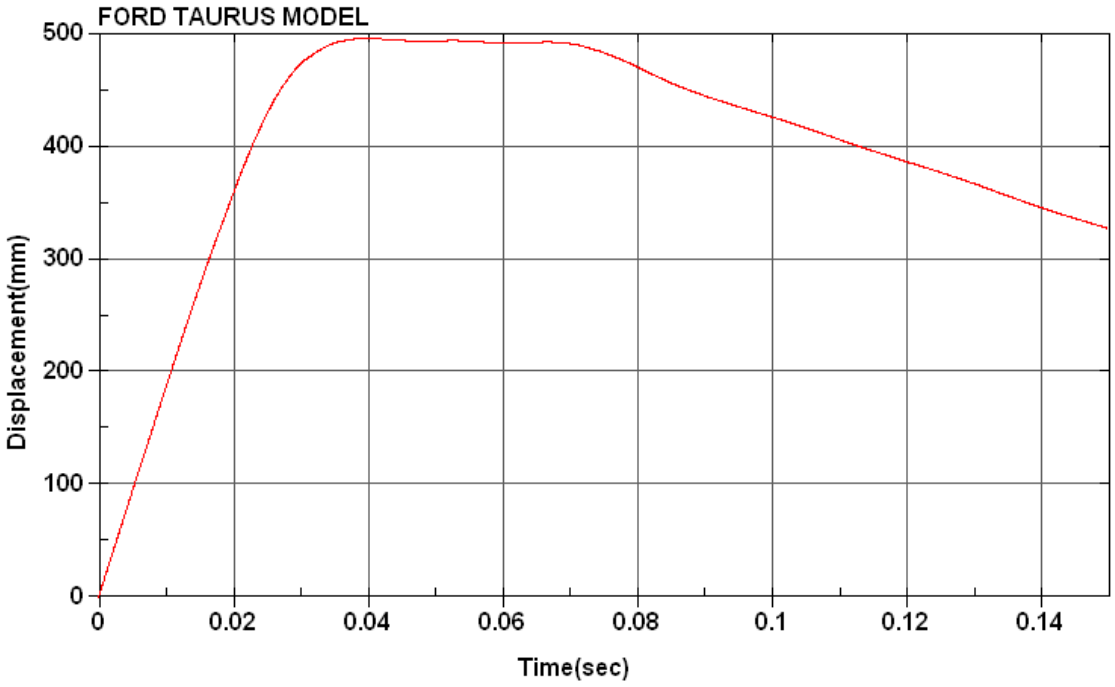

Figure 6.4 Displacement vs. time for Ford Taurus for actual bumper at T=0.14 sec.

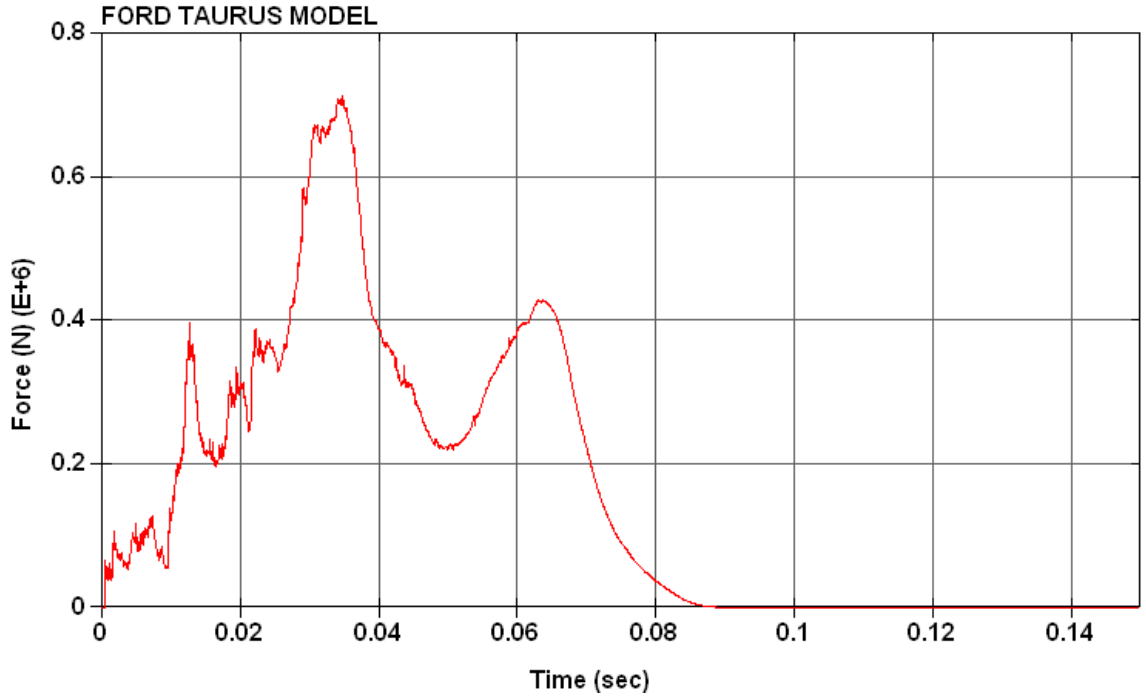

Figure 6.5 Force vs. time for Ford Taurus for actual bumper at T=0.14 sec.

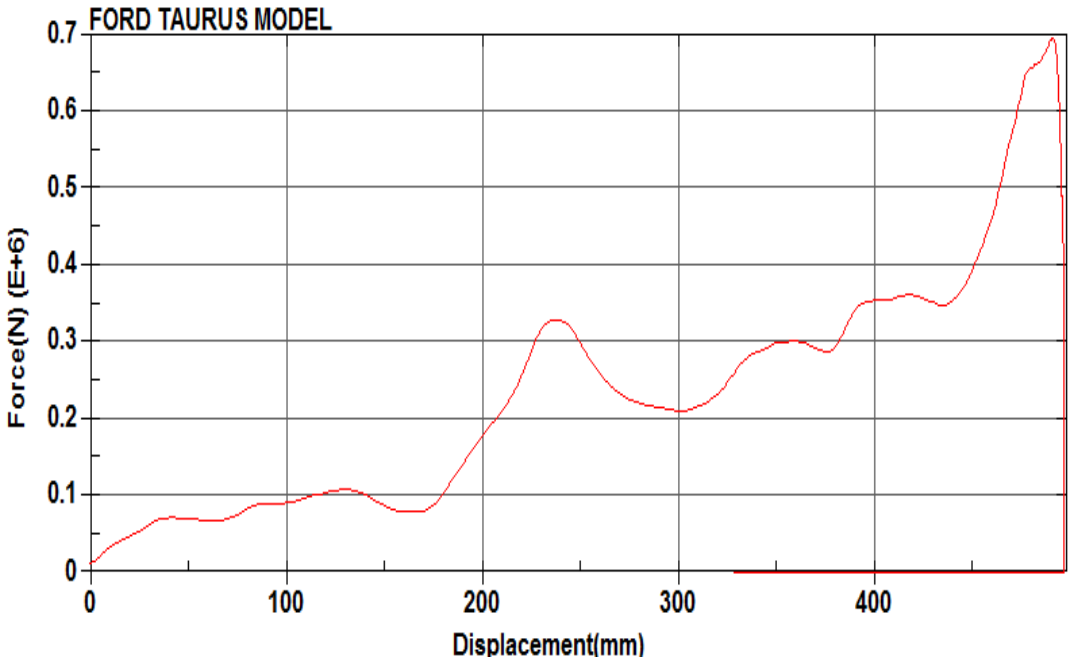

Figure 6.6 Force vs. displacement for Ford Taurus for actual bumper at T=0.14 sec.

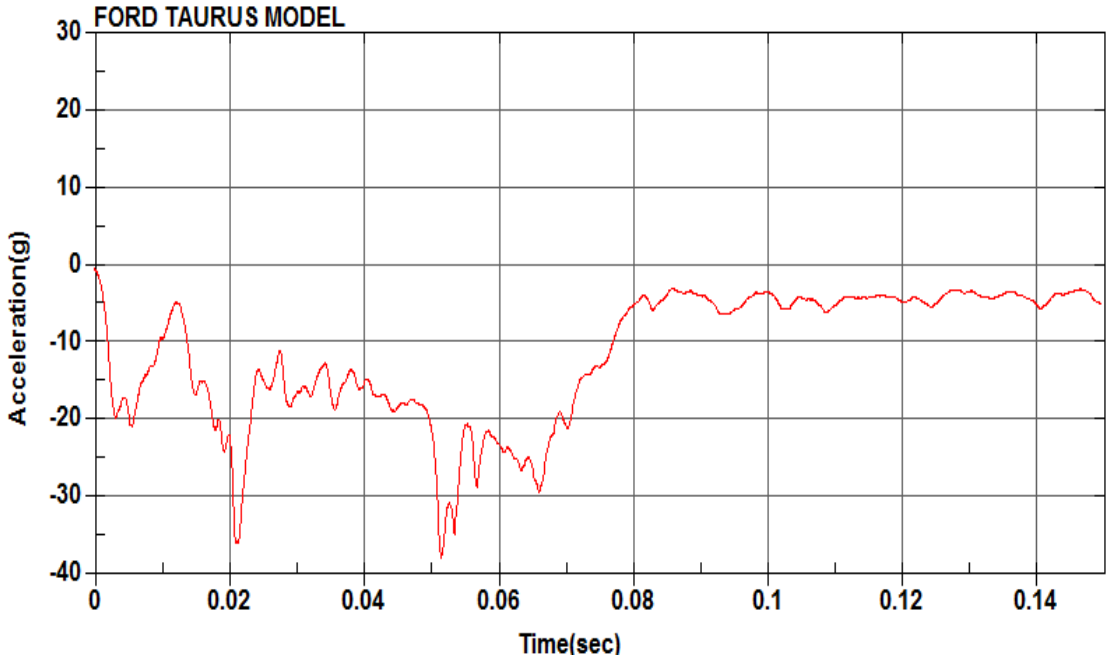

Figure 6.7 Acceleration vs. time for Ford Taurus for actual bumper at T=0.14 sec.

FE analysis results for the optimized sandwich beam in front bumper

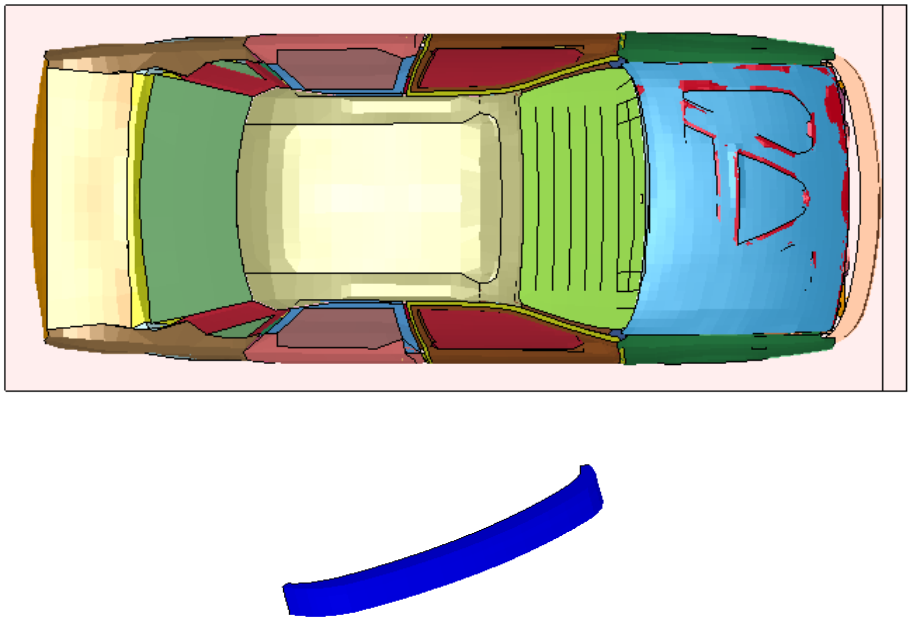

Figure 6.8 Frontal impact of Ford Taurus with sandwich beam at T=0.0 sec.

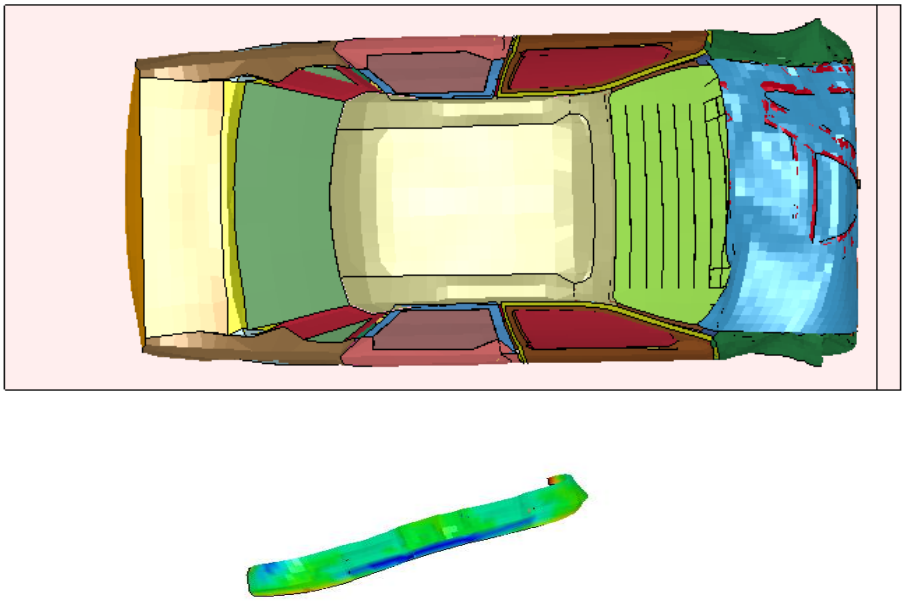

Figure 6.9 Frontal impact of Ford Taurus with sandwich beam at T=0.14 sec.

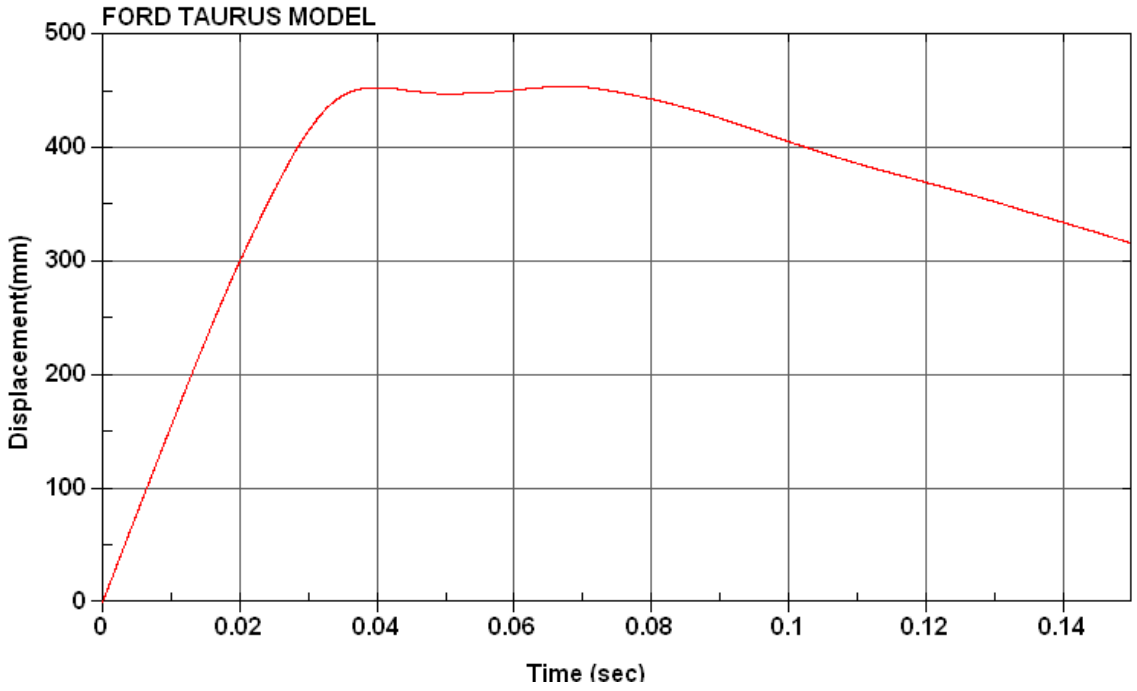

Figure 6.10 Displacement vs. time for Ford Taurus sandwich beam at T=0.14 sec.

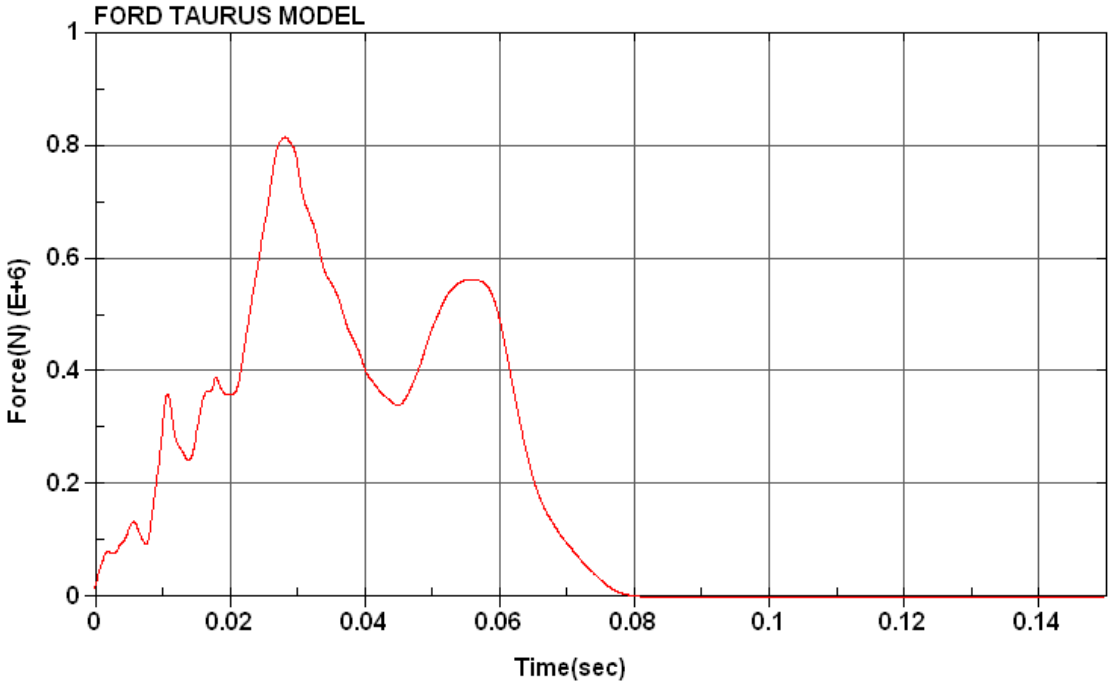

Figure 6.11 Force vs. time for Ford Taurus sandwich beam at T=0.14 sec.

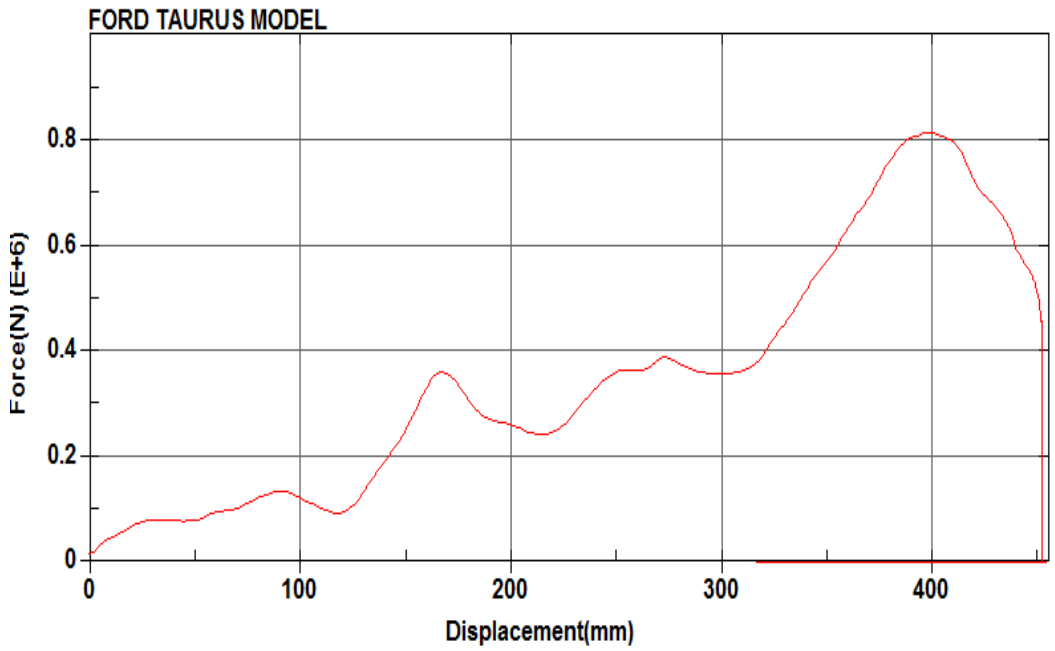

Figure 6.12 Force vs. displacement for Ford Taurus for sandwich beam at T=0.14 sec.

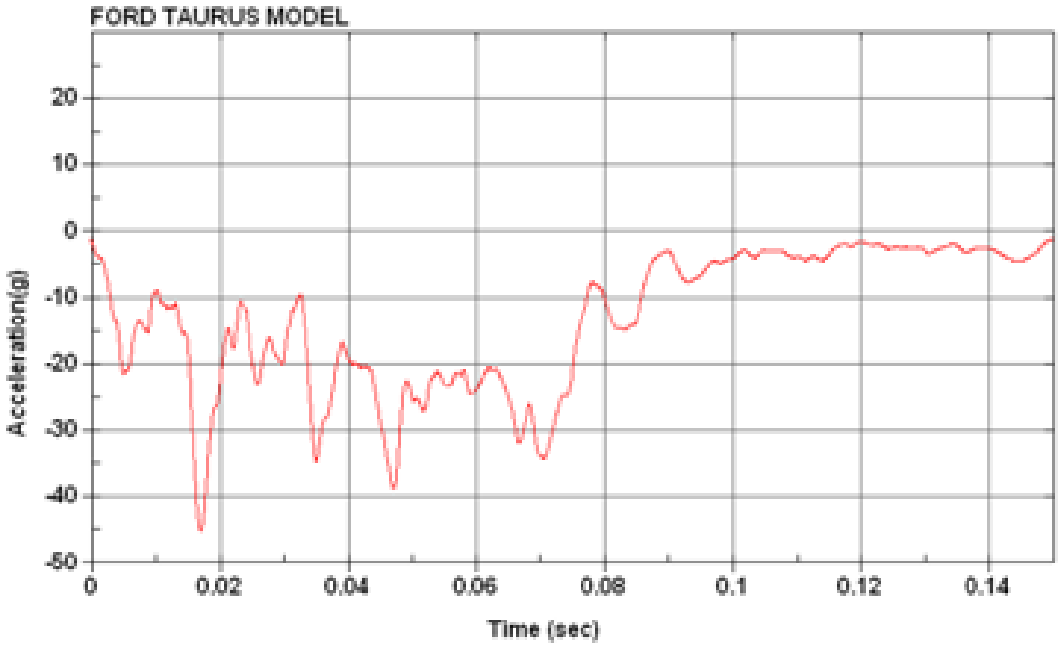

Figure 6.13 Acceleration vs. time for Ford Taurus for actual bumper at T=0.14 sec.

Frontal impact at 10 mph actual bumper

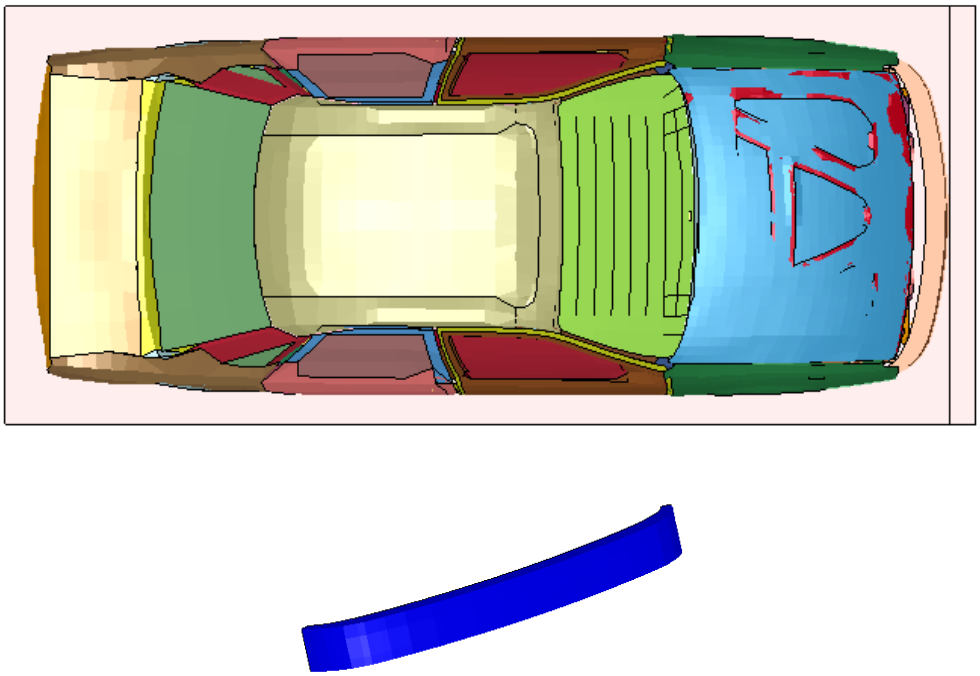

Figure 6.14 Frontal impact of Ford Taurus at T=0.0 sec.

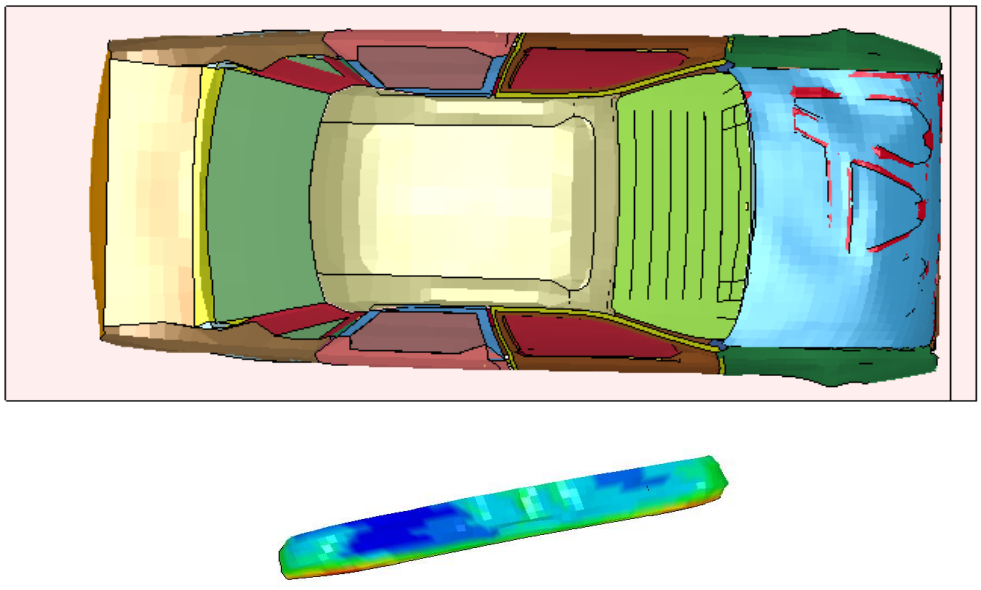

Figure 6.15 Frontal impact of Ford Taurus at T=0.14 sec.

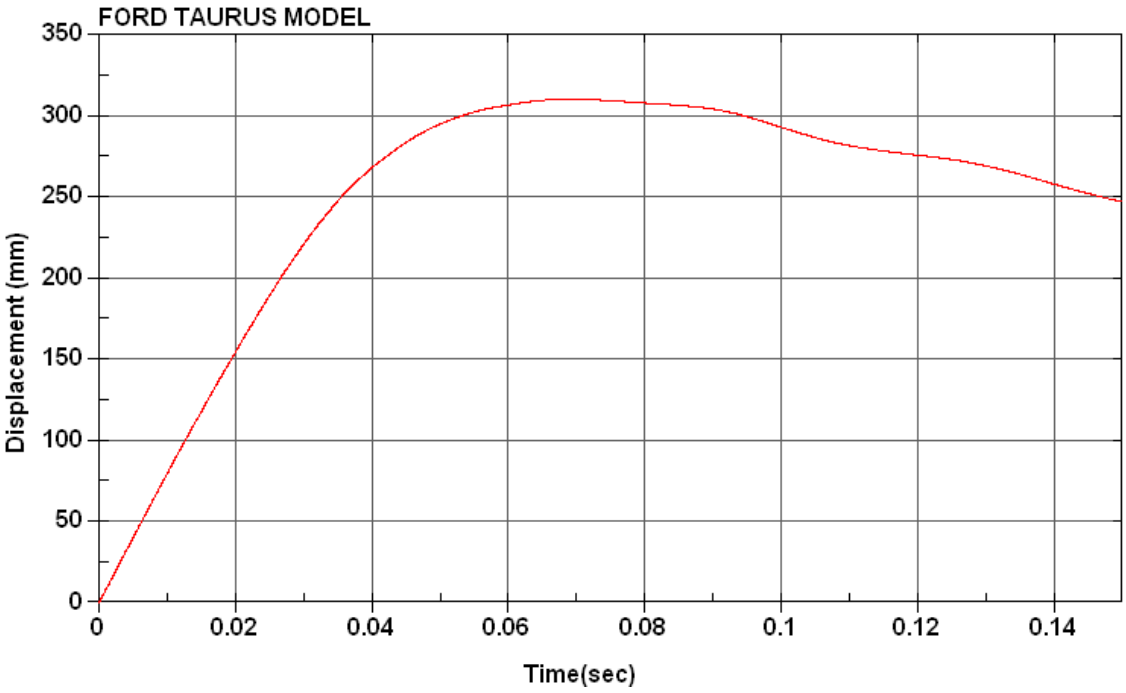

Figure 6.16 Displacement vs. time for Ford Taurus for actual bumper at T=0.14 sec.

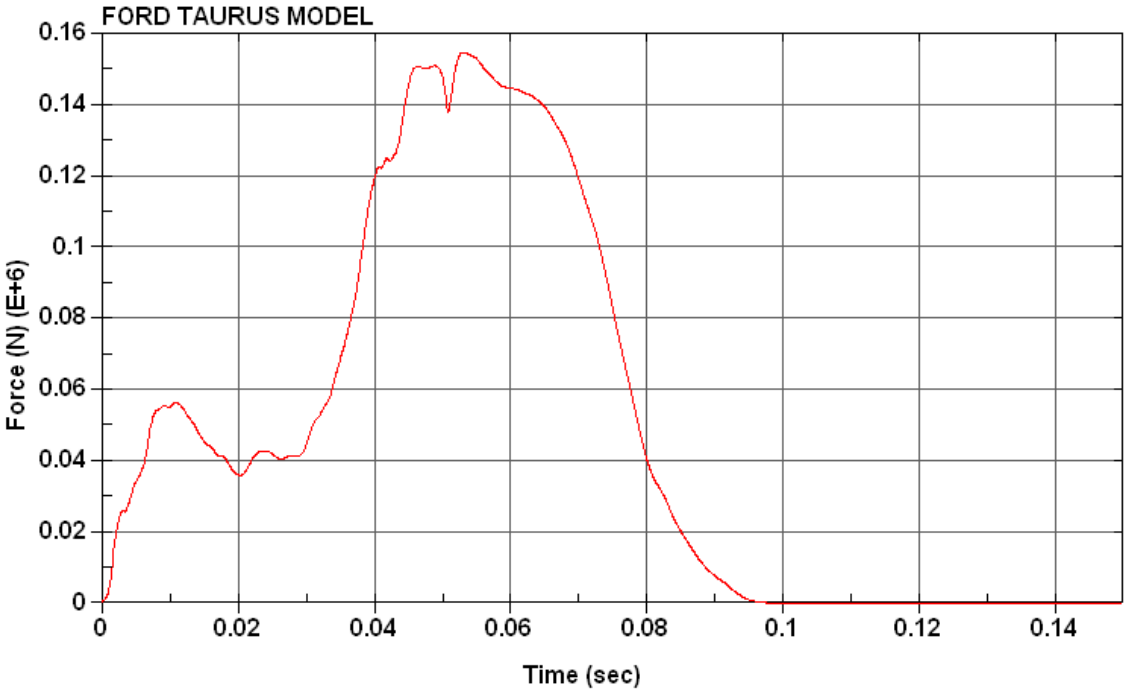

Figure 6.17 Force vs. time for Ford Taurus for actual bumper at T=0.14 sec.

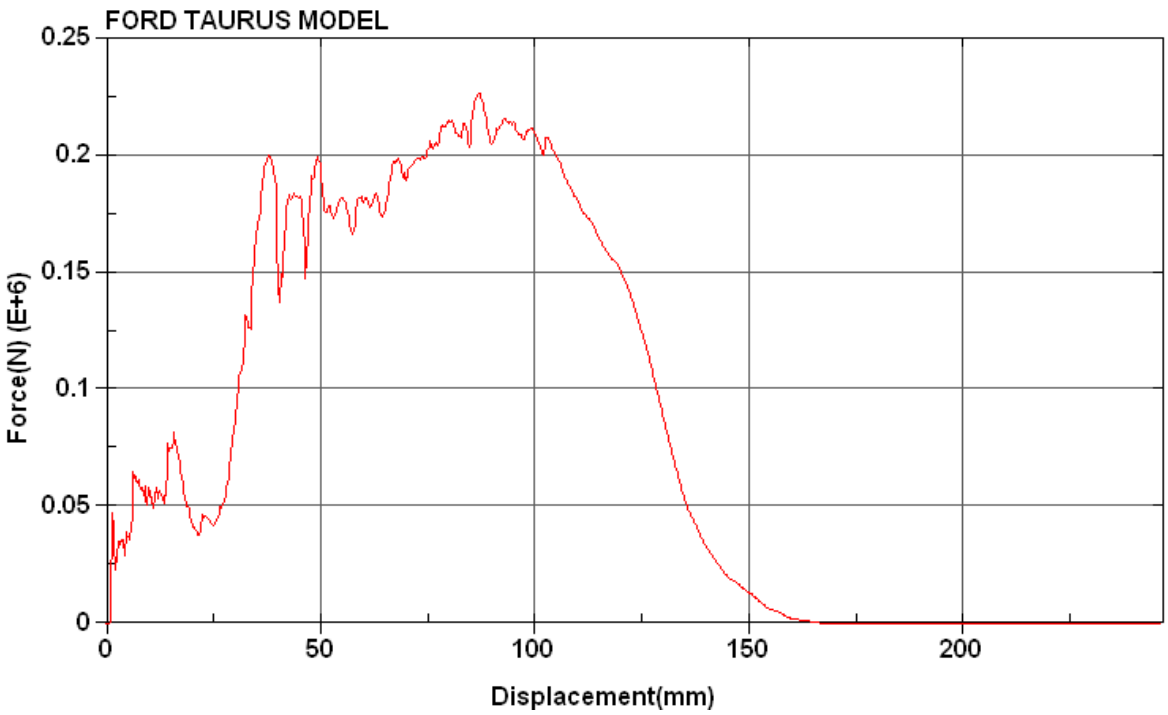

Figure 6.18 Force vs. displacement for Ford Taurus for actual bumper at T=0.14 sec.

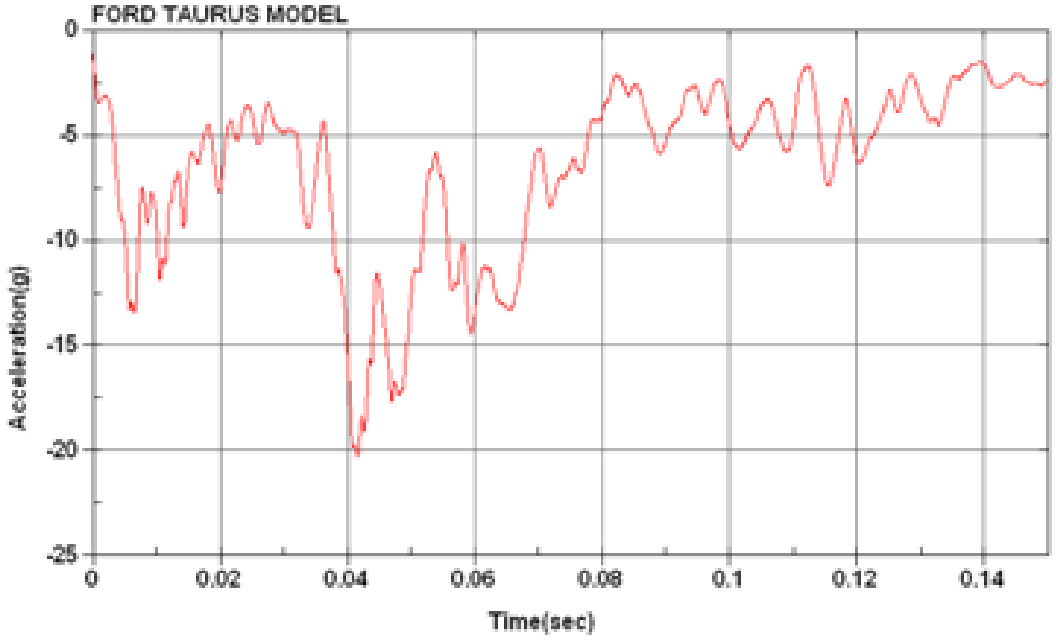

Figure 6.19 Acceleration vs. time for Ford Taurus for actual bumper at T=0.14 sec.

Frontal impact at 10 mph sandwich material front bumper

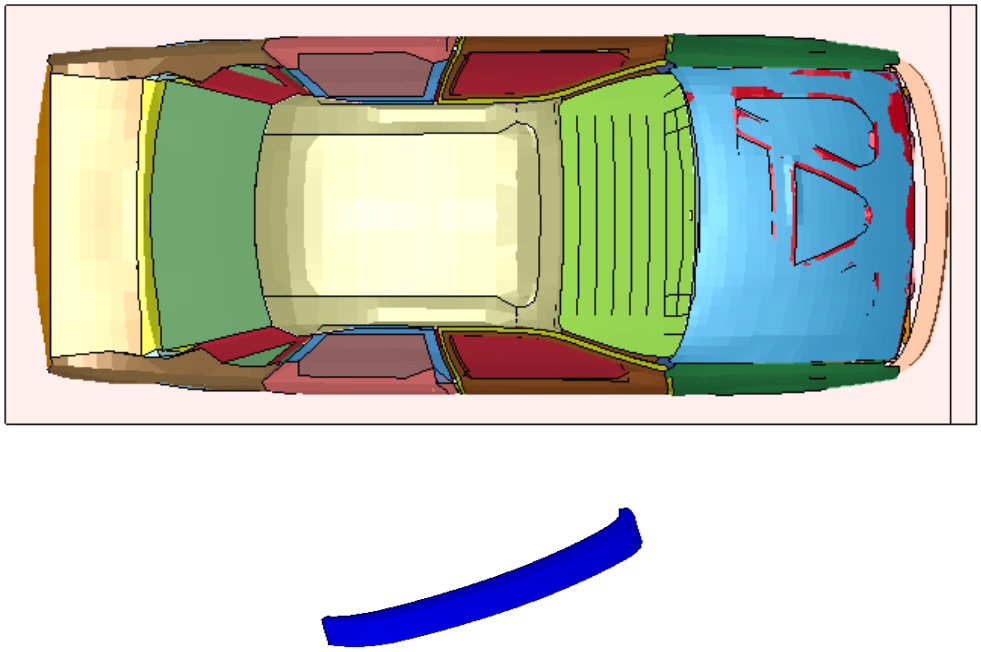

Figure 6.20 Frontal impact of Ford Taurus at T=0.0 sec.

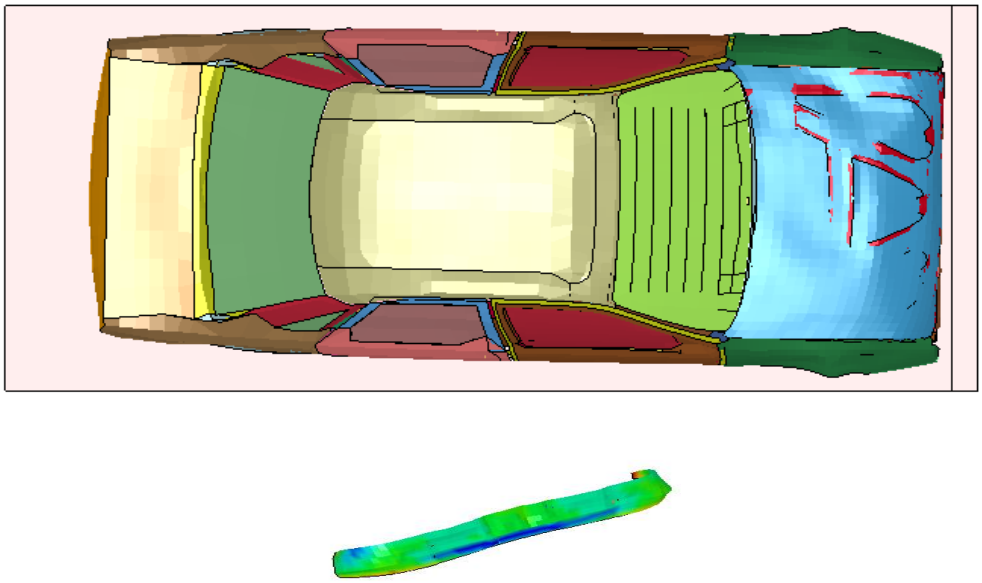

Figure 6.21 Frontal impact of Ford Taurus at T=0.14 sec.

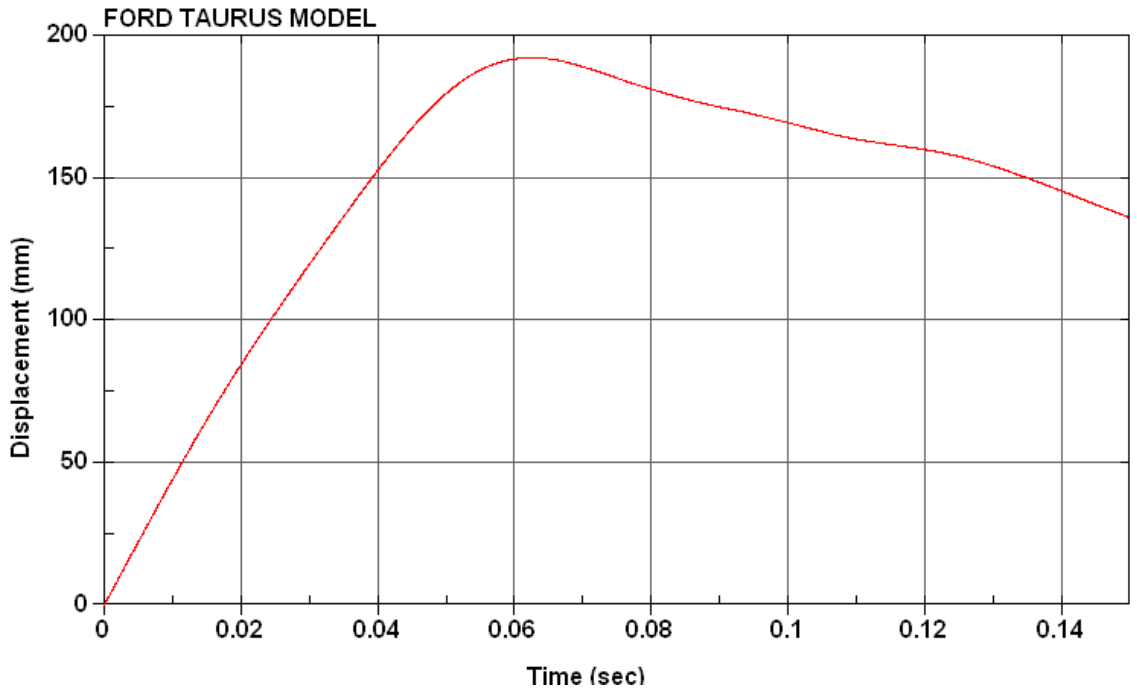

Figure 6.22 Displacement vs. time for Ford Taurus for sandwich beam at T=0.14 sec.

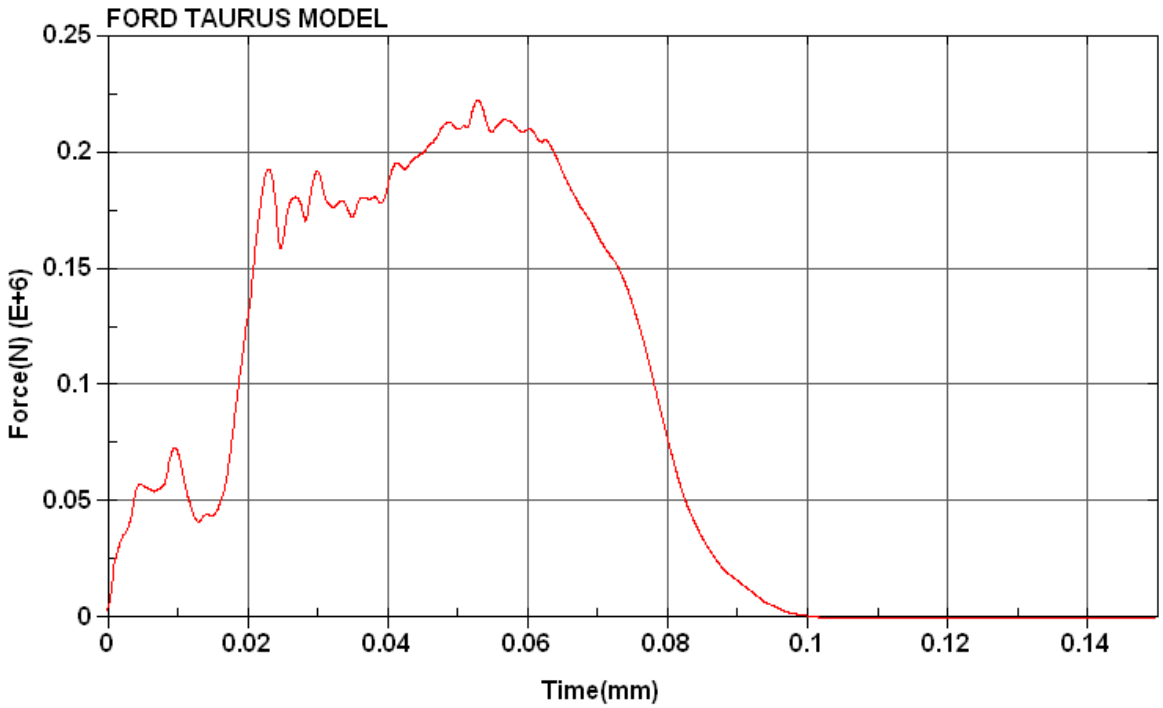

Figure 6.23 Force vs. time for Ford Taurus for sandwich beam at T=0.14 sec.

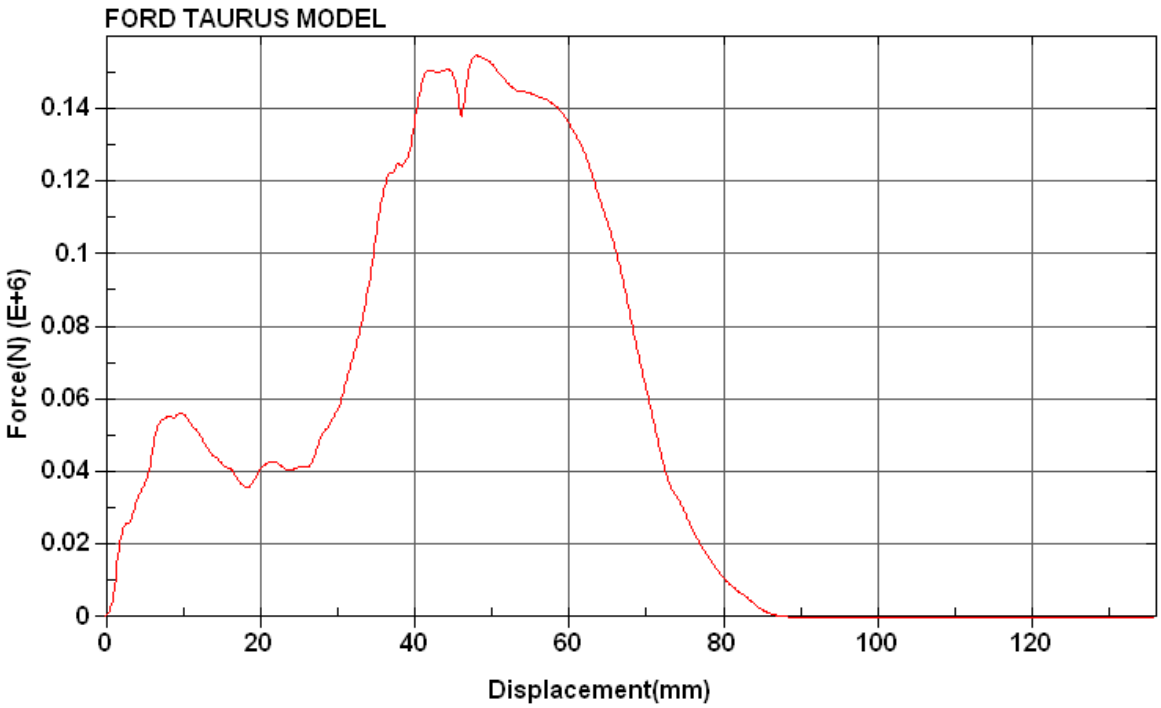

Figure 6.24 Force vs. displacement for Ford Taurus for sandwich beam at T=0.14 sec.

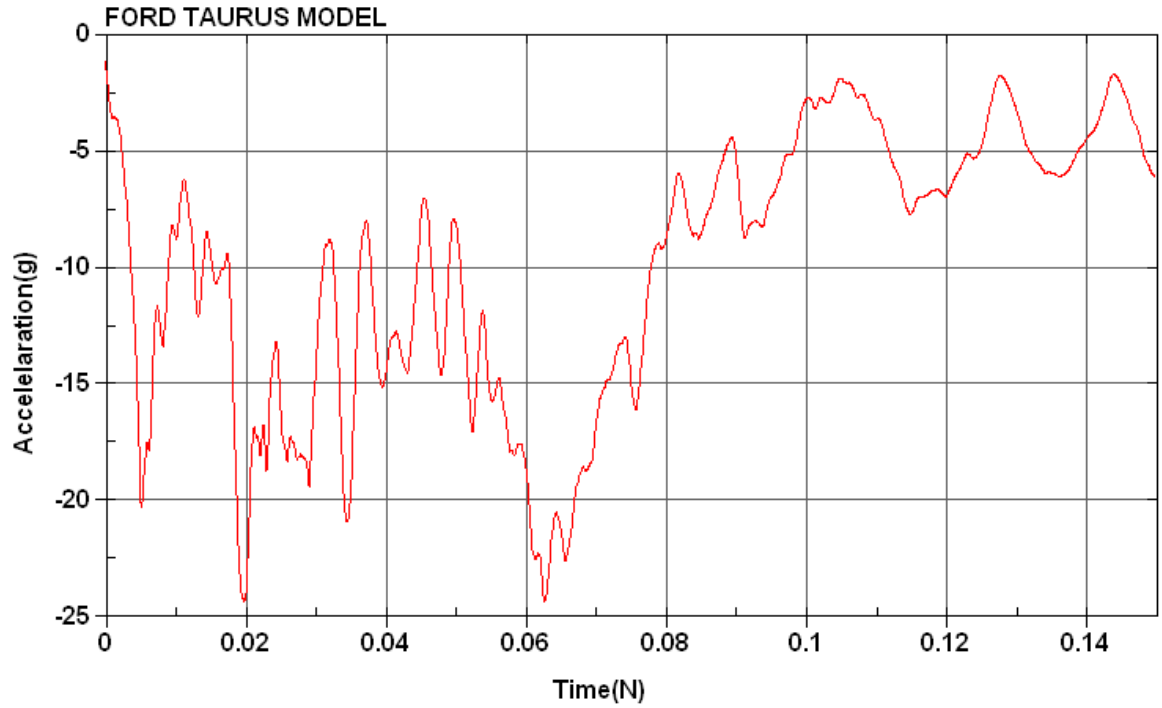

Figure 6.25 Acceleration vs. time for Ford Taurus for sandwich beam at T=0.14 sec.

Figures 6.2 through 6.7 show the reconstruction of frontal impact of the Ford Taurus at 35 mph, and observed bumper deformations on hitting a rigid wall. Displacement vs. time, force vs. time, force vs. displacement (energy absorption), and acceleration vs. time response graphs are plotted to understand the overall structural stability of the Ford Taurus.

Figures 6.8 through 6.12 show the frontal impact of the Ford Taurus at 35 mph with the front bumper composed of optimized sandwich material. The figures also detail observed bumper deformations on hitting a rigid wall. Displacement vs. time, force vs. time, force vs. displacement (energy absorption), and acceleration vs. time response graphs are plotted to understand the overall structural stability of the Ford Taurus.

Figures 6.13 through 6.18 show the frontal impact of the Ford Taurus at 10 mph with actual frontal bumper and observed bumper deformations on hitting a rigid wall. Displacement vs. time, force vs. time, force vs. displacement (energy absorption), and acceleration vs. time response graphs are plotted to understand the overall structural stability of the Ford Taurus.

Figures 6.18 through 6.25 show the frontal impact of the Ford Taurus at 10 mph with the front bumper composed of optimized sandwich material. The figures also detail observed bumper deformations on hitting a rigid wall. Displacement vs. time, force vs. time, force vs. displacement (energy absorption), and acceleration vs. time response graphs are plotted to understand the overall structural stability of the Ford Taurus.

Oblique impact (30^0) at 35 mph with actual front bumper

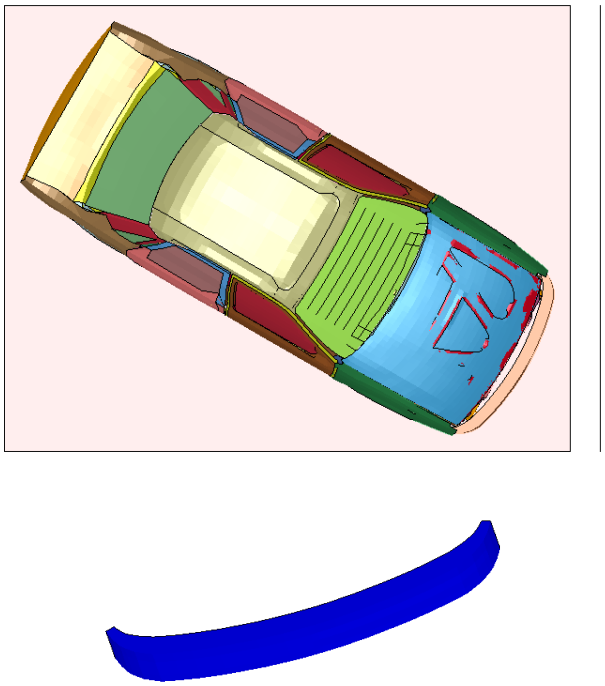

Figure 6.26 Oblique impact of Ford Taurus at T=0.0 sec.

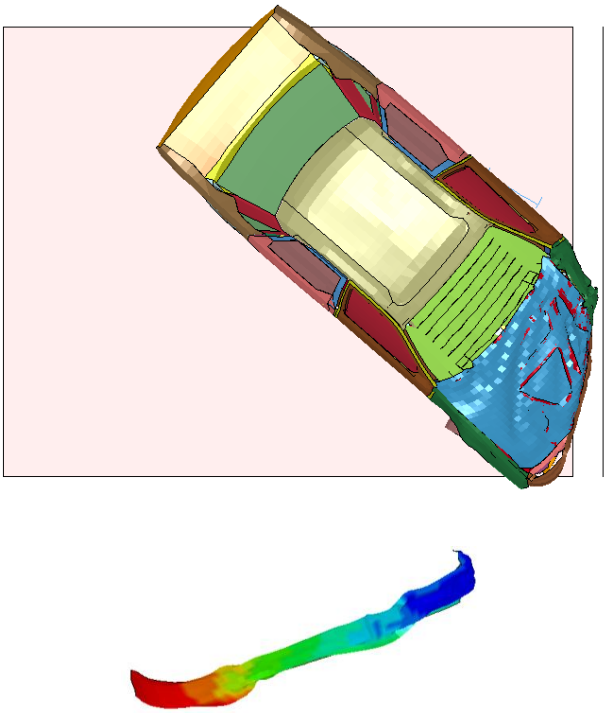

Figure 6.27 Oblique impact of Ford Taurus at T=0.0 sec.

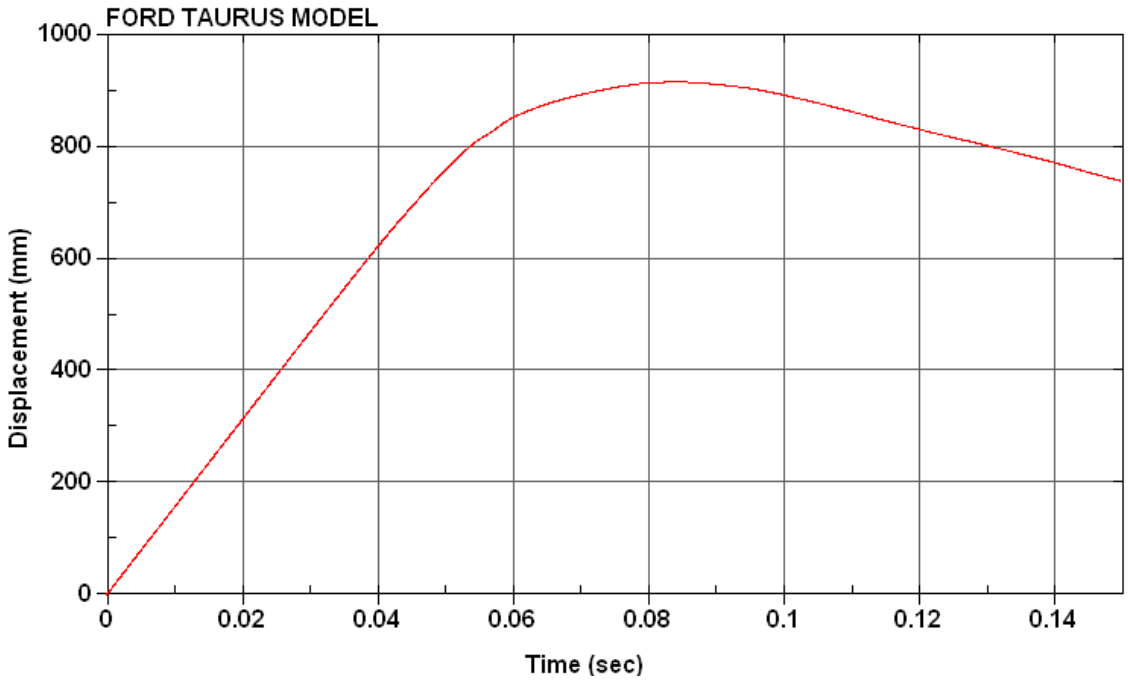

Figure 6.28 Displacement vs. time for oblique impact with actual bumper at T=0.14 sec.

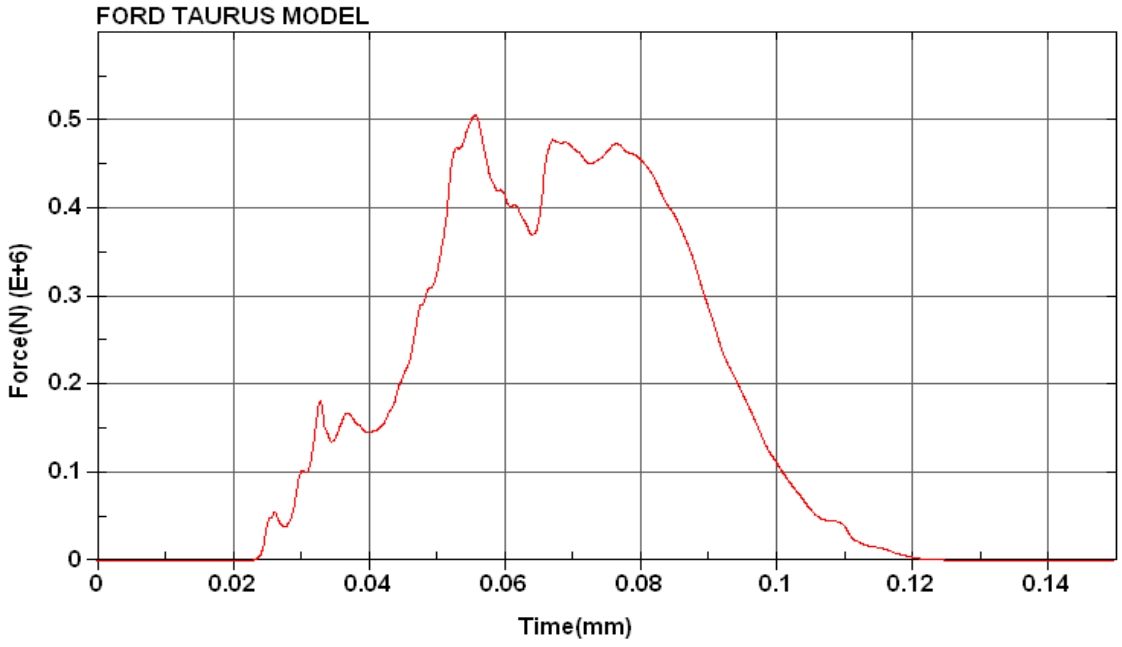

Figure 6.29 Force vs. time for oblique impact with actual bumper at T=0.14 sec.

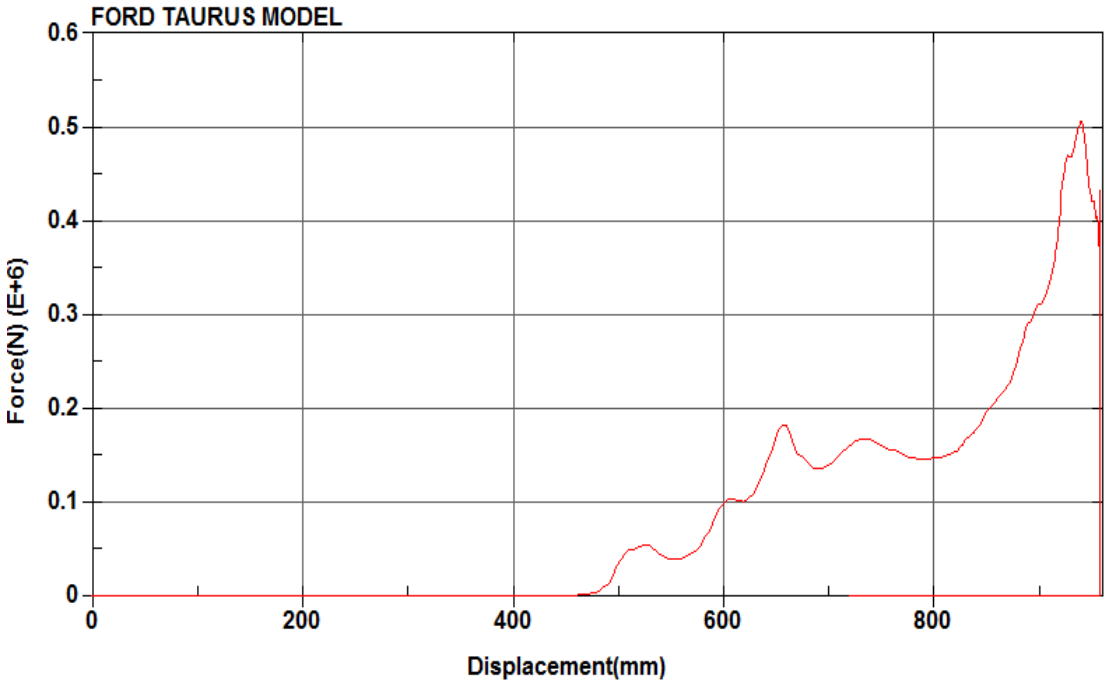

Figure 6.30 Force vs. displacement for oblique impact with actual bumper at T=0.14 sec.

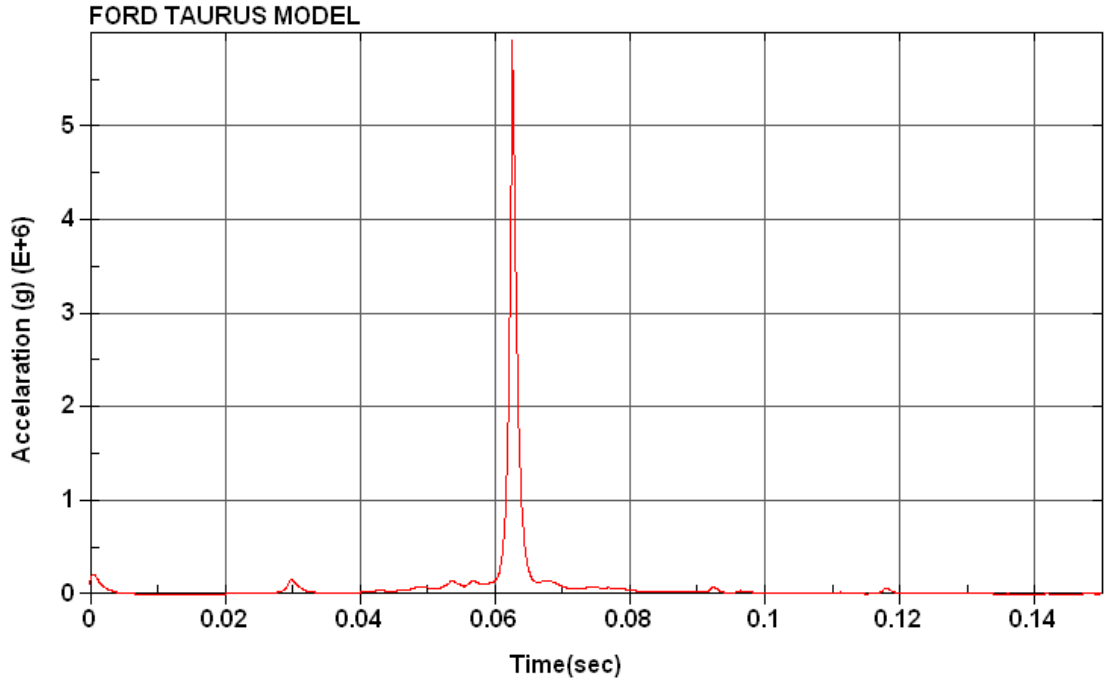

Figure 6.31 Acceleration vs. time for oblique impact actual bumper at T=0.14 sec.

Oblique impact (30^0) at 35 mph with sandwich material in front bumper

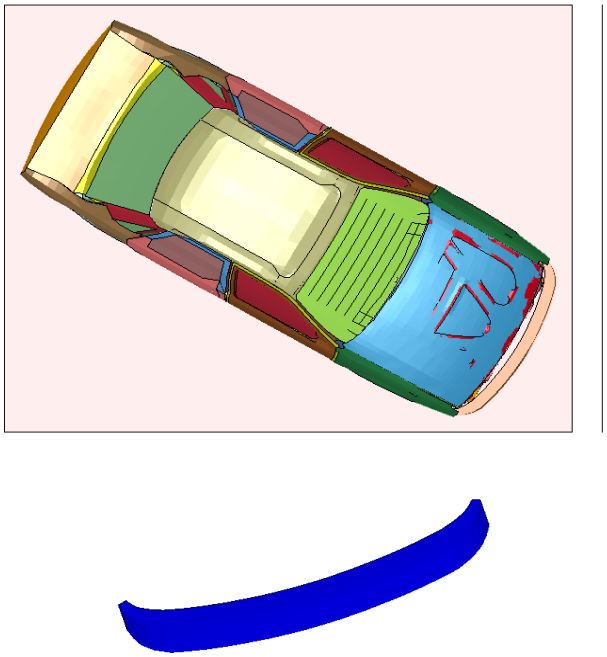

Figure 6.32 Frontal impact of Ford Taurus at T=0.0 sec.

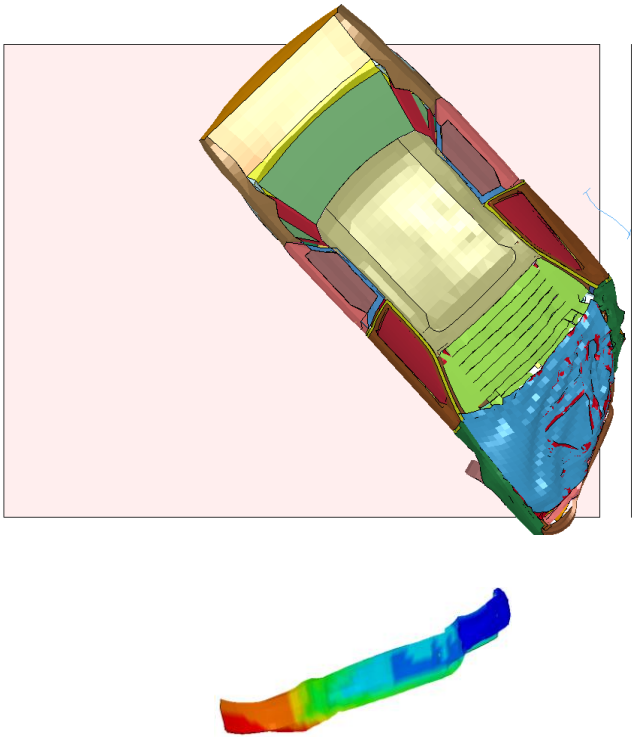

Figure 6.33 Frontal impact of Ford Taurus at T=0.14 sec.

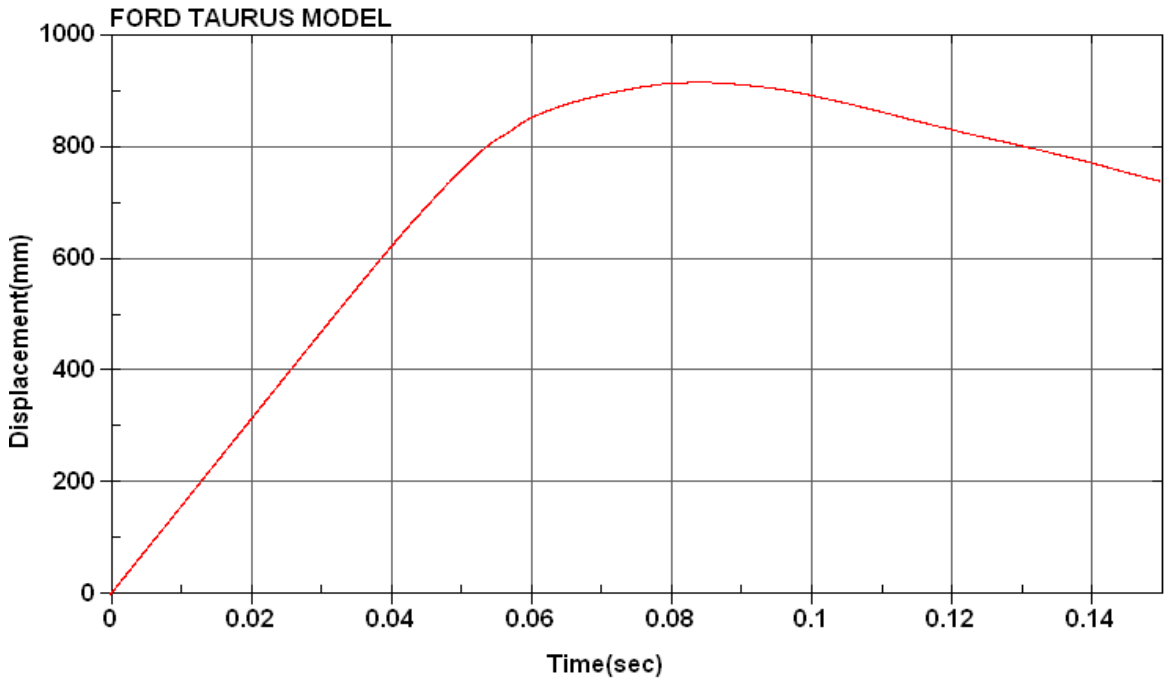

Figure 6.34 Displacement vs. time for oblique impact with sandwich beam at T=0.14 sec.

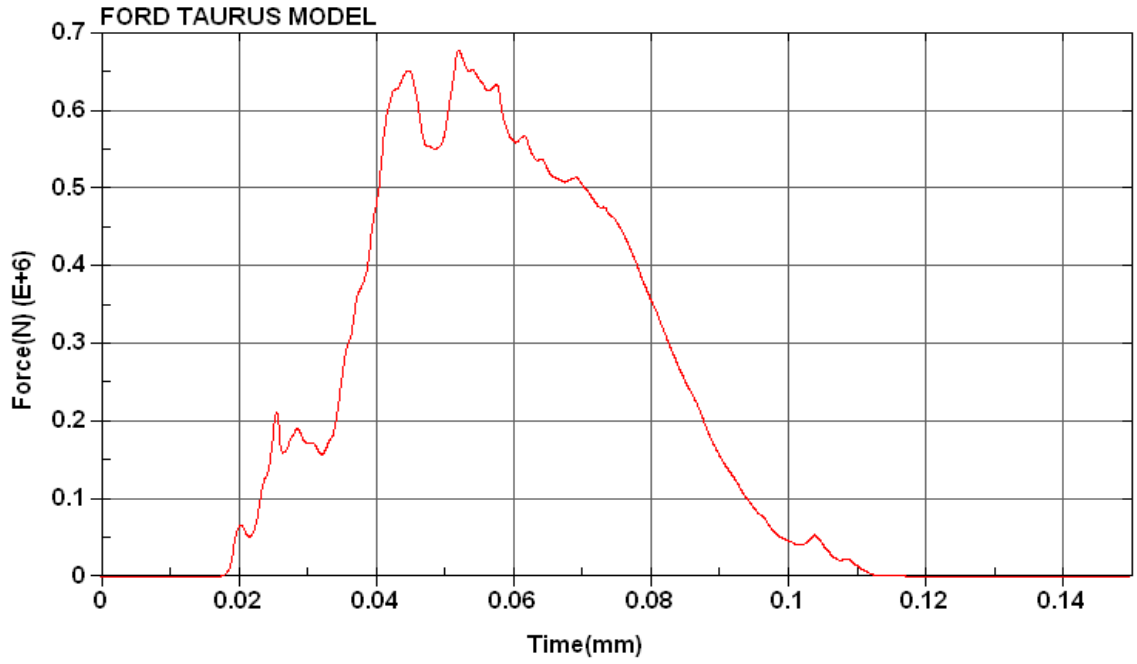

Figure 6.35 Force vs. time for oblique impact with sandwich beam at T=0.14 sec.

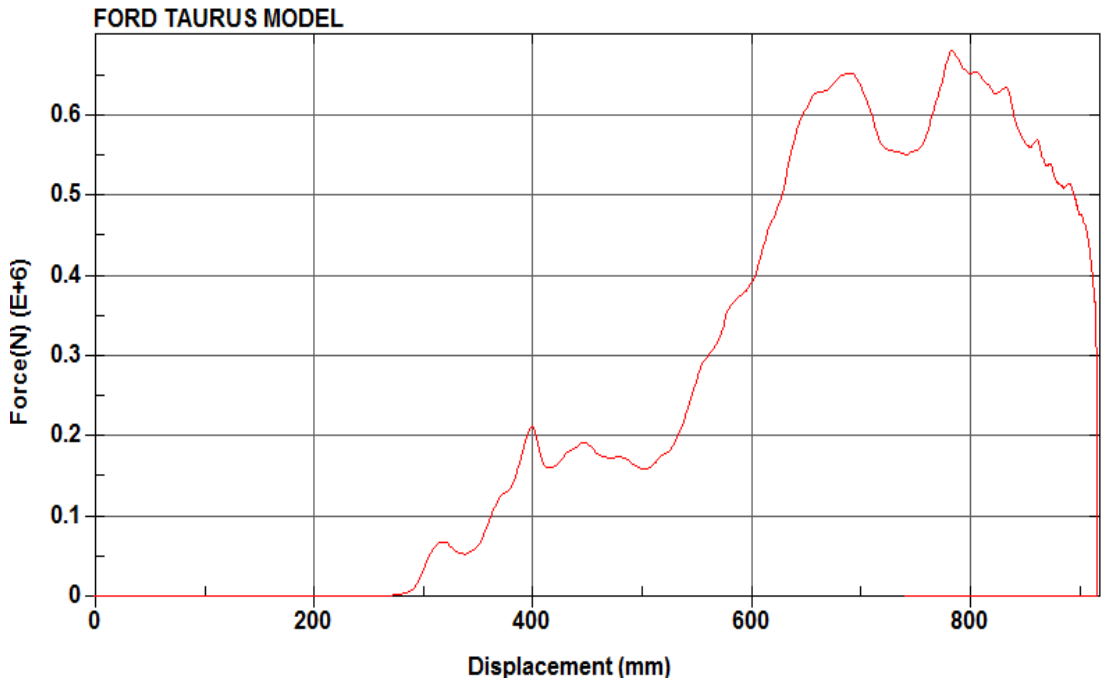

Figure 6.36 Force vs. displacement for oblique impact with sandwich beam at T=0.14sec.

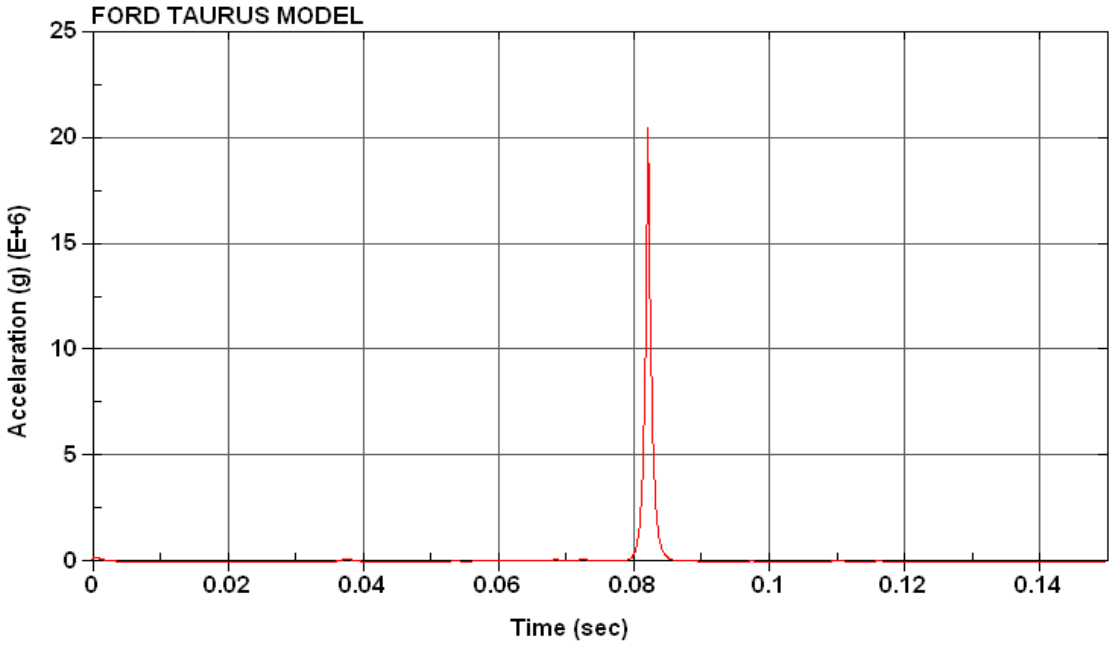

Figure 6.37 Acceleration vs. time for oblique impact with beam at T=0.14 sec.

Figures 6.26 through 6.31 show the oblique impact (30^0) of the Ford Taurus at 35 mph, with actual frontal bumper and observed bumper deformations on hitting a rigid wall. Displacement vs. time, force vs. time, force vs. displacement (energy absorption) and acceleration vs. time response graphs are plotted to understand the overall structural stability of the Ford Taurus.

Figures 6.32 through 6.37 show the oblique impact (30^0) of the Ford Taurus at 35mph, with the front bumper composed of optimized sandwich material. The figures also detail observed bumper deformations on hitting a rigid wall. Displacement vs. time, force vs. time, force vs. displacement (energy absorption), and acceleration vs. time response graphs are plotted to understand the overall structural stability of the Ford Taurus.

Table 6.2 and Table 6.3 summarize the results obtained from the frontal and oblique impact crash analyses of the Ford Taurus.

Table 6.2 Crash analysis summary for Ford Taurus with actual front bumper

Steel	Front Impact @ 35 mph	Front Impact @ 10 mph	Oblique impact @ 35mph
Displacement (mm)	500	310	930
Force (KN)	700	140	500
Acceleration (g)	38	20	6

Table 6.3 Crash analysis summary of Ford Taurus with sandwich front bumper

Sandwich	Front Impact @ 35 mph	Front Impact @ 10 mph	Oblique impact @ 35mph
Displacement (mm)	450	200	900
Force (KN)	810	225	680
Acceleration (g)	44	25	20

Upon comparing Tables 6.2 and 6.3, it is observed that the Ford Taurus with sandwich material in the front bumper is showing less deformation with increased contact force, resulting in increased acceleration. This hints that sandwich material shows high structural stability, resulting in less overall deformation. Structural performance for oblique impact of the Ford Taurus with sandwich material bumper is better than the original.

From Tables 6.2 and 6.3, it can be concluded that sandwich material performs better for load in normal and oblique loading. Therefore, the optimized sandwich material used in the front bumper performs better in frontal impacts.

Using the acceleration pulse obtained in Figure 6.13, tests will be done relating to occupant kinematics and injuries sustained due to frontal impact of the Ford Taurus. The frontal impact sled FE model will be used to evaluate results, when existing front bumpers are replaced with sandwich material.

CHAPTER 7

OCCUPANT BIODYNAMICS

Full vehicle crash testing is used to reproduce the dynamic conditions of real-world car accidents. The complex and destructive nature of these crash tests makes them very expensive. Because of these issues, sled testing becomes the preferred evaluation method for occupant injury. Sled testing allows engineers to reproduce the occupant injury of a full-scale crash test, in a controlled environment, and at a fraction of the cost. Sled simulations were conducted using the LS-Dyna finite element code. HyperMesh was used as a preprocessor for setting up the sled deck, and HyperView as a post-processor to measure the dummy responses. To confirm the accuracy of the sled FE model, it is necessary to compare the simulation results with the physical tests. Since we have the published data for the frontal impact sled test using the Ford Taurus, we can compare the results obtained through the frontal impact of the Ford Taurus with sandwich material in the front bumper. In the current study, the frontal impact sled test is performed to evaluate the occupant injury sustained. By utilizing the acceleration pulse obtained from the frontal impact of the Ford Taurus with sandwich material in front bumper as the input to the sled FE model, a simulation was carried out to predict the occupant kinematics. In the present study, a 50th percentile Hybrid III FE dummy model was used as the occupant for studying the biomechanical [6] responses. Responses concerning chest deflection, head-acceleration, pelvis acceleration, torso belt forces, upper neck loads, and neck injury criteria were studied.

The overall research question of the project is how automotive safety systems can be improved through deep studies of accident events, with consideration of the interaction [6] between classic mechanics and biomechanics.

7.1 Biomechanics

The mechanical characteristics of the human body can be specified in terms of physical parameters in the same manner as any mechanical structure. This special field of [6] mechanics is referred to as *biomechanics*. As defined, biomechanics is mechanics applied to biology. The biological world is a part of the physical world around us, and is naturally an object of inquiry in mechanics.

Biomechanics seeks to understand the mechanics of living systems. In full-scale crash tests, human cadavers or crash test dummies are used, and sometimes, animals. At present, there are no mathematical models that can completely replace tests with real cars and animals or cadavers. However, research and development of mathematical models are constantly being improved [6].

7.2 Simulation of Hybrid III 50TH Percentile Dummy

This dummy weighs 74.4 kg and its stature is 180 cm. The dummy is placed, belted-up, in a natural sitting position. In motor vehicle crashes, three types of collision forces that can cause injuries. The first force is the direct impact due to the collision between the motor vehicle and another object. The second force is any collision that may occur between the intruded parts of the vehicle and the passenger body. The third involves the violent collision of body organs within the body frame. The last two forces increase the importance of consistent use of safety restraints in motor vehicles.

7.3 Head injury

Injuries to head are divided into skull injuries, brain injuries, and scalp injuries. Scalp injuries are quite common in accidents, but they are considered to be of minor importance. In general terms, it is convenient to view head injuries as comprising these three distinct varieties.

7.4 Head injury criteria

Head injury criterion (HIC) is used to assess head injury. Values greater than 1,000 indicate that there is likelihood of serious head injury. HIC is calculated when the head of the occupant comes in hard contact with another rigid object during a frontal (contact) impact. It is evaluated as

$$HIC = \max_{t_1, t_2} \left\{ (t_2 - t_1) \left[\frac{1}{t_2 - t_1} \int_{t_1}^{t_2} a(t) dt \right]^{2.5} \right\} \quad (7.1)$$

where

t1, t2 = arbitrary instances of time, when the head experiences acceleration or deceleration.

a (t) = resultant linear acceleration at the center of gravity of the head .The time interval, t2-t1, must be chosen such that the difference is less than 36 ms, and in such a way that the value of HIC is maximized

7.5 Neck Injury Criteria

Neck injury is due to excessive compressive or tensile forces along the neck axis, or excessive shear forces acting perpendicular to the neck axis. The duration of the load acting on the neck, also affects the level of injury. In this study, the neck injury criteria formulated by Mertz and Patrick was used.

The criteria for compressive loading was

$F > 900 – 20t$ $t< 30$ ms (7.2)

$F > 250$ lb (f) $t> 30$ ms (7.3)

The criteria for tensile loading was

$F> 740 – 2.6\ t$ $t < 34$ ms (7.4)

$F> 1888 - 36.4t$ $34ms < t > 45$ ms (7.5)

$F> 250$ lb (f) $t > 45$ ms (7.6)

Neck injuries can also occur due to excessive moments. A limiting value of 504 in-lb and 1680 in-lb was set for moments in extension and flexion, respectively. (The SI equivalent of 1 lb-f is 4.484 N and in 1 in-lbf is 0.1130 N-m)

7.6 Chest 3ms Criteria

A chest 3ms criterion gives the acceptable limit of the maximum acceleration experienced by the occupant over a 3ms time interval. For this criterion, chest acceleration should not exceed 60 G over a time interval of 3ms, during a crash event.

7.7 Chest Deflection Criteria

The chest deflection criteria suggest that chest deflection should not exceed more than 63mm during a crash event. If the chest deflection value goes beyond the recommended value, it shows serious chest injuries in the chest cavity.

7.8 FMVSS 208 Injury Criteria

The FMVSS 208 was developed to reduce the number of fatalities, and number of severe injuries to occupants involved in frontal crashes**.** This standard also specifies

injury criteria for various crash test dummies, also known as anthropomorphic test devices (ATDs). This standard is used for estimating the fatalities from a frontal impact. Parameters from FMVSS 208 are used to compare the results obtained from the FE model of a frontal impact involving a Ford Taurus.

7.9 Computer-aided Computation and Simulation

The parametric study conducted in the present chapter is completed by the use of numerical analysis methods. The performance of computer hardware and software [6] is steadily increasing. Concerning engineering applications, the use of computer-aided tools can be seen in all sectors, e.g. computer-aided design (CAD), and computer-aided [6] manufacturing (CAM), and computation and simulation with FE analysis.

Explicit FE codes for crashworthiness engineering applications have been [6] developed since the 1960s. The first full-vehicle car crash models were built and analyzed in the mid 1980s. In the field of vehicle design and crashworthiness engineering, FE analysis today is a fully integrated tool in the product development process, and widely used in computation and simulation. Another advantage of the use of more sophisticated models, is that the need of full-scale development prototypes is reduced.

Since full-scale prototypes are relatively expensive, a lot of money and time is saved in the development process. Due to the steady increase in hardware and software performance, it is possible to use more and more detailed models and still keep the calculation times at reasonable levels [6]. In comparison to full-scale crash tests, mathematical models offer a very fast and cheap way to model a car occupant's motion. The modeling provides a quality and resolution that allow designers to make rough

decisions on how to proceed. This can, in turn, minimize the number of full-scale crash tests needed to establish the performance of different protective systems [6].

Another quality in this respect, is the complete repeatability by which models can resolve effects of infinitely small changes to a system [6]. As stated, this makes mathematical models very well-suited for parametric studies. Thus, the use of mathematical models makes it possible to perform simulations over and over with equivalent circumstances, e.g. in order to perform crash test simulations [6].

7.10 Process Methodology

7.10.1 FE model of seat structure development

A generic finite element model (FE model) including a seat structure and a sled was established [6]. The lower seat frame and the sled were modeled as rigid material. The seat structure and the sled were modeled with shell elements as per the requirement of [6] FMVSS 208. A FTSS Hybrid III 50 percentile finite element adult male dummy was positioned according to the prescribed H-point, torso angle, thigh angle and other positioning requirements of FMVSS 208.

Belt routing was done in LS-Dyna. Lap and shoulder belts were modeled with a combination of 2d shell element and 1d seat belt element. Fabric properties were defined by shell elements of belt, and 1d belts were defined by MAT_SEATBELT material model. Slip rings and retractors were defined at the appropriate locations. Crash pulse was applied to a rigid floor of vehicle longitudinal direction (X-axis). Rigid base of seat was connected to the floor and the BOUNDARY_PRESCRIBED_RIGID_MOTION card has been used to apply the deceleration pulse corresponding to 35 mph (15m/s) full frontal crash. Gravity was applied to the seat using the LOAD_BODY card. Contacts

were defined with segment-based soft constraint formulation for dummy with belt, seats and vehicle interiors. AUTOMATIC_SINGLE_SURFACE contact was defined for the seat parts.

Simulation was carried for 400 msec. Dummy responses after 300 msec were not believed to be very significant. The LS-Dyna 971 version has been used as solver. Post-processing has been done in HyperView 8.0. All the dummy injuries were calculated by the default calculator available in HyperView. Responses have been filtered by different SAE filters, prescribed by FMVSS 208 regulation dummy kinematics were plotted.

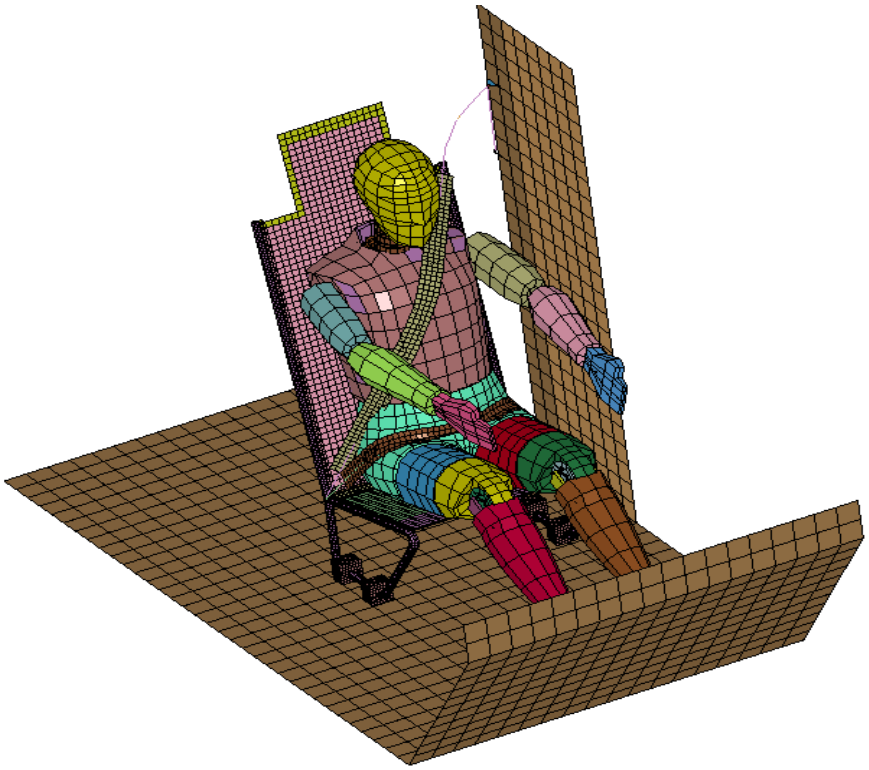

Figure 7.1 FE modeling of the frontal impact sled test setup (FMVSS 208)

The tasks performed in this phase were as follows:

- Review of CAD geometry
- Preparation of 3D CAD model geometry for meshing with finite elements

- Meshing CAD model with finite elements
- Definition of model properties: material, thickness, etc
- Verification of finite element model mass properties
- Evaluation of numerical stability of the finite element analysis
- Verification of the finite element model for parametric study

7.10.2 Mesh quality criteria

To control the minimum time step for the whole model, the following quality criterion is shown in Table 7.1. Parameters such as minimum length of the element, and number of trias are most significant. Minimum length of the element is directly related to the characteristic length of the element, which affects the minimum time step. Also, the percent of trias should be less than 5 percent of the total elements in the component, because trias behave stiffly during contact.

Table 7-1 Mesh quality criteria for seat strained belt FE model

No	Quality Parameter	Min./Max.	Allowable Min./Max.
1	Min Side Length	5.1	5
2	Max Side Length	30.9	100
3	Max Aspect Ratio	2.9	5
4	Min Quad Internal Angle	45	45
5	Max Quad Internal Angle	134.6	135
6	Min Tria Internal Angle	23.8	15
7	Max Tria Internal Angle	108.7	120
8	Max Warp Angle	14.8	15
9	Percent of Trias	0.4	5

7.10.3 Injury Parameters

The main result from crash testing is the various injury responses. These responses are used to predict the severity and type of injuries that the occupant may suffer in various crash scenarios. These injury criteria are also utilized as the basis for certification by government agencies. The injury levels predicted in the crash tests and simulations were used to validate the simulations. The values predicted by the simulations must be within the tolerance range of those predicted by the actual tests. Some of the injury criterion, such as head injury, was evaluated within specified time windows. The position of this window is also of importance in predicting the validity of the simulations. Thus, time windows for such injury criterions were also utilized in establishing the various neck injury criteria. Figures 7.2 through 7.7 are the simulation results for the frontal impact sled test, where the acceleration pulse used is the acceleration obtained from the optimized sandwich material in the front bumper of the Ford Taurus. Figures 7.2 through 7.8 are the responses of the occupant during different time intervals. The restraint system employed tries to restrict the occupant's movement by tightening the seat belt which is done though the retractors that are present in the seat belt FE model.

NCAP frontal impact with seat belt restrained sled test at 35 mph

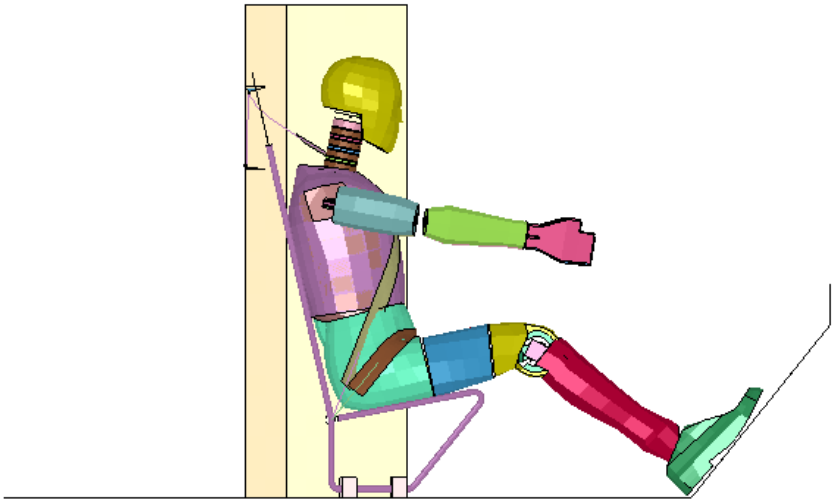

Figure 7.2 Occupant dynamics response for frontal impact at time T=0.0 sec.

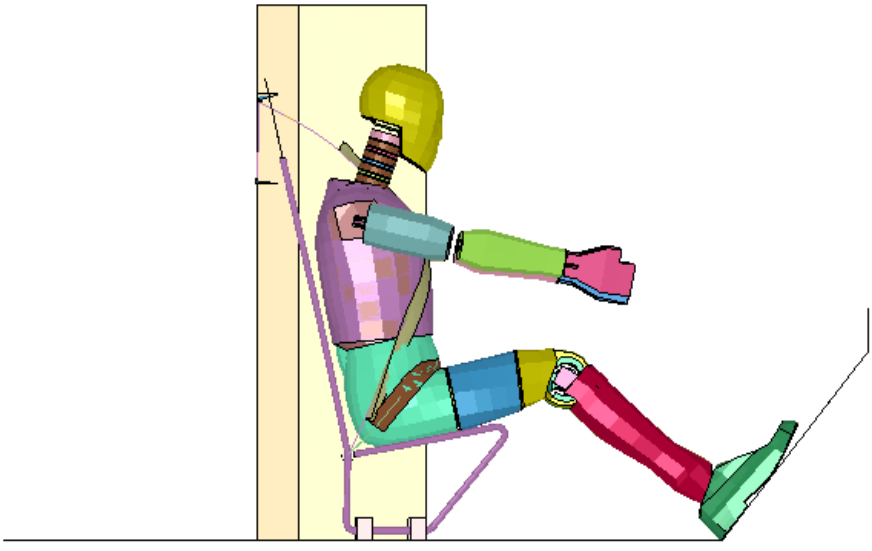

Figure 7.3 Occupant dynamics response for frontal impact at time T=0.08 sec.

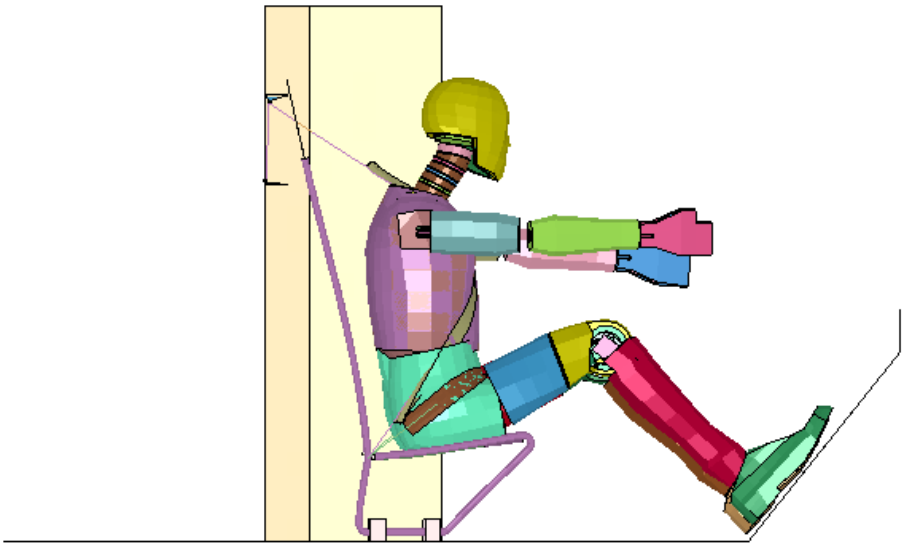

Figure 7.4 Occupant dynamics response for frontal impact at time T=0.14 sec.

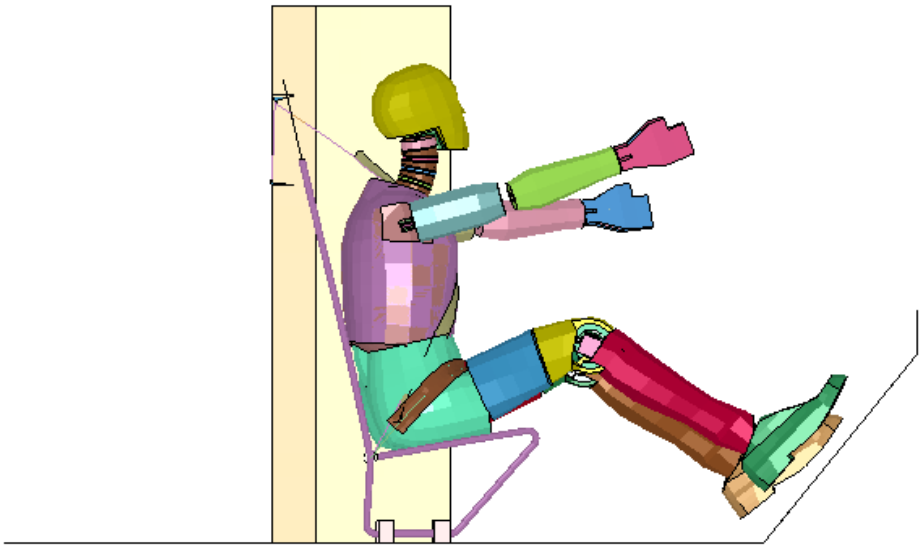

Figure 7.5 Occupant dynamics response for frontal impact at time T=0.2 sec.

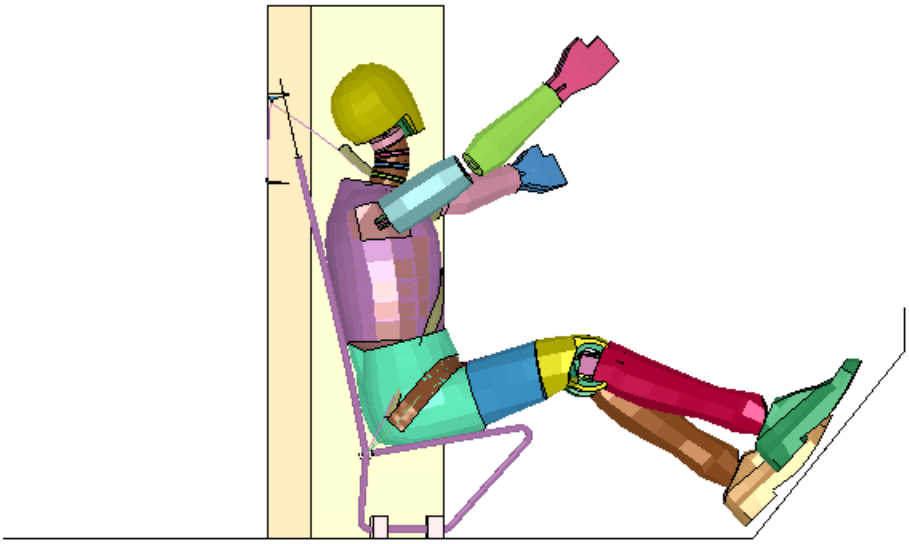

Figure 7.6 Occupant dynamics response for frontal impact at time T=0.26 sec.

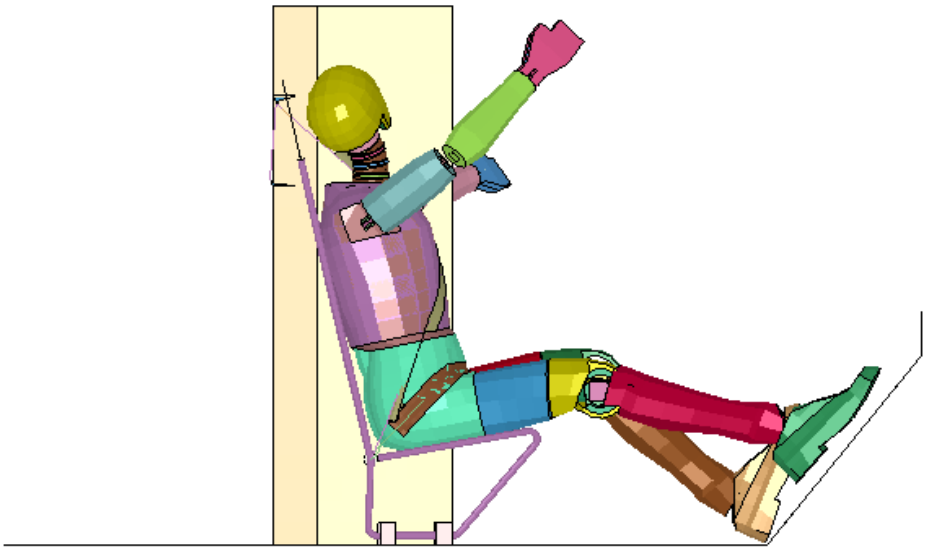

Figure 7.7 Occupant dynamics for frontal impact at time T=0.32 sec.

Occupant response for frontal impact at 35 mph

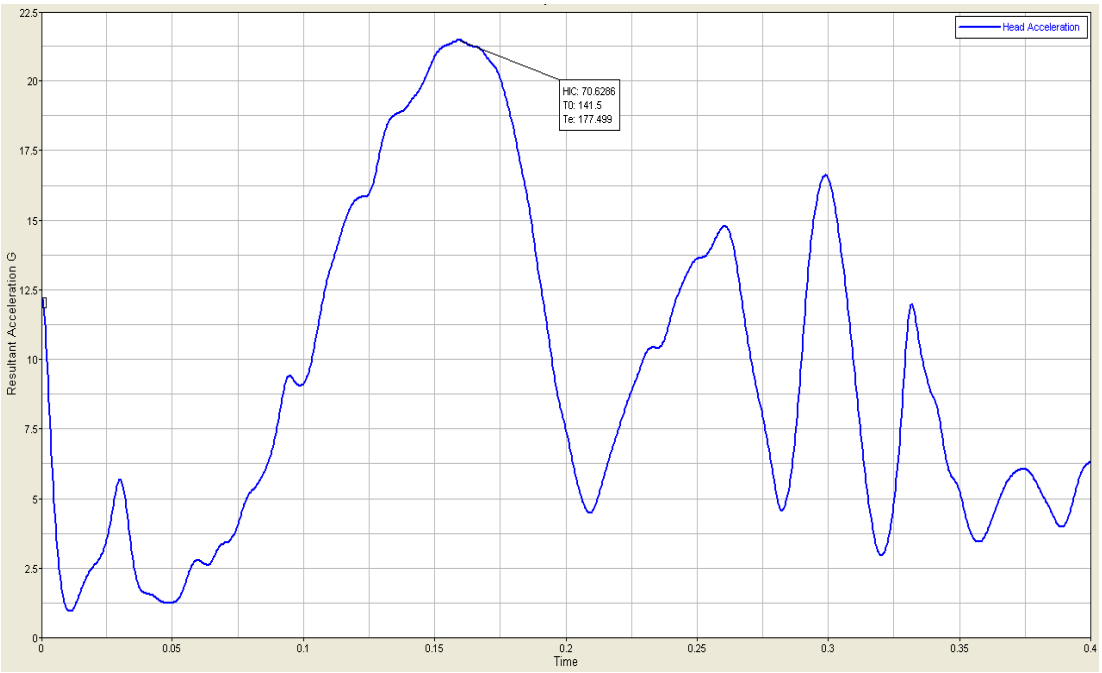

Figure 7.8 Head acceleration

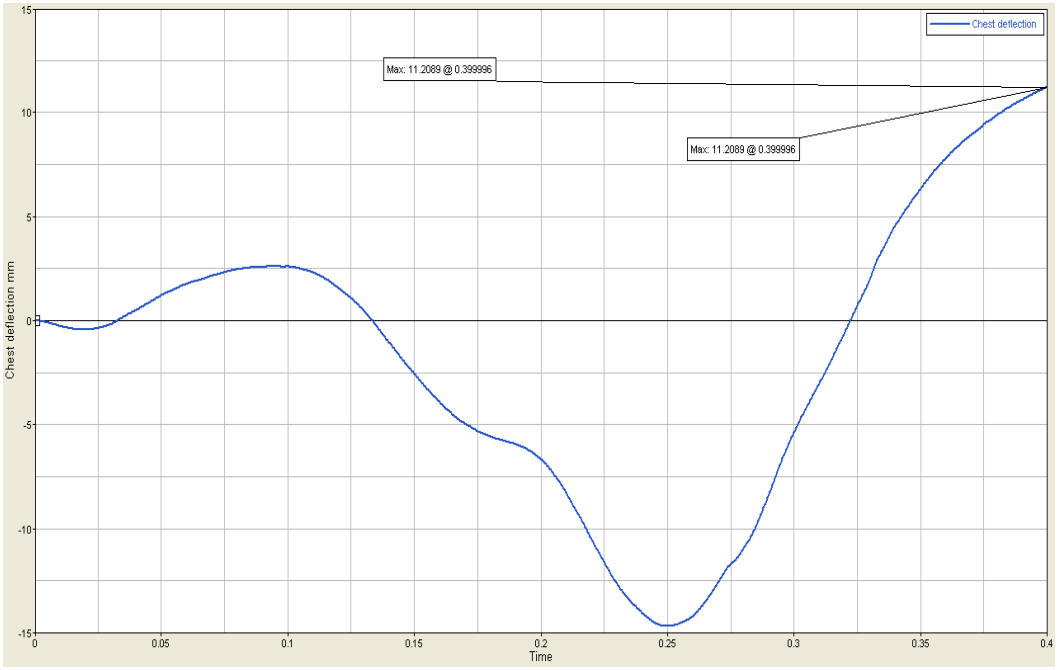

Figure 7.9 Chest deflection

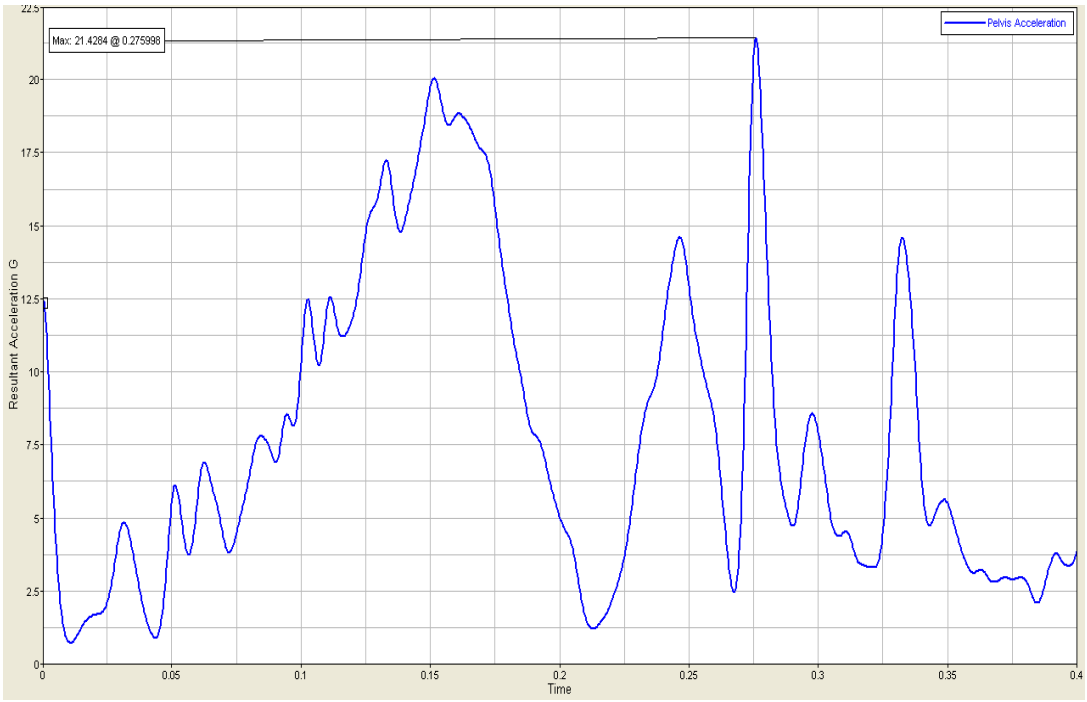

Figure 7.10 Pelvis acceleration

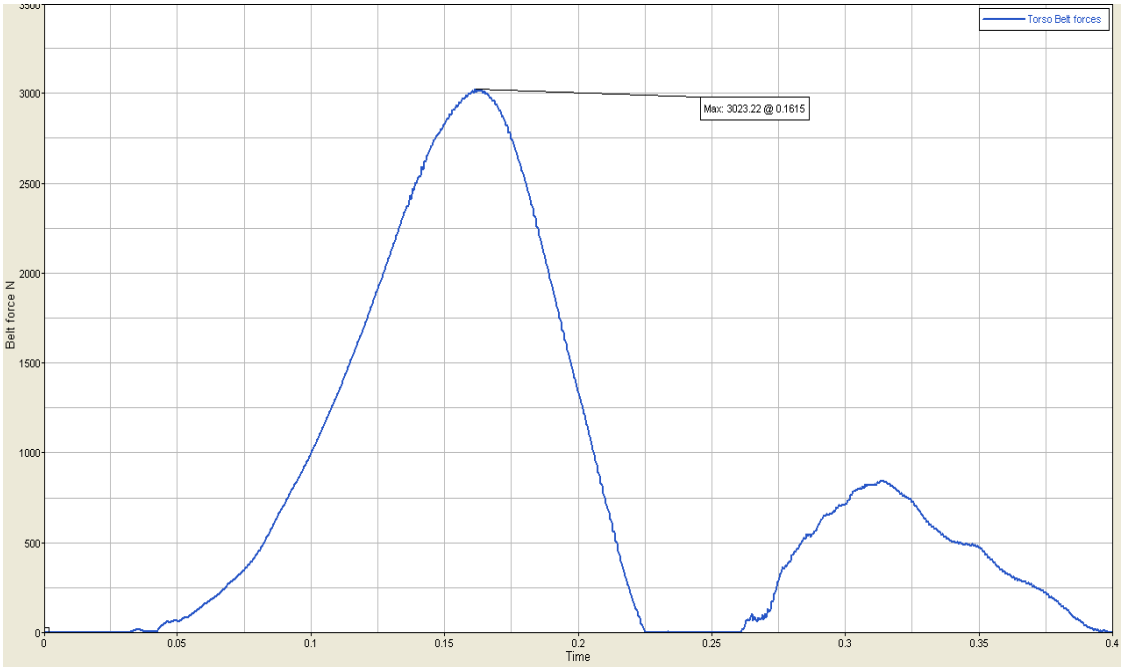

Figure 7.11 Torso belt forces

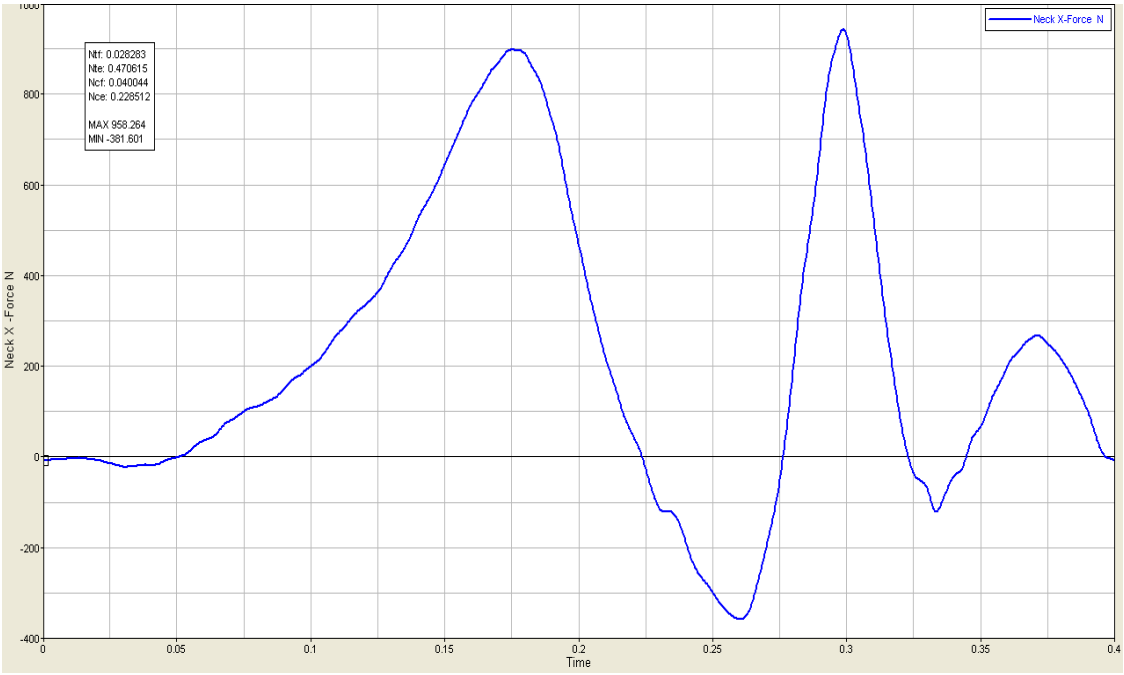

Figure 7.12 Neck injury criteria NIC Neck X-Force

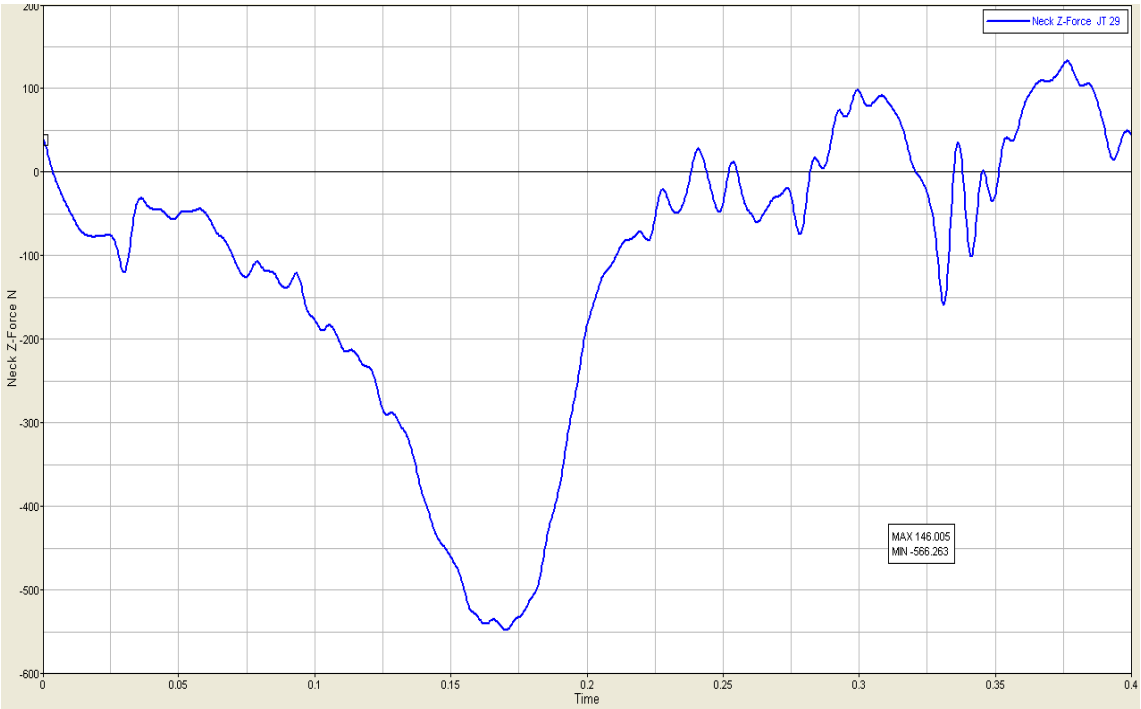

Figure 7.13 Neck injury criteria NIC Neck Z-Force

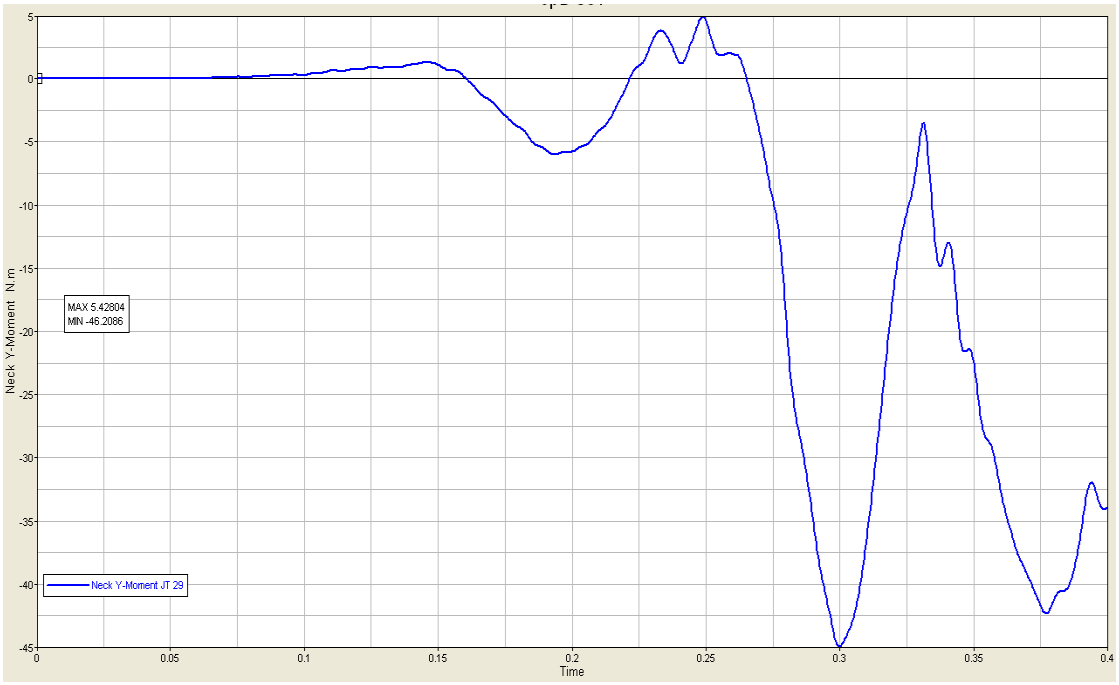

Figure 7.14 Neck injury criteria NIC Neck Y-Moment

Figures 7.8 through 7.14 are the results for the dynamic response of the occupant for the frontal impact sled test. It was conducted using the acceleration pulse obtained for the frontal crash analysis of Ford Taurus, with optimized sandwich material in the front bumper, at a speed of 35 mph.

Figure 7.8 is the graph for the head acceleration, with the peak value of 22 g's with HIC value of 70.6 g's. Figure 7.9 is the graph for chest deflection, with a maximum value of 11.99 mm at time T=.25 sec. This is within the acceptable range as mentioned in Section 7.9. Figure 7.10 is the graph for pelvis acceleration, with a maximum acceleration of 21.42g at t=0.275 sec. Figure 7.11 is the occupant response for the seat belt restraint system due to frontal impact, and the torso belt force measured from the graph was 3023 N, at t=0.1615 sec. Figure 7.12 is the graph plotted for the occupant's

graph was 3023 N, at t=0.1615 sec. Figure 7.12 is the graph plotted for the occupant's neck force along the X-axis during frontal crash test at 35 mph. The peak maximum load observed is 958.27 N. Figure 7.13 is the occupant neck force along the Z-axis during frontal crash test at 35 mph. The peak load observed is 500 N. Figure 7.14 is the moment experienced by the occupant's neck due to the frontal crash impact. The peak values recorded are a maximum of 5.42 N-mm and a minimum of -46.20 N-mm.

The occupant dynamic response for the frontal impact sled test results were obtained by using the acceleration pulse obtained when the steel front bumper was replaced with the optimized sandwich beam. When compared with the frontal impact of the actual front bumper results show that sandwich beam is performing better, and the occupant injury levels sustained, are reduced.

Table 7.2 Summary of occupant bio-dynamic

Biomechanical Responses	Tested Data	Modified Material
Head Acceleration G	40	22
Torso Belt forces N	3033	3023
Chest Deflection	15	12
HIC_{36}	242	102
Pelvis Acceleration G	97	22
Neck Compression N	1177	958
Neck Tension N	847	500
Neck Flexion N-m	46	18

It can be observed from table 7.3, that injuries sustained by the occupant for the frontal impact sled test are within the allowable injury level. There is a noticeable change in head acceleration, chest deflection, neck tension and neck flexion of the occupant.

CHAPTER 8

CONCLUSIONS AND RECOMMENDATIONS

8.1 Conclusion

The goal of this study was to investigate the use of composite sandwich panel as an alternative to the present automobile front bumper, and thus help in reducing the risk of injuries to the occupant. The composite sandwich beam model was cumputationally tested under the three-point bending. The optimization of the sandwich beam was then carried out by increasing the number of plies used in the face sheet, and trying different orientations. Orientations of 30^0, 60^0, and 45^0 were used to find out the layup configuration that gives the highest possible energy absorption, meeting the design requirements of specific strength and energy absorption during the crash event. The FMVSS 208 and US-NCAP tests were conducted on the Ford Turus vechicle with the current and the new bumper model to discover the decrease in accelerations and energy absorption provided by the vehicle, before and after the use of sandwich beam.

The following conclusions can be made from this study.

- Optimization of the sandwich beam has shown high energy absorption, which can be seen by examining the area under the force vs. displacement curve.
- Sandwich beam absorbs more energy and hence the deformation sustained by the beam is more. This leads to a decrease in the displacement and the acceleration of the car, to about 10 Percent and 24 Percent, respectively.
- The use of sandwich beam would reduce the weight of the front bumper by about 18 Percent.

- Injury levels reduce to 40 Percent, assuring that the sandwich beam is better energy-absorbing than the present front bumper.
- This sandwich front bumper is efficient in both FMVSS 208 (24% reduction in acceleration) and oblique impact (70 Percent reduction in acceleration).
- Performance of the Ford Taurus with sandwich beam and actual beam is almost similar, thus suggesting that more angled plies should be used in the sandwich beam.
- With the present production technology involved, the manufacturing of sandwich beams is simple and cost efficient.
- There is no complexity in the use of this sandwich beam in automobile manufacturing, as it is a simple structure and can replace the existing front bumper easily.

As the front bumper is always a highly impacted structure of an automobile, the proposed sandwich beam also fails at very high impacts. By considering still better combination skin and core materials, the failure of the composite front bumper can be avoided.

8.2 Future work

The following recommendations are made for future work in this thesis:

- Improvement can be made in the design of the sandwich beam, by varying the core thickness and the orientation of the layers used in the laminate (currently 0/30/-30/-60/60/90/0/S is used).
- A multiple-cored sandwich beam can be designed with two different foam cores bonded together by an adhesive material.

- In this present research, face sheet and foam are joined together rigidly, but still better results can be obtained if the adhesive material properties are defined in detail while modeling the sandwich beam.
- To better define the improvement observed due to sandwich beam, it is suggested to perform the crash analysis at different angles and at different speeds. Since we are using the FRP composite face sheet, its strength might vary according to the direction of the loading.

REFERENCES

REFERENCES

[1] Siruvole, S.K. (2007), "Evaluation of the occupant response and structural damage according to the newly proposed pole test under federal motor vehicle safety standard side impact regulation," (Master's thesis), Wichita State University, Wichita.

[2] Sheshadri, A. (2006), "Design and analysis of a composite bean for side-impact protection of occupants in a sedan," (Master's thesis), Wichita State University, Wichita.

[3] Nguyen, M.Q.,Jacombs, S.S., Thomson, R.S., Hachenberg, D. and Scott, M. L. (2005). Simulation of impact on sandwich structures, "*Composite Structures*, 67 (2), 217-227.

[4] Cantwell, W.J., Scudamore, R., Ratcliffe, J., and Davies, P. (1999). "Interfacial fracture in sandwich laminates," *Composites Science and Technology*. *59*. 2079-2085.

[5] Mines, R. A. and Alias, A. (2002), "Numerical simulation of the progressive collapse of polymer composite sandwich beams under static loading," *Composites Part A: Applied Science and Manufacturing***,** 33 (1), 11-26.

[6] Gavelin, A, (2006), "Seat integrated safety belts: A parametric study using finite element simulations", (Doctoral thesis). Lulea University of Technology, Lulea, Sweden. Retrieved from http://epubl.luth.se/1402-1757/2006/21/LTU-LIC-0621-SE.pdf. (retrieved May 2011)

[7] Mamalis, A.G., Manolakos, D.E., Ioannidis, M.B. and Papapostolou, D.P.,(2005), "The crushing response of composite sandwich panels subjected to edgewise compression: experimental," *Composite Structures*, 71 (2), 246–257.

[8] NCAC, (2010) "Applications: Finite element model archive", Retrieved from http://www.ncac.gwu.edu/vml/models.html. (retrieved May 2011)

[9] Dassault Systems. (2007), "Abaqus/CAE user's manual," Retrieved from http://www.engin.brown.edu:2080/v6.7/. (retrieved May 2011)

[10] ScienceAlert Pty Ltd, (2008), "The sandwich factor for safer cars," *Swinburne Magazine*. Retrieved from www.sciencealert.com.au/features/20081109-17939.html. (retrieved May 2011)

[11] http://antholonet.com/EngineerisCars/Delorean/delorean.html (retrived on May 2011)

[12] Cantwell, W. J.,(1994), "A comparative study of the mechanical properties of sandwich materials for nautical construction," *SAMPE Journal*, 30 (4), 45-51.

[13] Cameron, C. J., Wennhage, P., Göransson, P., and Rahmqvist, S. (2010), "Structural-acoustic design of a multi-functional sandwich panel in an automotive context," *Journal of Sandwich Structures and Materials*, 12 (6), 684-708.

[14] Vinson, J. R. (1999), "The behavior of sandwich structures of isotropic and composite materials," New York: Technomic Publishing.

[15] U. S. Government Printing Office, (1999), "Federal Motor Vehicle Safety Standards (FMVSS) and Regulations," Retrieved from http://www.nhtsa.gov/cars/rules/import/FMVSS/index.html.(retrieved May 2011)